

NONLINEAR INTERACTIONS BETWEEN LONG WAVES IN A TWO-LAYER
FLUID

A Dissertation

by

NAVID TAHVILDARI

Submitted to the Office of Graduate Studies of
Texas A&M University
in partial fulfillment of the requirements for the degree of

DOCTOR OF PHILOSOPHY

December 2011

Major Subject: Civil Engineering

NONLINEAR INTERACTIONS BETWEEN LONG WAVES IN A TWO-LAYER
FLUID

A Dissertation

by

NAVID TAHVILDARI

Submitted to the Office of Graduate Studies of
Texas A&M University
in partial fulfillment of the requirements for the degree of

DOCTOR OF PHILOSOPHY

Approved by:

Chair of Committee,	James M. Kaihatu
Committee Members,	William S. Saric
	Scott A. Socolofsky
	Jun Zhang
Head of Department,	John Niedzwecki

December 2011

Major Subject: Civil Engineering

ABSTRACT

Nonlinear Interactions between Long Waves in a Two-Layer Fluid. (December 2011)

Navid Tahvildari, B.S., Amirkabir University of Technology (Tehran Polytechnic);

M.S., Sharif University of Technology

Chair of Advisory Committee: Dr. James M. Kaihatu

The nonlinear interactions between long surface waves and interfacial waves in a two-layer fluid are studied theoretically. The fluid is density-stratified and the thicknesses of the top and bottom layers are both assumed to be shallow relative to the length of a typical surface wave and interfacial wave, respectively. A set of Boussinesq-type equations are derived for potential flow in this system. The equations are then analyzed for the dynamics of the nonlinear resonant interactions between a monochromatic surface wave and two oblique interfacial waves. The analysis uses a second order perturbation approach. Consequently, a set of coupled transient evolution equations of wave amplitudes is derived. Moreover, the effect of weak viscosity of the lower layer is incorporated in the problem and the influences of important parameters on surface and interfacial wave evolution (namely the directional angle of interfacial waves, density ratio of the layers, thickness of the fluid layers, surface wave frequency, surface wave amplitude, and lower layer viscosity) are investigated. The results of the parametric study are discussed and are generally in qualitative agreement with previous studies.

In shallow water, a triad formed of surface waves (or interfacial waves) can be considered in near-resonant interaction. In contrast to the previous studies which limited the study to a triad (one surface wave and two interfacial waves or one interfacial

and two surface waves), the problem is generalized by considering the nonlinear interactions between a triad of surface waves and three oblique pairs of interfacial waves. In this system, each surface wave is in near-resonance interaction with other surface waves and in exact resonance with a pair of oblique interfacial waves. Similarly, each interfacial wave is in near-resonance interaction with other interfacial waves which are propagating in the same direction. Inclusion of all the interactions considerably changes the pattern of evolution of waves and highlights the necessity of accounting for several wave harmonics. Effects of density ratio, depth ratio, and surface wave frequency on the evolution of waves are discussed.

Finally, a formulation is derived for spatial evolution of one surface wave spectrum in nonlinear interaction with two oblique interfacial wave spectra. The two-layer Boussinesq-type equations are treated in frequency domain to study the nonlinear interactions of time-harmonic waves. Based on weakly two-dimensional propagation of each wave train, a parabolic approximation is applied to derive the formulation.

To My Family

ACKNOWLEDGMENTS

I could not fulfill this study without the support and encouragement of many people. I would like to express my deep gratitude to my advisor and mentor, Dr. James Kaihatu, for continuous financial support and advice not only on this course of research but also on all aspects of an academic career. I appreciate him for being nice and for respecting and supporting my ideas. Thanks also goes to my committee members Dr. William Saric, Dr. Scott Socolofsky, and Dr. Jun Zhang for their help and advice which undoubtedly improved my work. I would also like to thank Dr. Patrick Lynett for helpful hints and discussions.

I dedicate this work to my beloved fiancé, Saba, whose love and passion have encouraged me to improve myself in every way. I also dedicate it to my parents and my sister for their unconditional love and for supporting and encouraging me throughout all years of my studies. I also wish to dedicate this work to the memory of my grandfather who with his peaceful mind, always motivated his children and grandchildren to study hard and do well.

I thank all my friends for their help and encouragement and for making my experience in Texas A&M a great one.

I would like to acknowledge the support for this research provided by the United States Office of Naval Research through National Oceanographic Partnership Program (ONR-NOPP) (grant N00014-10-1-0389).

TABLE OF CONTENTS

CHAPTER	Page
I	INTRODUCTION 1
II	ANALYSIS OF THE NONLINEAR INTERACTIONS 9
	A. Introduction 9
	B. Governing equations 10
	1. Basic equations 12
	C. Boussinesq-type equations in a two-layer fluid 13
	D. Perturbation analysis 17
	1. Linear solution 19
	2. Second order solution and solvability condition 21
	3. Viscous effects 30
	E. Parametric study 34
	1. Comparison with Jamali (1998) 47
	F. Near-resonant interactions 50
	G. Concluding remarks 68
III	FREQUENCY DOMAIN FORMULATION 70
	A. Introduction 70
	B. Boussinesq equations for a two-layer fluid 72
	C. Resonant triad interaction 74
	D. Time-harmonic equations 76
	E. Parabolic approximation 79
	F. Summary 86
IV	CONCLUSIONS 87
	A. Summary 87
	B. Recommendations 90
	REFERENCES 92
	VITA 99

LIST OF TABLES

TABLE	Page
I Variation of θ (directional angle) with variation of T (surface wave period)	71

LIST OF FIGURES

FIGURE	Page
1	Configuration of the problem 11
2	(ω, k) roots of the dispersion relation and possible resonances among surface and interfacial modes. The dot lines are identical images of surface 2 and interface 2 which are shifted to pass point A. 22
3	Comparison of surface and interfacial roots of fully dispersive, weakly dispersive and non-dispersive dispersion relations. The slower branches (with significantly smaller ω for a given k) represent the interfacial roots. 24
4	Temporal variation of dimensionless amplitudes of interacting surface and interfacial modes. $h = 0.8m, d = 0.2m, r = 0.926, T = 7s, \theta = 70, a_0 = 0.01m, b_0 = 0.001m$ 29
5	Temporal variation of dimensionless amplitudes of interacting surface and interfacial modes. $h = 0.8m, d = 0.2m, r = 0.926, T = 7s, \theta = 70^\circ, \nu = 3 \times 10^{-6}m^2/s, a_0 = 0.01m, b_0 = 0.001m$ 33
6	Variations of initial growth rate of interfacial wave I against θ . $h = 0.8m, d = 0.2m, r = 0.926, T = 7s, a_0 = 0.01m, b_0 = 0.001m$ 35
7	Symmetric configuration of interfacial waves exhibits maximum growth rate; $\theta = 84^\circ$ when $h = 0.8m, d = 0.2m, r = 0.926$ and $T = 7s, a_0 = 0.01m, b_0 = 0.001m$ 36
8	Three-dimensional pattern of nearly-standing interfacial waves. $\theta = 84^\circ, h = 0.8m, d = 0.2m, r = 0.926$ and $T = 7s, a_0 = 0.01m, b_0 = 0.001m$ 36
9	Temporal variation of (a) interfacial wave amplitude, (b) surface wave amplitude for different values of lower layer viscosity ν . $h = 0.8m, d = 0.2m, r = 0.926, T = 7s, a_0 = 0.01m, b_0 = 0.001m$ 38

FIGURE	Page
10	Variation of temporal damping rate, β , against viscosity ν . $h = 0.8m, d = 0.2m, r = 0.926, T = 7s, a_0 = 0.01m, b_0 = 0.001m$ 39
11	Temporal variation of (a) interfacial wave amplitude, (b) surface wave amplitude for values of surface wave frequency T_3 . $h = 0.8m, d = 0.2m, r = 0.926, a_0 = 0.01m, b_0 = 0.001m$ 40
12	Magnitudes of growth rate of interfacial mode against k_3H . $h = 0.8m, d = 0.2m, r = 0.926, a_0 = 0.05m$ 41
13	Magnitudes of damping rate of surface and interfacial mode against k_3H . $h = 0.8m, d = 0.2m, r = 0.926, \nu = 3.00 \times 10^{-6}m^2/s, a_0 = 0.05m, b_0 = 0.001m$ 42
14	Temporal variation of mode amplitudes for various values of $1/r$. $h = 0.8m, d = 0.2m, T = 7s, a_0 = 0.01m, b_0 = 0.001m$ 43
15	Growth rate of interfacial mode and dissipation rate of surface and interfacial mode against variation of density ratio $1/r$. $h = 0.8m, d = 0.2m, T = 7s, \nu = 3.00 \times 10^{-6}m^2/s, a_0 = 0.01m, b_0 = 0.001m$ 44
16	Temporal variation of mode amplitudes for different upper layer depths h/H . $r = 0.926, T = 7s, a_0 = 0.01m, b_0 = 0.001m$ 45
17	Growth rate of interfacial mode (Int. gr) and dissipation rate of surface (Surf. dr) and interfacial modes (Int. dr) against variations of relative upper layer depth, h/H . $r = 0.926, T = 7s, \nu = 3.00 \times 10^{-6}m^2/s, a_0 = 0.01m, b_0 = 0.001m$ 46
18	Temporal variation of mode amplitudes for different initial values of surface wave amplitude a_{30} . $r = 0.926, T = 7s, h = 0.8m, d = 0.2m, b_0 = 0.001m$ 48
19	Growth rate of interfacial mode against variations of surface wave initial amplitude a_{30} . $r = 0.926, T = 7s, h = 0.8m, d = 0.2m, \nu = 3.00 \times 10^{-6}m^2/s, b(0) = 0.001m$ 49

FIGURE	Page	
20	Sketch of the configuration of the interactions between 3 surface waves and corresponding interfacial wave pairs. Surface (or interfacial) waves in the same direction exchange energy due to near-resonant condition. Surface and interfacial waves exchange energy due to exact resonance condition.	52
21	Temporal evolution of (a) surface waves amplitudes in interaction with their subharmonic interfacial waves and (b) Subharmonic interfacial wave amplitudes in resonant triads with corresponding surface waves (the interaction is decoupled from other resonant triads), $H = 2.00m$, $d = 0.50m$, $\omega_3 = 0.3rad/s$, $r = 0.926$, $a_1(0) = a_2(0) = a_3(0) = 0.05m$ $b_1(0) = b_2(0) = b_3(0) = 0.001m$	56
22	Temporal evolution of (a) surface wave amplitudes in interaction triad with other surface waves (decoupled from interfacial waves) and (b) interfacial wave amplitudes in resonant triads with other interfacial waves (decoupled from surface waves) $H = 2.00m$, $d = 0.50m$, $\omega_3 = 0.3rad/s$, $r = 0.926$, $a_1(0) = a_2(0) = a_3(0) = 0.05m$	57
23	Time variation of the amplitude of surface wave 1, $H = 2.00m$, $d = 0.50m$, $\omega_3 = 0.3rad/s$, $r = 0.926$, $a_1(0) = a_2(0) = a_3(0) = 0.05m$	58
24	Time variation of the amplitude of surface wave 2, $H = 2.00m$, $d = 0.50m$, $\omega_3 = 0.3rad/s$, $r = 0.926$, $a_1(0) = a_2(0) = a_3(0) = 0.05m$	58
25	Time variation of the amplitude of surface wave 3, $H = 2.00m$, $d = 0.50m$, $\omega_3 = 0.3rad/s$, $r = 0.926$, $a_1(0) = a_2(0) = a_3(0) = 0.05m$	59
26	Time variation of the amplitude of interfacial wave 1, $H = 2.00m$, $d = 0.50m$, $\omega_3 = 0.3rad/s$, $r = 0.926$, $a_1(0) = a_2(0) = a_3(0) = 0.05m$	59
27	Time variation of the amplitude of interfacial wave 2, $H = 2.00m$, $d = 0.50m$, $\omega_3 = 0.3rad/s$, $r = 0.926$, $a_1(0) = a_2(0) = a_3(0) = 0.05m$	60
28	Time variation of the amplitude of interfacial wave 3, $H = 2.00m$, $d = 0.50m$, $\omega_3 = 0.3rad/s$, $r = 0.926$, $a_1(0) = a_2(0) = a_3(0) = 0.05m$	60
29	Temporal evolution of surface waves for different density ratios, $H = 2m$, $d = 0.5m$, $\omega_3 = 0.3rad/s$, $a_1(0) = a_2(0) = a_3(0) = 0.05m$, $b_1(0) = b_2(0) = b_3(0) = 0.001m$	62

FIGURE	Page
30	Temporal evolution of interfacial waves for different density ratios, $H = 2m, d = 0.5m, \omega_3 = 0.3rad/s, a_1(0) = a_2(0) = a_3(0) = 0.05m, b_1(0) = b_2(0) = b_3(0) = 0.001m.$ 63
31	Temporal evolution of surface waves for different depth ratios, $H = 2m, \omega_3 = 0.3rad/s, r = 0.926, a_1(0) = a_2(0) = a_3(0) = 0.05m, b_1(0) = b_2(0) = b_3(0) = 0.001m.$ 64
32	Temporal evolution of interfacial waves for different depth ratios, $H = 2m, \omega_3 = 0.3rad/s, r = 0.926, a_1(0) = a_2(0) = a_3(0) = 0.05m, b_1(0) = b_2(0) = b_3(0) = 0.001m.$ 65
33	Temporal evolution of surface waves for different frequencies ratios, $H = 2m, d = 0.5m, r = 0.926, a_1(0) = a_2(0) = a_3(0) = 0.05m, b_1(0) = b_2(0) = b_3(0) = 0.001m.$ 66
34	Temporal evolution os surface waves for different frequencies ratios, $H = 2m, d = 0.5m, r = 0.926, a_1(0) = a_2(0) = a_3(0) = 0.05m, b_1(0) = b_2(0) = b_3(0) = 0.001m.$ 67

CHAPTER I

INTRODUCTION

The evolution of oceanic internal waves has been the subject of numerous studies in the past several decades. Internal gravity waves are commonly found in stably density stratified fluids in various scales. The density stratification can be due to temperature (as in lakes) or salinity (as in ocean) gradient. A two-fluid system is a common, although simplified, model for ocean stratification. The internal waves propagate along the density interface (thus the term "interfacial" waves). Although nonlinear evolution of internal waves often makes it impossible to track their source of generation (Staquet & Sommeria, 2002), several mechanisms, which are not well investigated, are known to lead to generation of interfacial waves in the ocean. Among others are interaction of tides with topography, interfacial shear instability, and nonlinear interactions with surface waves.

Stokes (1847) was the first to show that two modes of oscillation are possible in a two-layer fluid. The modes are called barotropic or surface mode, corresponding to the mode in which the largest fluid oscillations occur at the surface, and baroclinic or internal mode in which maximum oscillation is at the interface. It was found that the interface between the layers allows for presence of waves which are very similar to the surface waves. Helland-Hansen & Nansen (1909) reported the first observation of internal wave effects as fluctuation of the temperature at a fixed depth. Having established the evidence of their presence, researchers focused on possible mechanisms of generation and dissipation of interfacial waves and their interaction with other waves in the ocean. After initial studies by Philips (1960) on nonlinear wave inter-

The journal model is the *Journal of Fluid Mechanics*.

actions, Ball (1964) showed that in a two-layer shallow fluid, nonlinear interactions are possible between surface and interfacial waves. The nonlinear interactions among different wave components have been widely studied since then (Philips, 1981). Nonlinear interactions in a two-layer fluid are of practical importance in coastal dynamics, limnology and oceanography. The focus of the studies on internal waves have mostly been in deep ocean conditions (Thorpe, 1975) and there are only a few accounts of observation of interfacial waves in coastal areas where the seabed boundary conditions becomes influential. However, theoretical and experimental results of Hill & Foda (1998) and Jamali (1998) confirm that surface waves can induce interfacial waves in intermediate and shallow waters. Study of interface processes also has implications in investigation of wave-sediment interactions.

Vast areas of mud, silt and fine sediments line the adjacent shorelines of many areas of the world (e.g., the coastlines of Louisiana, USA (Jaramillo *et al.*, 2009); the Korean Peninsula; the Amazon River delta (Cacchoine *et al.*, 1995); coast of Surinam; the Persian Gulf (Soltanpour *et al.*, 2010)). Generally, the immediate effect of cohesive sediments on the surface waves has been that of very strong damping, as reported by Wells & Coleman (1981). However, in addition to the direct damping of surface waves, several other physical phenomena occur during the propagation of surface waves over bottom mud. An example is the interaction between surface waves which can lead to the energy transfer from short to long waves (Sheremet & Stone, 2003; Kaihatu *et al.*, 2007). In addition, surface waves can generate short internal waves over a sediment-water interface (Hill & Foda, 1996). The bottom mud can become fluidized due to the dynamic forcing of surface waves and form a two-layer fluid admitting nonlinear generation of instabilities over lutocline (mud-water interface). Surface waves can lose energy to grow such instabilities to become interfacial waves. Therefore, one possible damping mechanism for surface waves which is often disregarded is the generation

of interfacial waves. In addition, interfacial waves may break and result in vertical mixing in the water column (Thorpe, 1968). These phenomena highlight the practical importance of the evolution of the interfacial waves in coastal regions. The nonlinear interactions among surface and interfacial modes of motion or their interaction with bottom topography has been studied only to a small degree.

In contrast to a single layer fluid where completely resonant nonlinear interactions are third order effects and occur among four waves in deep to intermediate depth water (Philips, 1960), exact resonance is possible among triads of waves in second order in a two-layer fluid (Ball, 1964). Either two surface waves with one interfacial wave or two interfacial waves with a single surface wave can form a resonant triad. The former triad was first studied by Ball (1964). He specifically focused on the triad in very shallow water (non-dispersive limit) and showed that the interfacial wave gains energy from opposite-traveling surface wave pair. Thorpe (1966) studied the same triad using Euler equations. In addition, Segur (1980) noted that a two-layer system mathematically admits resonant interactions between two internal waves and a single surface wave. The physical consequence of this resonant triad was examined later in the theoretical studies of Wen (1995) and theoretical and experimental studies of Hill & Foda (1998) and Jamali (1998). The experiments generally indicated the generation of a pair of oblique short interfacial waves and their growth due to subharmonic resonance with a monochromatic surface wave. These studies used second order perturbation approach and predicted initial exponential growth of the interfacial waves. Hill (2004) extended the analysis to the third order by providing an inviscid analysis for internal waves propagating over a deep lower layer. His results indicate that the second order analysis significantly overestimates the interfacial wave amplitudes. Recently, Tahvildari & Jamali (2009) extended the third order study to intermediate depth water and incorporated the effect of viscosity in the evolution equations of

wave amplitudes. Their analysis could predict the long-term saturation of interfacial waves due to viscous effects, which was in agreement with experimental observations (Jamali, 1998). All of these analyses use deep water scaling, with the small parameter as $\epsilon = ka$, where a and k are respectively a typical wave amplitude and wave number, limiting the analysis to fluid layers of large to intermediate depths. However, the interaction between surface waves and seabed becomes significant in shallow waters where Stokes theory breaks down and Boussinesq-type equations provide a more consistent description of wave forms.

The classical Boussinesq equations of Peregrine (1967), are the extension of weakly nonlinear shallow water equations to include weak dispersiveness. Therefore, they can provide an appropriate formulation for the relatively shallow to intermediate depth waters corresponding to coastal regions. Numerical simulations of the standard Boussinesq equations have compared quite well in their range of validity with field observations (Chen *et al.*, 2003; Elgar & Guza, 1985; Freilich & Guza, 1984) and laboratory data (Liu *et al.*, 1985; Rygg, 1988). There have been several attempts to overcome the shallow water limitation of the conventional Boussinesq equations by improving the linear dispersion properties (Madsen *et al.*, 1991; Nwogu, 1993) which have led to introduction of extended Boussinesq equations. The numerical investigation of Nwogu (1993) equations has shown improved comparisons with experimental results (Wei & Kirby, 1995). A fully nonlinear extension of Nwogu (1993) equations was derived and modeled by Wei *et al.* (1995). On long internal waves, early studies were based on the Korteweg-De Vries (KdV) equation Benjamin (1966). Some researchers used KdV-type equations with incorporation of dissipative and shoaling effects (Lewis *et al.*, 1974; Liu, 1988; Maxworthy, 1979). Koop & Butler (1981) studied the behavior of weakly nonlinear KdV models for long internal waves against experimental measurements and concluded that the model behaves

fairly well where both layers of fluid are in shallow range. Based on the KdV or the Kadomtsev-Petviashvili (K-P) equations, all these models have the limitation of uni-directional or weakly two-dimensional waves in horizontal plane. Weakly nonlinear and weakly dispersive (Choi & Camassa, 1996; Lynett & Liu, 2002) and fully nonlinear and weakly dispersive (Choi & Camassa, 1999) models were derived for evolution of internal waves. Recently, Debsarma *et al.* (2010) improved the fully nonlinear model of Choi & Camassa (1999) with inclusion of higher order dispersive terms. Among the aforementioned two-fluid models, all assume a rigid lid condition except for Choi & Camassa (1996). The rigid lid assumption eliminates the complications due to nonlinear interactions between surface and interfacial modes. However, a two-layer fluid with free surface boundary condition is a more realistic analogy for oceanic environment. It is noted that derivation of extended Boussinesq equations in the manner of Madsen *et al.* (1991) and Nwogu (1993) can also be accompanied following this general approach; this would allow for more accurate wave propagating modeling at frequencies beyond the weakly dispersive limit. However, our focus here is on the nonlinear processes in shallow water (small μ^2) rather than on enhancement of the model performance in intermediate-deep water.

In deep-intermediate water, neither the surface wave nor the interfacial waves can be in near-resonance condition with other surface or interfacial modes in second order. On the other hand, study of waves in non-dispersive limit confines the results to very shallow waters. The work in this dissertation contributes to the research on nonlinear wave interactions, and in particular, focuses on generalization of study of nonlinear interactions between a surface wave and a pair of interfacial waves by including shallow water scaling. Accounting for shallow water scaling extends the previous research on the topic from intermediate-deep water to shallow-intermediate depths. On the other hand, other resonant interactions are possible in shallow water; a

triad formed of surface waves (or interfacial waves) can exchange energy if they satisfy near-resonance condition. These interactions are also influential on the evolution of waves. In an effort to take this interaction into account, we consider a triad of surface waves which are in near-resonance with each other and simultaneously in exact resonance with two oblique interfacial waves. The interfacial waves on the other hand, are in shallow water range as well and thus, are in near-resonant interaction with other interfacial waves in the same wave train. Therefore, we have expanded the problem by considering a system of 9 waves which interact to varying degrees.

In Chapter (2), the governing equations for the propagation of weakly dispersive waves in a two-layer fluid are derived. These equations form a two-dimensional Boussinesq-type model with depth-averaged velocities in which the nonlinearity and dispersiveness are in balance, i.e. $O(\epsilon) = O(\mu^2) \ll 1$, where $\mu = kh$ is the dispersion parameter in which k and h are a typical wave number and water depth respectively. The equations are shown to be compatible with the system derived by Choi & Camassa (1996) in the limit of shallow lower layer and slightly varying bottom. This system of equation follows is consistent with the ordering in the conventional Boussinesq equations and thus is valid in shallow water range. The equations are analyzed for the nonlinear wave interactions in the system. Initially, the problem of subharmonic generation of two oblique interfacial waves due to resonant interaction with a long surface wave is studied. A second order perturbation approach is used and coupled evolution equations of the amplitudes of the interacting waves are derived. The focus is on dynamics of transient evolution of wave amplitudes. Furthermore, the effect of weak viscosity of the lower layer is incorporated in the amplitude evolution equations. Finally, the influence of important parameters in the system such as directional angle of interfacial waves, viscosity of the lower layer, surface wave frequency and initial amplitude, relative thickness of the layers and density difference

on temporal evolution of surface and interfacial wave amplitudes are discussed. Finally, the problem is generalized to include the near-resonant terms and the effects of stratification, depth ratio and surface wave frequency on the evolution of waves are discussed. The study provides invaluable insight on the dynamics of surface-interface interactions by studying their temporal evolution. It is also desirable to investigate the spatial evolution of waves when they have reached their steady-state amplitude.

As mentioned earlier, Tahvildari & Jamali (2009) investigated the third order effects on the evolution of interfacial waves. The significant result of the study was that after initial exponential growth, the interfacial wave amplitudes inhibit growth and approach a constant magnitude in long time due to weak viscosity effects. In other words, interfacial waves approach a time-periodic steady-state behavior. There are a few studies on the spectral energy transfer between surface and interfacial waves. Watson *et al.* (1976) discussed the spectral growth of internal waves due to coupling with surface waves. The study was limited to linear theory. Olbers & Herterich (1979) studied the energy transfer from the spectrum of surface wave to internal wave field in deep ocean. Parau & Dias (2001) showed that nonlinear interaction is possible between a long internal mode and a short surface mode in oceanic conditions. However, the study was formulated in deep water conditions and was limited to one horizontal dimension. Recently, Liu (2006) studied the energy transfer in random surface and internal wave field using Stokes theory. However, there is no study on the evolution of interacting spectra of long surface and interfacial waves.

In Chapter (3), the nonlinear interactions between surface and interfacial waves is extended to one spectrum of surface waves and a pair of spectra of interfacial waves. The spatial evolution of interacting waves in the steady-state stage is formulated. Time evolution of spatially periodic waves was studied by Bryant (1973, 1974). He applied a Fourier transform, periodic in space, for velocity potential and

free surface displacement and formulated a model for flat bottom. However, as most wave records are taken as time-series in spatially fixed gages, a time periodic spatial varying formulation is a more suitable model for practical applications. Liu *et al.* (1985) studied refraction-diffraction of time periodic waves by Boussinesq equations using a parabolic approximation. Agnon *et al.* (1993) derived a nonlinear spatially varying, temporally periodic shoaling model. Kaihatu & Kirby (1995) extended the model in Agnon *et al.* (1993) to two dimensions and derived a nonlinear mild-slope elliptic model. A parabolic approximation was used to develop the evolution equations in two-dimensions. The model showed an improvement in comparison with experimental data. Furthermore, Kaihatu & Kirby (1998) used the parabolic approximation to model the extended Boussinesq equations. In this chapter, the quadratic nonlinear interactions between components of one surface wave spectrum and two oblique interfacial wave spectra is studied. The interfacial wave trains are assumed to be generated due to subharmonic resonance with the surface wave. Therefore, the considered interactions include second order near-resonant interactions among surface waves harmonics and also among interfacial wave harmonics in each wave train, as well as second order exact resonance between surface and subharmonic interfacial harmonics. As frequency domain formulation allows for explicit modeling of the nonlinear wave interactions and provides the suitable tool to extend the study of triad interactions to steady-state condition, this framework is adopted. In Chapter (4), the conclusions and suggestions for future work are discussed.

CHAPTER II

ANALYSIS OF THE NONLINEAR INTERACTIONS

A. Introduction

In a two fluid system, energy can be exchanged between a surface wave in barotropic mode to a pair of interfacial waves in baroclinic mode. This interaction is a potential mechanism for parametric instability of internal gravity waves in near-inertial frequency band (Foda & Hill, 1998). In shallow waters, in addition to this energy exchange, components in a surface or interfacial wave train can form resonant triads. The purpose of this chapter is to analyze these processes. As a first step, a suitable formulation is derived to analyze the dynamics of the nonlinear interactions. Then the parametric instability of the interfacial waves is investigated and finally, the analysis is expanded to include more possible nonlinear interactions between waves in a two-layer shallow water.

Initially, a system of Boussinesq-type equations is derived for shallow flows in a two-layer fluid. The resulting model is composed of four equations for conservation of mass and momentum in both layers and can be used for numerical simulation of surface and interfacial waves propagation. The model is verified by comparing to Choi & Camassa (1996). The model retains second order of nonlinearity and first order of dispersion, i.e. the truncation error is $O(\epsilon^2, \epsilon\mu^2)$. Then, using a standard approach (second order perturbation), the equations are analyzed for the dynamics of the generation of two oblique interfacial waves due to nonlinear interactions with a surface wave. Consequently, temporal evolution equations of the waves are derived and the interaction between the surface and interfacial waves is studied. Furthermore, the influence of important parameters in the problem, i.e. directional angle of interfacial

waves, viscosity, surface wave frequency, surface wave amplitude, stratification, and depth ratio on the evolution of interacting waves are studied.

In addition to the aforementioned coupling between surface and interfacial waves, triads of nonlinear interaction can be formed among harmonics of surface or interfacial waves. To allow for such interactions, we generalize the problem by considering a triad of surface waves. A triad is a basic structure to study nonlinear energy transfer between modes. The nonlinear interactions between the same type of waves in weakly-dispersive limit, is a *near-resonant* interaction. In such condition, the frequencies exactly and the wave numbers approximately satisfy the kinematic conditions of resonance. Due to exact resonance condition, each surface wave component generates two oblique interfacial waves and thus, two trains of oblique interfacial waves each having three waves are generated. The component of generated interfacial waves are also long waves and can form an interacting triad. In Section (II-F), these possible nonlinear interactions are analyzed and the changes in the evolution of waves due to alteration of the important parameter values are examined.

B. Governing equations

Figure 1 illustrates the configuration of the problem. The Cartesian coordinate system is introduced with origin at still interface, (x, y) at the interfacial plane and z -axis positive upward. The fluid is two-layer and density stratified with an upper layer of density ρ' and thickness h , and lower layer of density ρ and thickness d (prime quantities refer to upper layer hereafter). The fluid layers are assumed inviscid (initially), incompressible, homogeneous and immiscible and flows are assumed irrotational within each fluid. Therefore, velocity potential functions ϕ' and ϕ can be defined for the upper and lower layer, respectively. We allow for mild spatial variation

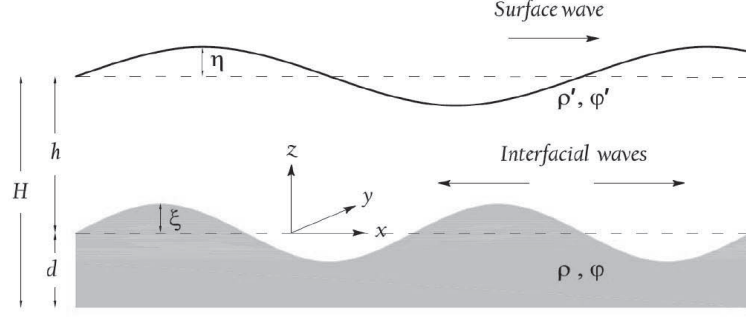


Fig. 1. Configuration of the problem

of bathymetry; $z = -d(x, y)$ where $\nabla d = \mathcal{O}(\mu^2)$. Resonant generation of interfacial waves due to interaction with a surface wave is a three dimensional process, and to capture this three dimensionality, the fluid layers are assumed to be horizontally infinite, corresponding to a laterally unbounded ocean. The free surface and interface displacements are $\eta(x, y)$ and $\xi(x, y)$ respectively.

In the derivation of a depth-averaged model, we scale the problem in a manner consistent with a shallow water formulation. Using a typical wave amplitude, a_0 , characteristic wave number, k_0 , and a typical upper layer thickness, h_0 , the following dimensionless variables are introduced (Mei *et al.*, 2005):

$$\begin{aligned} (x^*, y^*) &= k_0(x, y), & z^* &= \frac{z}{h_0}, & t^* &= k_0 \sqrt{gh_0} t, & \omega^* &= \frac{\omega}{k \sqrt{gh_0}}, \\ (\xi^*, \eta^*) &= \frac{(\xi, \eta)}{a_0}, & (d^*, h^*) &= \frac{(d, h)}{h_0}, & \phi^* &= \phi \frac{k}{\epsilon \sqrt{gh_0}}, & k^* &= \frac{k}{k_0}, \end{aligned} \quad (2.1)$$

where g is the gravity acceleration and the asterisks denote dimensionless quantities. The parameter $\epsilon = a_0/h_0$ is a measure of relative smallness of the wave amplitudes and the nonlinearity parameter. In scaling the long wave motion, another small parameter is defined to represent frequency dispersion ; $\mu = k_0 h_0$. By substituting the dimensionless variables, the equations become non-dimensional. The asterisks are dropped hereafter for convenience.

1. Basic equations

One approach to deriving the Boussinesq-type equations is to start from the potential flow boundary value problem (e.g. see Mei *et al.*, 2005) where the fluid is inviscid. The internal kinematics of the two layers are thus governed by the Laplace equation. The equations are written in terms of velocity potentials in the two layers and are scaled using (2.1):

$$\mu^2 \nabla^2 \phi' + \phi'_{zz} = 0, \quad \epsilon \xi < z < h + \epsilon \eta \quad (2.2)$$

$$\mu^2 \nabla^2 \phi + \phi_{zz} = 0, \quad -d < z < \epsilon \xi \quad (2.3)$$

where $\nabla = (\partial/\partial x, \partial/\partial y)$ and subscripts of coordinates or time denote partial derivatives. The free surface kinematic and dynamic boundary conditions are given by

$$\mu^2 [\eta_t + \epsilon \nabla \phi' \cdot \nabla \eta] = \phi'_z, \quad z = h + \epsilon \eta \quad (2.4)$$

$$\mu^2 \left[\phi_t + \eta + \frac{1}{2} \epsilon (\nabla \phi')^2 \right] + \frac{1}{2} \epsilon (\phi'_z)^2 = 0, \quad z = h + \epsilon \eta \quad (2.5)$$

where $z = h$ is the elevation of the undisturbed free surface, and the atmospheric pressure on the free surface is assumed to be zero. Similarly, the kinematic and dynamic interface boundary conditions are,

$$\mu^2 [\xi_t + \epsilon \nabla \phi' \cdot \nabla \xi] = \phi'_z, \quad z = \epsilon \xi \quad (2.6)$$

$$\mu^2 [\xi_t + \epsilon \nabla \phi \cdot \nabla \xi] = \phi_z, \quad z = \epsilon \xi \quad (2.7)$$

$$r \mu^2 \left[\phi'_t + \xi + \frac{\epsilon}{2} (\nabla \phi')^2 \right] + \frac{\epsilon}{2} (\phi'_z)^2 = \mu^2 \left[\phi_t + \xi + \frac{\epsilon}{2} (\nabla \phi)^2 \right] + \frac{\epsilon}{2} (\phi_z)^2, \quad z = \epsilon \xi \quad (2.8)$$

where the parameter $r = \rho'/\rho < 1$ is the density ratio of the layers in a stable stratification. Equations (2.6) and (2.7) respectively account for the particles at the interface in the upper and lower fluid to remain on the interface. Equation (2.8) is the

Bernoulli equation at the interface where the pressures in the lower layer and upper layer are identical. It is evident in the scaled equations that the displacements at the free surface and interface are in the same order of magnitude and both surface and interfacial modes are assumed to be long waves. The bottom topography is assumed to be mildly varying in space and a no flux kinematic boundary condition is used at the seabed:

$$\mu^2 \nabla \phi \cdot \nabla d + \phi_z = 0, \quad z = -d(x, y) \quad (2.9)$$

C. Boussinesq-type equations in a two-layer fluid

In this section, we derive Boussinesq equations for propagation of weakly nonlinear and weakly dispersive waves in the two-fluid system. The Boussinesq approximation results in a simplifying assumption to the governing equations that nonlinearity and frequency dispersion are in balance, i.e. $\mathcal{O}(\epsilon) \sim \mathcal{O}(\mu^2)$. We express the depth dependence of the velocity potentials in the layers as power series in vertical coordinate, z , for both layers,

$$\phi'(x, y, z, t) = \sum_{n=0}^{\infty} z^n \phi'_n(x, y, t) \quad (2.10)$$

$$\phi(x, y, z, t) = \sum_{n=0}^{\infty} (z + d)^n \phi_n(x, y, t) \quad (2.11)$$

The above expansions are substituted in the bottom boundary condition, (2.9), and kinematic interfacial boundary condition, (2.6), respectively. Therefore, ϕ_1 and ϕ'_1 are obtained in terms of potential function values at the seabed and interface (ϕ_0 and ϕ'_0 respectively),

$$\phi'_1 = \mu^2 \xi_t + \epsilon \mu^2 \nabla \phi'_0 \cdot \nabla \xi \quad (2.12)$$

$$\phi_1 = -\mu^2 \nabla \phi_0 \cdot \nabla d + \mu^4 \nabla \phi_0 \cdot \nabla d (\nabla d)^2 \quad (2.13)$$

By substituting (2.10) and (2.11) respectively in the upper and lower layer Laplace equations, (2.2) and (2.3), the following recursion expressions are obtained,

$$\phi'_{n+2} = -\mu^2 \frac{\nabla^2 \phi'_n}{(n+1)(n+2)} \quad (2.14)$$

$$\phi_{n+2} = \mu^2(\mu^2 - 1) \frac{\nabla^2 \phi_n + (n+1) [\nabla \phi_{n+1} \cdot \nabla d + \nabla \cdot (\phi_{n+1} \nabla d)]}{(n+1)(n+2)} \quad (2.15)$$

We rewrite (2.10) using (2.12) and (2.14) and rewrite (2.11) using (2.13) and (2.15) and retain terms of $\mathcal{O}(\mu^3)$ and larger. The expressions for velocity potential functions are then given by,

$$\phi' = \phi'_0 + \mu^2 \xi_t - \frac{\mu^2}{2} \nabla^2 \phi'_0 z^2 + \mathcal{O}(\mu^4) \quad (2.16)$$

$$\phi = \phi_0 - \mu^2 \nabla \phi_0 \cdot \nabla d (z+d) - \frac{\mu^2}{2} \nabla^2 \phi_0 (z+d)^2 + \mathcal{O}(\mu^4) \quad (2.17)$$

The above expressions for the velocity potentials will be used to obtain the depth-integrated momentum equations. Horizontal gradients of these equations give the horizontal velocities in the upper and lower layers in terms of the horizontal velocity at the interface and the seabed respectively. In the upper layer, (2.2) is integrated over the layer thickness and the kinematic boundary conditions at the interface, equation (2.6), and at the free surface, equation (2.4), are used. Similarly, in the lower layer, equation (2.3) is integrated from the seabed, $z = -d(x, y)$, to the interface, $z = \epsilon \xi$, and the kinematic boundary conditions, (2.7) and (2.9) are used. Therefore, the depth-integrated continuity equations in the layers are obtained as:

$$(h + \eta - \xi)_t + \nabla \cdot \int_{\epsilon \xi}^{h+\epsilon \eta} \nabla \phi' dz = 0 \quad (2.18)$$

$$\xi_t + \nabla \cdot \int_{-d}^{\epsilon \xi} \nabla \phi dz = 0 \quad (2.19)$$

The initial assumption that the waves are long allows for definition of depth-averaged horizontal velocities in the layers:

$$\bar{\mathbf{u}}' = \frac{1}{H'} \int_{\epsilon\xi}^{h+\epsilon\eta} \mathbf{u}' dz, \quad \bar{\mathbf{u}} = \frac{1}{H} \int_{-d}^{\epsilon\xi} \mathbf{u} dz \quad (2.20)$$

where $\bar{\mathbf{u}}' = \nabla\phi'$ and $\bar{\mathbf{u}} = \nabla\phi$. The total thickness of the top and bottom layers are defined by $H' = h + \epsilon(\eta - \xi)$ and $H = d + \epsilon\xi$ respectively. Substituting the velocity for velocity potential in equations (2.18) and (2.19) and also substituting the total depth in terms of surface and interface displacements and the layer depths, the continuity equations are written in terms of depth-averaged velocities:

$$(h + \eta - \xi)_t + \nabla \cdot [(h + \epsilon\eta - \epsilon\xi)\bar{\mathbf{u}}'] = 0 \quad (2.21)$$

$$\xi_t + \nabla \cdot [(d + \epsilon\xi)\bar{\mathbf{u}}] = 0 \quad (2.22)$$

The above equations are exact to all orders of nonlinearity and dispersiveness for viscous and inviscid fluids and for rotational and irrotational flows. In deriving the momentum equations, it is convenient to define horizontal velocities at interface and seabed:

$$\mathbf{u}'_0 = \nabla\phi'_0, \quad \mathbf{u}_0 = \nabla\phi_0 \quad (2.23)$$

The horizontal gradients of velocity potentials are integrated in the depth of the respective layers and equations (2.16) and (2.17) are used to write the velocity potential of the upper and lower layer in terms of the velocity potential at the interface and the seabed, respectively. Therefore, the horizontal velocities in the layers can be written as:

$$\bar{\mathbf{u}}' = \bar{\mathbf{u}}'_0 + \frac{\mu^2}{2} h \nabla \xi_t - \frac{\mu^2}{6} h^2 \nabla \nabla \cdot \bar{\mathbf{u}}' + \mathcal{O}(\epsilon\mu^2, \mu^4) \quad (2.24)$$

$$\bar{\mathbf{u}} = \bar{\mathbf{u}}_0 - \frac{\mu^2}{2} d \left[\nabla(\bar{\mathbf{u}}_0 \cdot \nabla d) + \nabla d \cdot \nabla \bar{\mathbf{u}}_0 + \frac{d}{3} \nabla \nabla \cdot \bar{\mathbf{u}}_0 \right] + \mathcal{O}(\epsilon\mu^2, \mu^4) \quad (2.25)$$

Noting that $\bar{\mathbf{u}}_0 = \bar{\mathbf{u}} + \mathcal{O}(\mu^2)$ and $\bar{\mathbf{u}}'_0 = \bar{\mathbf{u}}' + \mathcal{O}(\mu^2)$, the above equations can be reverted to obtain $\bar{\mathbf{u}}_0$ and $\bar{\mathbf{u}}'_0$ as:

$$\bar{\mathbf{u}}'_0 = \bar{\mathbf{u}}' - \frac{\mu^2}{2} h \nabla \xi_t + \frac{\mu^2}{6} h^2 \nabla \nabla \cdot \bar{\mathbf{u}}' + \mathcal{O}(\epsilon \mu^2, \mu^4) \quad (2.26)$$

$$\bar{\mathbf{u}}_0 = \bar{\mathbf{u}} + \frac{\mu^2}{2} d \left[\nabla (\bar{\mathbf{u}} \cdot \nabla d) + \nabla d \cdot \nabla \bar{\mathbf{u}} + \frac{d}{3} \nabla \nabla \cdot \bar{\mathbf{u}} \right] + \mathcal{O}(\epsilon \mu^2, \mu^4) \quad (2.27)$$

Using (2.26) and (2.27) in the dynamic boundary conditions at the surface and interface will give the momentum equations for horizontal velocities in the upper and lower layer, respectively:

$$\bar{\mathbf{u}}'_t + \epsilon \bar{\mathbf{u}}' \cdot \nabla \bar{\mathbf{u}}' + \nabla \eta = \mu^2 h \nabla \left(\frac{h}{3} \nabla \cdot \bar{\mathbf{u}}'_t - \frac{1}{2} \xi_{tt} \right) \quad (2.28)$$

$$\begin{aligned} \bar{\mathbf{u}}_t + \epsilon \bar{\mathbf{u}} \cdot \nabla \bar{\mathbf{u}} + (1-r) \nabla \xi + \nabla \eta = \\ \mu^2 \left[\frac{d}{2} \nabla \nabla \cdot (d \bar{\mathbf{u}}_t) - \frac{d^2}{6} \nabla \nabla \cdot \bar{\mathbf{u}}_t + r \left(\frac{h^2}{2} \nabla \nabla \cdot \bar{\mathbf{u}}'_t - h \nabla \xi_{tt} \right) \right] \end{aligned} \quad (2.29)$$

It is noted that the momentum equations retain $\mathcal{O}(\epsilon, \mu^2)$ terms and thus are weakly dispersive and weakly nonlinear in the sense of conventional Boussinesq equations; components of $\mathcal{O}(\epsilon \mu^2)$ and smaller are neglected in these equations. A similar approach is taken to derive the momentum equation in the lower layer using the interfacial dynamic boundary condition, (2.8). Equations (2.21), (2.22), (2.28) and (2.29) are essential equations for describing long surface and interfacial wave motion in a two-fluid system. The equations can readily be converted to dimensional form using (2.1):

$$(h + \eta - \xi)_t + \nabla \cdot [(h + \eta - \xi) \bar{\mathbf{u}}'] = 0 \quad (2.30)$$

$$\bar{\mathbf{u}}'_t + \bar{\mathbf{u}}' \cdot \nabla \bar{\mathbf{u}}' + g \nabla \eta = \frac{-h}{2} \nabla \xi_{tt} + \frac{h^2}{3} \nabla \nabla \cdot \bar{\mathbf{u}}'_t \quad (2.31)$$

$$\xi_t + \nabla \cdot [(d + \xi) \bar{\mathbf{u}}] = 0 \quad (2.32)$$

$$\bar{\mathbf{u}}_t + \bar{\mathbf{u}} \cdot \nabla \bar{\mathbf{u}} + g(1-r) \nabla \xi + gr \nabla \eta =$$

$$\frac{d}{2} \left[\nabla \nabla \cdot (d \bar{\mathbf{u}}_t) - \frac{d}{3} \nabla \nabla \cdot \bar{\mathbf{u}}_t \right] + r \left(\frac{h^2}{2} \nabla \nabla \cdot \bar{\mathbf{u}}'_t - h \nabla \xi_{tt} \right) \quad (2.33)$$

The derived equations reduce to classical nonlinear shallow water equations (e. g. Ball, 1964) in the non-dispersive limit ($\mu \rightarrow 0$). In the limit of $r \rightarrow 0$, the equations can be combined to reduce to the single layer Boussinesq equations (Peregrine, 1967). Using horizontal velocity at the interface for the lower layer and depth averaged velocity for the upper layer, Choi & Camassa (1996) derived a similar system via a different approach. The equations in Choi & Camassa (1996) are derived for arbitrary lower layer depth. If the limit of shallow lower layer, flat bottom (or slightly varying bottom where $|\nabla d| \leq \mathcal{O}(\mu)$), and free surface condition is applied, equations (2.30)-(2.33) reduce to the system of equations provided in Choi & Camassa (1996) (see their appendix). The long wave approximation allows for substituting the fully dispersive terms in polynomial of dispersion orders, and thus, significantly facilitates the application of the derived Boussinesq equations for numerical modeling. Derived equations can be modeled numerically in time or frequency domain.

It is noted that derivation of extended Boussinesq equations in the manner of Madsen *et al.* (1991) and Nwogu (1993) can also be accompanied following this general approach; this would allow for more accurate wave propagating modeling at frequencies beyond the weakly dispersive limit. However, our focus here is on the nonlinear processes in shallow water (small μ^2) rather than on enhancement of the model performance in intermediate-deep water.

D. Perturbation analysis

The Boussinesq-type equations derived above represent the comprehensive behavior of surface and interfacial waves as they propagate and evolve in time and space. Due to the nonlinearity of the system of equations, super and subharmonic generation of

modes occur. While numerical modeling of this set of equations in the time-domain can replicate this comprehensive view, it cannot do so in isolation from other effects. In this section, based on the derived model (2.30)-(2.33) and by using a perturbation approach, we directly focus on the transient evolution of the interacting surface and interfacial modes. For simplification, we assume that the depth of the layers, h and d are constant. It is more convenient to carry out the analysis in dimensional form.

The triad of resonance is composed of either two surface modes and a single interfacial mode (Ball, 1964) or a single surface mode and two interfacial modes (Hill & Foda, 1998; Jamali, 1998). The triad of waves in resonance satisfy the following kinematic conditions on wave frequencies and vector wave numbers:

$$\begin{aligned}\omega_1 \pm \omega_2 \pm \omega_3 &= 0 \\ \mathbf{k}_1 \pm \mathbf{k}_2 \pm \mathbf{k}_3 &= 0\end{aligned}\tag{2.34}$$

where ω_i and \mathbf{k}_i are the wave frequency and wave numbers respectively. The triad under consideration is composed of interfacial waves 1 and 2 and surface wave 3. Wave amplitudes are assumed to be slowly varying functions of time. The nonlinearity parameter, ϵ , is chosen as the small perturbation parameter and the following expansions are introduced for the variables,

$$\begin{aligned}\eta &= \eta_0 + \epsilon\eta_1 + \mathcal{O}(\epsilon^2), & \xi &= \xi_0 + \epsilon\xi_1 + \mathcal{O}(\epsilon^2) \\ \mathbf{u}' &= \mathbf{u}'_0 + \epsilon\mathbf{u}'_1 + \mathcal{O}(\epsilon^2), & \mathbf{u} &= \mathbf{u}_0 + \epsilon\mathbf{u}_1 + \mathcal{O}(\epsilon^2)\end{aligned}\tag{2.35}$$

These expansions are substituted in the governing equations (2.30)-(2.33) and the ordered equations up to the second order are obtained. We recall that the velocities are depth-averaged and drop the overbar signs hereafter.

1. Linear solution

The linear solution, $\mathcal{O}(1)$, is obtained using continuity equations, (2.21) and (2.22), and the linearized momentum equations of the two layers, (2.28) and (2.29),

$$(h + \eta_0 - \xi_0)_t + h \nabla \cdot \mathbf{u}'_0 = 0 \quad (2.36)$$

$$(\mathbf{u}'_0)_t + g \nabla \eta_0 + h \nabla \left(\frac{h}{3} \nabla \cdot (\mathbf{u}'_0)_t - \frac{1}{2} (\xi_0)_{tt} \right) = 0 \quad (2.37)$$

$$(\xi_0)_t + d \nabla \cdot \mathbf{u}_0 = 0 \quad (2.38)$$

$$\begin{aligned} (\mathbf{u}_0)_t + g(1-r) \nabla \xi_0 + gr \nabla \eta_0 - \left[\frac{d^2}{3} \nabla \nabla \cdot (\mathbf{u}_0)_t \right] + \\ r \left[\frac{h^2}{2} \nabla \nabla \cdot (\mathbf{u}'_0)_t - h (\nabla \xi_0)_{tt} \right] = 0 \end{aligned} \quad (2.39)$$

The eigensolution of the above homogeneous equations are the free propagating surface and interfacial modes. It is evident that dispersive terms are important in the linear solution. Surface and interface displacements and velocities are written as,

$$\eta_0 = \sum_{n=1}^3 \eta_{0n} = \sum_{n=1}^3 a_{0n}(T) e^{i\psi_n} + c.c., \quad (2.40)$$

$$\xi_0 = \sum_{n=1}^3 \xi_{0n} = \sum_{n=1}^3 b_{0n}(T) e^{i\psi_n} + c.c., \quad (2.41)$$

$$\mathbf{u}'_0 = \sum_{n=1}^3 \hat{\mathbf{u}}'_{0n} e^{i\psi_n} + c.c., \quad (2.42)$$

$$\mathbf{u}_0 = \sum_{n=1}^3 \hat{\mathbf{u}}_{0n} e^{i\psi_n} + c.c. \quad (2.43)$$

where $\psi_n = \mathbf{k}_n \cdot \mathbf{x} - \omega_n t$ is the phase function and *c.c.* denotes complex conjugate. Wave amplitudes, a_{0n} and b_{0n} , are slow functions of time. The variables η_{0n} , ξ_{0n} , $\hat{\mathbf{u}}'_{0n}$ and $\hat{\mathbf{u}}_{0n}$ represent the contribution of wave n on the surface and interface displacement and velocity fields of the upper and lower layer respectively. It is noted that the above definition of phase function requires constant wave numbers which are connected to the assumption of constant depth. Using equations (2.36)-(2.40), the linear velocities

are obtained as,

$$\hat{\mathbf{u}}_{0n} = \left(\frac{\omega_n}{k^2 d} \right) b_{0n} \mathbf{k}_n \quad (2.44)$$

$$\hat{\mathbf{u}}'_{0n} = \left(\frac{g - \frac{1}{2} h \omega^2}{\omega \left(1 + \frac{k^2 h^2}{3} \right) - g \frac{k^2 h}{\omega}} \right) b_{0n} \mathbf{k}_n \quad (2.45)$$

where $k = |\mathbf{k}|$ is the wave number magnitude. The relationship between the surface and interfacial amplitudes is also obtained,

$$a_{0n} = b_{0n} \left(\frac{1 - \frac{k^2 h^2}{6}}{1 - g \frac{h k^2}{\omega^2} + \frac{h^2 k^2}{3}} \right) \quad (2.46)$$

Equations (2.44)-(2.46) are the long wave asymptotes of the fully dispersive linear solutions (e.g. Lamb 1932). The eigenpair (ω, k) of a free surface or interfacial wave satisfy the dispersion relation associated with linear equations (2.36)-(2.40),

$$\begin{aligned} \omega^4 \left[\left(1 + \frac{k^2 h^2}{3} \right) \left(\frac{1 + \frac{k^2 d^2}{3}}{k d} \right) + r k h \left(1 + \frac{1}{12} k^2 h^2 \right) \right] \\ - \omega^2 g k \left[k h \left(\frac{1 + \frac{k^2 d^2}{3}}{k d} \right) + 1 + \frac{k^2 h^2}{3} \right] + (1 - r) g^2 k^3 h = 0 \end{aligned} \quad (2.47)$$

The above equation is the small kh and kd limit of the fully dispersive linear dispersion relation for a two-fluid system (see Lamb 1932). Equation (2.47) is a quartic function of ω and provides two independent sets of real roots for wave number magnitude, k . Each set of roots includes two real roots equal in magnitude and opposite in sign and represent the surface or interfacial mode of motion. Surface and interfacial roots of the dispersion relation and the possible triads of resonance are shown in Figure 2. For a given surface wave number, in triad 1 where ($OA = OB + BA$), one surface wave (S_1) is in resonant interactions with another surface wave (S_2) traveling in opposite direction and an interfacial wave (I_2) propagating in the same direction as S_1 . Although all waves are within the long wave limit ($kh \approx kd \leq \pi/10$), all the modes have comparable wave lengths in this triad. On the other

hand, in triad 2 ($OA = OC + CA$), a surface wave is in resonant interaction with two opposite-traveling interfacial waves and the interfacial modes are evidently short relative to the surface mode. Figure 3 illustrates the solutions to the dispersion relation, equation (2.47), compared to the fully dispersive expression (Lamb, 1932) and its non-dispersive shallow water limit. As expected, the solutions coalesce in very shallow water and the fully dispersive solution deviates from other solutions in higher frequencies ($kh > 0.75$). However, it is noted that the interfacial branch of weakly dispersive expression provides accurate approximation of the full dispersion relation in higher frequencies as well. In studying the interfacial wave behavior, it is more convenient to use equations (2.44)-(2.46) to write all the linear variables in terms of interfacial wave amplitude, b . The expressions for velocities in terms of the interfacial wave amplitudes can readily be expressed in terms of surface wave amplitudes using (2.46). Therefore, while the evolution of b is obtained, it is always possible to obtain the evolution of its surface signature. Conversely, the surface wave also has an interfacial signature. As mentioned, the linear solutions form the components of the forcing functions of the second order solution. In next section we analyze the second order solution, solvability condition and evolution of the wave amplitudes.

2. Second order solution and solvability condition

Applying the perturbation expansions (2.35), the second order system is obtained as,

$$(h + \eta_1 - \xi_1)_t + h\nabla \cdot \mathbf{u}'_1 = -\nabla \cdot [(\eta_0 - \xi_0)\mathbf{u}'_0] \quad (2.48)$$

$$(\mathbf{u}'_1)_t + g\nabla\eta_1 + h\nabla \left(\frac{h}{3}\nabla \cdot (\mathbf{u}'_1)_t - \frac{1}{2}(\xi_1)_{tt} \right) = -\mathbf{u}'_0 \cdot \nabla \mathbf{u}'_0 \quad (2.49)$$

$$(\xi_1)_t + d\nabla \cdot \mathbf{u}_1 = -\nabla \cdot (\xi_0 \mathbf{u}_0) \quad (2.50)$$

$$(\mathbf{u}_1)_t + g(1-r)\nabla\xi_1 + gr\nabla\eta_1 - \left[\frac{d^2}{3}\nabla\nabla \cdot (\mathbf{u}_1)_t \right] + \quad (2.51)$$

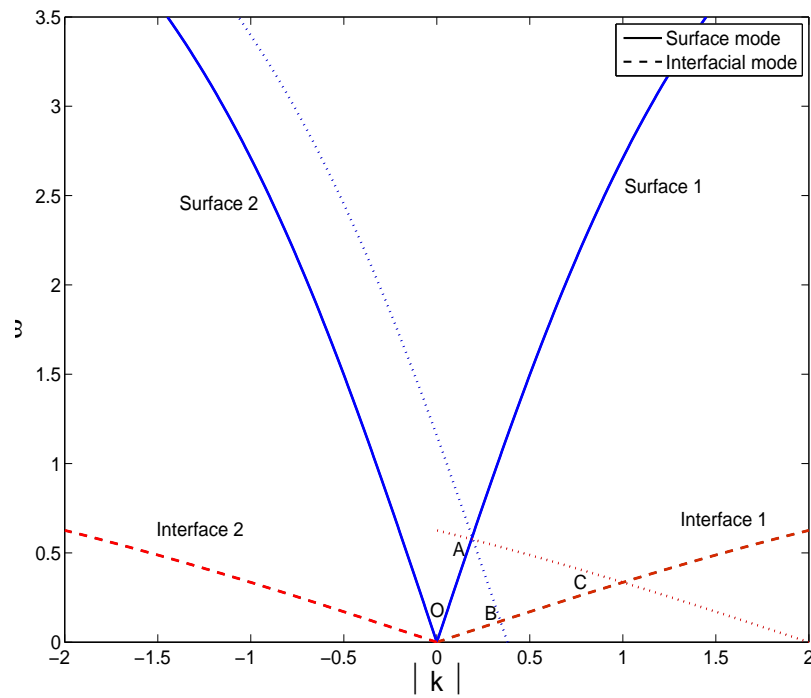


Fig. 2. (ω, k) roots of the dispersion relation and possible resonances among surface and interfacial modes. The dot lines are identical images of surface 2 and interface 2 which are shifted to pass point A.

$$r \left[\frac{h^2}{2} \nabla \nabla \cdot (\mathbf{u}'_1)_t - h(\nabla \xi_1)_{tt} \right] = -\mathbf{u}_0 \cdot \nabla \mathbf{u}_0 \quad (2.52)$$

The linear solutions obtained in the previous section are now the components of the forcing functions for the second order solution. Quadratic nonlinear interactions among the linear components result in a secular term in the second order solution. As the homogeneous system of equations, corresponding to the linear system, has a nontrivial solution, the above inhomogeneous second order system will not have a nonsecular solution unless the components of forcing functions satisfy a certain solvability condition.

It is convenient to combine the above equations to eliminate the linear terms of free surface and interface displacements in favor of velocities in the fluid layers (e. g. Dingemans, 1993). By cross differentiation, four equations reduce to two equations expressed in terms of velocities,

$$\begin{aligned} (\mathbf{u}'_1)_{tt} - gd\nabla\nabla \cdot \mathbf{u}_1 - gh\nabla\nabla \cdot \mathbf{u}'_1 - \frac{h^2}{3} \nabla\nabla \cdot \mathbf{u}'_{tt} - \frac{hd}{2} \nabla\nabla \cdot \mathbf{u}_{tt} = \\ -(\mathbf{u}'_0 \cdot \nabla \mathbf{u}'_0)_{tt} + g\nabla\nabla \cdot (\xi_0 \mathbf{u}_0 + \eta \mathbf{u}'_0 - \xi_0 \mathbf{u}'_0) + \frac{h}{2} \nabla\nabla \cdot (\xi_0 \mathbf{u}_0)_{tt} \end{aligned} \quad (2.53)$$

$$\begin{aligned} (\mathbf{u}_1)_{tt} - gd\nabla\nabla \cdot \mathbf{u}_1 - grh\nabla\nabla \cdot \mathbf{u}'_1 - d \left(\frac{d}{3} + rh \right) \nabla\nabla \cdot (\mathbf{u}_1)_{tt} - r \frac{h^2}{2} \nabla\nabla \cdot (\mathbf{u}'_1)_{tt} = \\ -(\mathbf{u}_0 \cdot \nabla \mathbf{u}_0)_{tt} + g\nabla\nabla \cdot (\xi_0 \mathbf{u}_0) + gr\nabla\nabla \cdot ([\eta - \xi] \mathbf{u}'_0) + rh\nabla\nabla \cdot (\xi_0 \mathbf{u}_0)_{tt} \end{aligned} \quad (2.54)$$

Equations (2.53) and (2.54) are used hereafter in the analysis. It can be shown that the determinant of the coefficient matrix of above equations is the dispersion relation, (2.47), and thus equals zero. Inserting (2.35) in above expression gives,

$$\begin{aligned} (\mathbf{u}'_1)_{tt} - gd\nabla\nabla \cdot \mathbf{u}_1 - gh\nabla\nabla \cdot \mathbf{u}'_1 - \frac{h^2}{3} \nabla\nabla \cdot \mathbf{u}'_{tt} - \frac{hd}{2} \nabla\nabla \cdot \mathbf{u}_{tt} = \mathcal{F}_1 \quad (2.55) \\ (\mathbf{u}_1)_{tt} - gd\nabla\nabla \cdot \mathbf{u}_1 - grh\nabla\nabla \cdot \mathbf{u}'_1 - d \left(\frac{d}{3} + rh \right) \nabla\nabla \cdot (\mathbf{u}_1)_{tt} - \end{aligned}$$

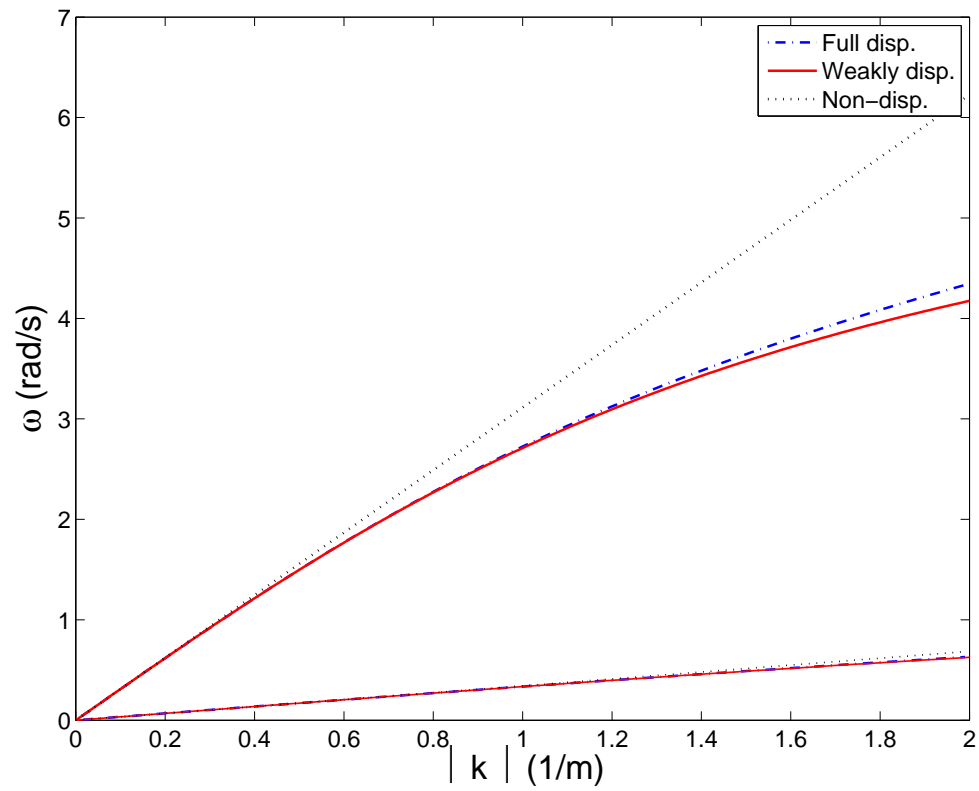


Fig. 3. Comparison of surface and interfacial roots of fully dispersive, weakly dispersive and non-dispersive dispersion relations. The slower branches (with significantly smaller ω for a given k) represent the interfacial roots.

$$r \frac{h^2}{2} \nabla \nabla \cdot (\mathbf{u}'_1)_{tt} = \mathcal{F}_2 \quad (2.56)$$

where \mathcal{F}_1 and \mathcal{F}_2 are the forcing functions formed of coupling of the linear terms in equations (2.53)-(2.54). The difference between Stokes and Boussinesq scaling stems from the disparity in scales of motion between horizontal and vertical velocities. In the Boussinesq scaling, the vertical motion is assumed to be one order smaller than the horizontal motion. In the Boussinesq equations, there is a balance between nonlinearity and dispersiveness. Therefore, while the linear solutions are long wave asymptotes of the fully dispersive solutions, the nonlinear terms in equations differ. The linear solutions, (2.40)-(2.43), are inserted in the above expressions for forcing functions, and \mathcal{F}_1 and \mathcal{F}_2 are rewritten as,

$$\mathcal{F}_1 = \sum_{n=1}^3 \left(\mathbf{S}_n \frac{db_{0n}}{dt} e^{i\psi_n} \right) + \sum_{m=1}^3 \sum_{n=m}^3 \left(\mathbf{T}_{mn} b_{0m} b_{0n} e^{i(\psi_m + \psi_n)} + \mathbf{T}_{\bar{m}n} \bar{b}_{0m} b_{0n} e^{i(\psi_n - \psi_m)} \right) + c.c. \quad (2.57)$$

$$\mathcal{F}_2 = \sum_{n=1}^3 \left(\mathbf{S}'_n \frac{db_{0n}}{dt} e^{i\psi_n} \right) + \sum_{m=1}^3 \sum_{n=m}^3 \left(\mathbf{T}'_{mn} b_{0m} b_{0n} e^{i(\psi_m + \psi_n)} + \mathbf{T}'_{\bar{m}n} \bar{b}_{0m} b_{0n} e^{i(\psi_n - \psi_m)} \right) + c.c. \quad (2.58)$$

where \mathbf{S}_n , \mathbf{S}'_n , \mathbf{T} and \mathbf{T}' are functions of layer thicknesses (h and d), surface wave frequency (ω_3), surface wave number (\mathbf{k}_3), the linear solutions for velocities in the layers (from equations 2.44-2.45), density ratio (r) and relative magnitude of surface wave amplitude to its interfacial signature (from 2.46). All these parameters are obtained from the dispersion relation and linear solutions. From the expressions for the forcing functions, it is evident that the second order solution for \mathbf{u} will have the following form,

$$\mathbf{u}_1 = \sum_{m=1}^3 \sum_{n=m}^3 \left(\widehat{\mathbf{u}}_{1mn} + \widehat{\mathbf{u}}_{1\bar{m}n} \right) + c.c. \quad (2.59)$$

where $\widehat{\mathbf{u}}_{1mn}$, and $\widehat{\mathbf{u}}_{1\bar{m}n}$ are the second order velocity component proportional to

$e^{i(\psi_m+\psi_n)}$ and $e^{i(\psi_n-\psi_m)}$, respectively. Velocity \mathbf{u}'_1 is written similarly. We now analyze the evolution of interfacial wave 2 as an example. The analysis for other waves in resonance are carried out similarly. Regarding the resonance conditions, (2.34), the second order component in the velocity associated with interfacial wave 2 is $\widehat{\mathbf{u}}_{1\bar{1}3}$. The combined equations, (2.55) and (2.56), are coupled equations with two degrees of freedom. This system should have a finite solution for uniformity of the perturbation expansions (2.35). To allow this, the aforementioned secularity of the second order solution is removed by applying a solvability condition: The forcing functions should be orthogonal to the solution of the adjoint system. It is noted that the homogeneous system is not self-adjoint. For interfacial wave 2, equations (2.55) and (2.56) become,

$$p_{11} \widehat{u}'_{\bar{1}3} + p_{12} \widehat{u}_{\bar{1}3} = S_2 \frac{db_{02}}{dt} + T_{\bar{1}3} b_{01}^- b_{03} + N.R.T \quad (2.60)$$

$$p_{21} \widehat{u}'_{\bar{1}3} + p_{22} \widehat{u}_{\bar{1}3} = S'_2 \frac{db_{02}}{dt} + T'_{\bar{1}3} b_{01}^- b_{03} + N.R.T \quad (2.61)$$

where $\widehat{\mathbf{u}}_{\bar{1}3} = \widehat{u}_{\bar{1}3} \mathbf{k}_2$, $\mathbf{S}_{\bar{1}3} = S_{\bar{1}3} \mathbf{k}_2$, $\mathbf{T}_{\bar{1}3} = T_{\bar{1}3} \mathbf{k}_2$ and so on. Coefficients p are given as,

$$p_{11} = -\omega_2^2 \left(1 + \frac{h^2}{3} k_2^2 \right) + ghk_2^2, \quad p_{12} = dk_2^2 \left(g - \frac{h}{2} \omega_2^2 \right) \quad (2.62)$$

$$p_{21} = rhk_2^2 \left(g - \frac{h}{2} \omega_2^2 \right), \quad p_{22} = -\omega_2^2 \left[1 + \mu^2 dk_2^2 \left(\frac{d}{3} + rh \right) \right] + gdk_2^2 \quad (2.63)$$

and $N.R.T$ denotes terms which oscillate at a non-resonant phase. As the triad of waves are in exact resonance, there will be no near-resonant terms. The velocities $\widehat{\mathbf{u}}'_{\bar{1}3}$ and $\widehat{\mathbf{u}}_{\bar{1}3}$ are the unknowns in these algebraic equations. In matrix form:

$$\begin{bmatrix} p_{11} & p_{12} \\ p_{21} & p_{22} \end{bmatrix} \begin{bmatrix} \widehat{u}'_{\bar{1}3} \\ \widehat{u}_{\bar{1}3} \end{bmatrix} = \begin{bmatrix} f_1 \\ f_2 \end{bmatrix}$$

or $\mathbf{P} \widehat{\mathbf{u}} = \mathbf{F}$. $|\mathbf{P}| = 0$ and in order for the above set of equations to have a solution,

the forcing matrix \mathbf{F} should be orthogonal to the solution of the adjoint system \mathcal{X} ,

$$\mathbf{F}^T \mathcal{X} = 0 \quad (2.64)$$

where \mathbf{F}^T is the transpose of forcing matrix. Inserting values for p_{ij} and f_i from (2.60), (2.61), (2.62) and (2.63) in the above equation yields the evolution equation of the amplitude of the interfacial wave 2.

The expressions for the interaction coefficients, α 's, are rather lengthy but straightforward to calculate. These coefficients govern the energy transfer among the interacting modes. Here we provide the interaction coefficient for interfacial wave 2 and the other two coefficients can be obtained similarly. T_{13} and T'_{13} in equations (2.57) and (2.58) are given by,

$$\begin{aligned} T_{13} = & -\omega_2 \widehat{u}'_{01} \widehat{u}'_{03} (\mathbf{k}_1 \cdot \mathbf{k}_3) + g [-(\widehat{u}_{01} k_1^2 + \widehat{u}_{03} k_3^2) - (\widehat{u}_{03} - \widehat{u}_{01})(\mathbf{k}_1 \cdot \mathbf{k}_3) - \\ & \widehat{\eta}_{01} \widehat{u}'_{03} k_3^2 - \widehat{\eta}_{03} \widehat{u}'_{01} k_1^2 + (\widehat{\eta}_{01} \widehat{u}'_{03} + \widehat{\eta}_{03} \widehat{u}'_{01})(\mathbf{k}_1 \cdot \mathbf{k}_3)] + \widehat{u}'_{01} k_1^2 + \widehat{u}'_{03} k_3^2 - \\ & (\widehat{u}'_{03} - \widehat{u}'_{01})(\mathbf{k}_1 \cdot \mathbf{k}_3)] + \frac{h}{2} \omega_2^2 [\widehat{u}_{01} k_1^2 + \widehat{u}_{03} k_3^2 - (\widehat{u}_{03} - \widehat{u}_{01})(\mathbf{k}_1 \cdot \mathbf{k}_3)] \quad (2.65) \end{aligned}$$

$$\begin{aligned} T'_{13} = & -\omega_2 \widehat{u}_{01} \widehat{u}_{03} (\mathbf{k}_1 \cdot \mathbf{k}_3) + g [(\widehat{u}_{01} k_1^2 + \widehat{u}_{03} k_3^2) - (\widehat{u}_{03} - \widehat{u}_{01})(\mathbf{k}_1 \cdot \mathbf{k}_3)] - \\ & gr [\widehat{\eta}_{01} \widehat{u}'_{03} k_3^2 + \widehat{\eta}_{03} \widehat{u}'_{01} k_1^2 - (\widehat{\eta}_{01} \widehat{u}'_{03} - \widehat{\eta}_{03} \widehat{u}'_{01})(\mathbf{k}_1 \cdot \mathbf{k}_3)] + \\ & gr [\widehat{u}'_{01} k_1^2 + \widehat{u}'_{03} k_3^2 - (\widehat{u}'_{03} - \widehat{u}'_{01})(\mathbf{k}_1 \cdot \mathbf{k}_3)] + rh \omega_2^2 [\widehat{u}_{01} k_1^2 + \widehat{u}_{03} k_3^2 - \\ & (\widehat{u}_{03} - \widehat{u}_{01})(\mathbf{k}_1 \cdot \mathbf{k}_3)] \quad (2.66) \end{aligned}$$

where ω_2 and k_i are obtained from dispersion relation (2.47). \widehat{u}_{0n} , \widehat{u}'_{0n} and $\widehat{\eta}_{0n}$ are obtained from linear solutions, (2.44), (2.45) and (2.46). In addition, linear coefficients S_n and S'_n are given by:

$$S_n = 2i\omega_n \left[\widehat{u}'_{0n} \left(\frac{h^2}{3} k_n^2 + 1 \right) + \frac{dh}{2} k_n^2 \widehat{u}_{0n} \right] \quad (2.67)$$

$$S'_n = 2i\omega_n \left(\widehat{u}_{0n} \left[1 + d \left(\frac{d}{3} + rh \right) k_n^2 \right] + \frac{rh^2}{2} k_n^2 \widehat{u}'_{0n} \right) \quad (2.68)$$

Knowing the required coefficients and p_{ij} from equations (2.62) and (2.63), the interaction coefficient associated with interfacial wave 2, α_2 , is given by,

$$\alpha_2 = \frac{1}{\hat{\eta}_{03}} \left(\frac{\frac{p_{11}+p_{12}}{p_{21}+p_{22}} T'_{13} - T_{13}}{S_2 - \frac{p_{11}+p_{12}}{p_{21}+p_{22}} S'_2} \right) \quad (2.69)$$

Similar approach is carried out and the evolution equations for the interfacial wave 1 and surface wave 3 are obtained. Therefore, the system of coupled evolution equations of the interacting harmonics is given by,

$$\frac{db_{01}}{dt} = \alpha_1 a_{03} b_{02}^-, \quad \frac{db_{02}}{dt} = \alpha_2 a_{03} b_{01}^-, \quad \frac{da_{03}}{dt} = \alpha_3 b_{01} b_{02} \quad (2.70)$$

where α_i are the interaction coefficients and found to be purely imaginary. The above set have exact solutions in terms of Jacobian elliptic functions (Mei & Unluata, 1972). However, it is straightforward to solve the evolution equations numerically. The calculation of interaction coefficients is carried out by Mathematica®[®], a symbolic computational software. One advantage of the present approach over the fully dispersive problem is the simple nature of the interaction coefficients, which reduces the required computation time. Temporal evolution of the harmonic amplitudes in a typical case is illustrated in Figure 4. The parameters in this case are, $T = 7s$, $H = 1m$, $d = 0.2m$, $r = 0.926$, $\theta = 70$, $\epsilon = 0.01$. It is seen that the interfacial waves grow in time, approach a maximum and reduce in amplitude until they lose energy; in contrast, the surface wave loses its energy from the initial stage. This pattern repeats periodically. Since inviscid flows are assumed, the total energy exchanged among the modes is conserved.

It is instructive to calculate the growth rate of amplitude harmonics using the derived evolution equations. The initial amplitude of interfacial waves are assumed such that $b_{01}(0) = b_{02}(0) \ll a_{03}(0)$. By cross differentiation, the initial growth rate of interfacial wave 2 is obtained and the approximate solution for the amplitude is

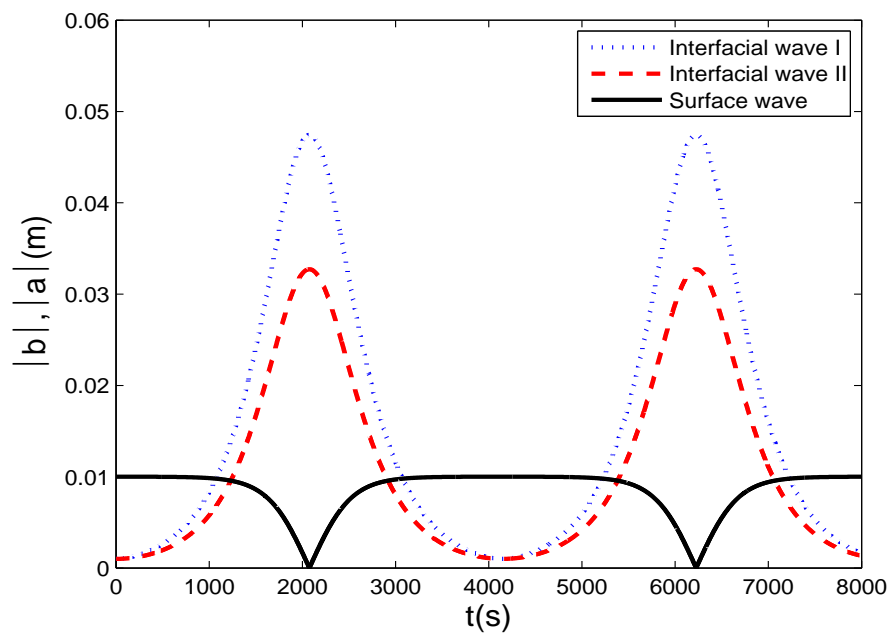


Fig. 4. Temporal variation of dimensionless amplitudes of interacting surface and interfacial modes. $h = 0.8m$, $d = 0.2m$, $r = 0.926$, $T = 7s$, $\theta = 70$, $a_0 = 0.01m$, $b_0 = 0.001m$

given by,

$$b_{02} \sim \exp\{\pm \sqrt{\alpha_2 \alpha_3 |b_{01}|^2 + \alpha_1 \bar{\alpha}_2 |a_{03}|^2} t\} \quad (2.71)$$

Similar expressions can be obtained for interfacial wave 2 and surface wave. It is evident that the behavior of harmonics amplitudes depend on the signs of the interaction coefficients as well as initial amplitudes of modes. If α_1 and α_2 have the same sign and α_3 has the opposite sign, the interfacial mode amplitudes grow exponentially resulting in instability at the interface while the surface wave amplitude shows oscillatory behavior. On the other hand, if the interfacial waves have opposite signs, all the harmonic amplitudes will merely oscillate and exhibit no growth. In such condition, the modes conduct suitable phase shifts to conserve energy in a phase period. If the variation of surface wave amplitude with time is neglected (corresponding to Hill & Foda, 1996; Jamali, 1998), the solution of the interfacial wave amplitudes becomes,

$$b_{01}, b_{02} \sim \exp\{\pm |a_{03}| \sqrt{\alpha_1 \bar{\alpha}_2} t\} \quad (2.72)$$

3. Viscous effects

In this section, the effects of lower layer viscosity is added to the analysis. Fluid viscosity affects the interfacial instabilities through two different mechanisms. The increase in viscosity will lead to stronger velocity shear at the interface and the increased shear can potentially lead to Kelvin-Helmholtz instabilities (e.g. see Turner, 1973). The other mechanism is viscous attenuation of wave amplitude (e.g. Davis & Acrivos 1967). In a slightly viscous system, the latter mechanism is dominant. On the other hand, the governing equations, (2.2)-(2.9), are based on an inviscid formulation, and thus the effect of viscosity should be sufficiently weak that the underlying assumption of irrotational flows is not violated. Consequently, the system under consideration here resembles clear water overlying lightly viscous mud (e.g.

mud assumed as newtonian fluid).

The attenuation of waves in two-layer systems has been widely studied with primary focus on surface waves. Dalrymple & Liu (1978), Hsiao & Shemdin (1980) and Macpherson (1980) among others, assuming different rheologies for the sediment, investigated the surface wave damping due to viscous dissipation in the lower sediment layer. Davis & Acrivos (1967) studied the damping of interfacial instabilities. They showed that in the case of weakly viscous fluids, the dissipation rate of wave energy can be superposed to the evolution equations of the harmonics. More recently, Hill (2002) and Troy & Koseff (2006) provided a more comprehensive treatment of the damping of interfacial waves in a flume. In this section we consider the damping effects in both surface and interfacial waves. Consequently, the inviscid set of evolution equations, (2.70) is modified as,

$$\frac{db_{01}}{dt} = \alpha_1 a_{03} b_{02}^- - \beta_1 b_{01}, \quad \frac{db_{02}}{dt} = \alpha_2 a_{03} b_{01}^- - \beta_2 b_{02}, \quad \frac{da_{03}}{dt} = \alpha_3 b_{01} b_{02} - \beta_3 a_{03} \quad (2.73)$$

where β_i is the dimensionless temporal damping rate of wave i . Inclusion of β in evolution equations will result in exponential damping effect on the harmonic amplitudes. If the viscosity of the upper layer is negligible comparing to the lower layer, corresponding to clear water over fluidized sediment, the damping rate can be obtained from Macpherson (1980). In it, a complex dispersion relation was provided, quartic in wave number and wave frequency, which accounts for viscoelasticity of the lower layer. Although only the attenuation of the surface mode was discussed, the derived dispersion relation can be solved numerically to obtain the damping rate of interfacial waves. Since the focus of the present study is on temporal attenuation, we feed the complex dispersion relation with wave numbers calculated from the inviscid dispersion relation, (2.47), and obtain the complex wave frequency. Therefore, if (ω, k) is an eigenpair in (2.47), (ω', k) is the eigenpair in the viscous dispersion

relation. Frequency ω' is a complex number where $Re[\omega'] \simeq \omega$, and $Im[\omega'] = \beta$ is the damping coefficient. Figure 5 illustrates the temporal variation of modes in viscous interaction. The parameters are the same as the inviscid case in Figure 4 with addition of viscosity $\nu = 3 \times 10^{-6} m^2/s$. It is seen in the figure that surface wave loses energy from the initial step of resonance. Interfacial wave 1 gains energy and exhibits initial growth, reach a maximum amplitude and undergo strong viscous attenuation thereafter but interfacial wave 2 is suppressed due to viscosity and is not excited.

By incorporation of viscous effects in both surface and interfacial waves evolution equations, we have made a more complete treatment of surface wave damping than previous studies; in addition to the direct damping of surface mode due to lower layer viscosity (represented by $-\beta_3 a_{03}$ in 2.73), some of surface wave energy is redirected to interfacial modes due to nonlinear interactions and is lost through viscous attenuation of interfacial waves (represented by $-\beta_1 b_{01}$ and $-\beta_2 b_{02}$ in equation (2.73)).

As in the inviscid case, by cross-differentiation of the viscous evolution equations, (2.73), the amplitudes of the harmonics are obtained as,

$$b_{02} \sim e^{\gamma' t} \quad (2.74)$$

where

$$\gamma' = \frac{-\beta_2}{2} \pm \left(\alpha_1 \alpha_3 |b_{01}|^2 + \alpha_1 \bar{\alpha}_2 |a_{03}|^2 + \beta_2^2 \right)^{\frac{1}{2}} \quad (2.75)$$

The expressions for interfacial wave 1 and the surface wave are similar. It is clear that the addition of viscosity leads to addition of exponential decay to harmonic amplitudes. In the next section, we investigate the influence of important parameters on resonant interaction.

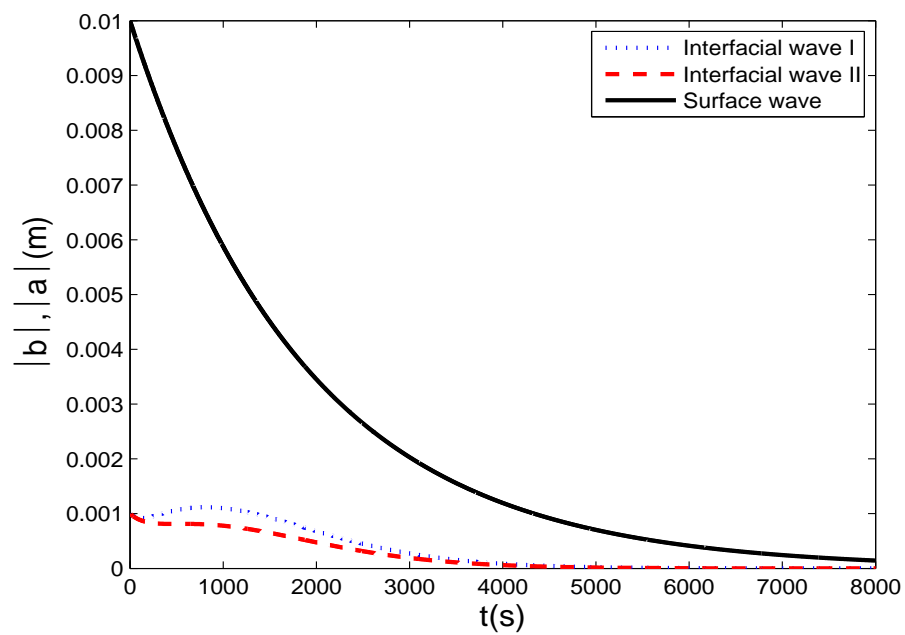


Fig. 5. Temporal variation of dimensionless amplitudes of interacting surface and interfacial modes. $h = 0.8m$, $d = 0.2m$, $r = 0.926$, $T = 7s$, $\theta = 70^\circ$, $\nu = 3 \times 10^{-6}m^2/s$, $a_0 = 0.01m$, $b_0 = 0.001m$

E. Parametric study

In this section, the important parameters controlling the resonant interaction are studied numerically. Variation of these parameters is translated into the variation of the interaction and damping coefficients in evolution equations of the amplitudes (equations 2.70). Directional angle of the interfacial waves, viscosity of the lower layer, surface wave frequency and amplitude, relative thickness of the layers as well as the density difference of the layers influence the energy exchange among the harmonics. In a fluid of constant total depth, H , these dimensionless parameters are mathematically independent and describe the problem,

$$\theta, \quad \nu/\sqrt{gH^3}, \quad a_0/H, \quad k_0H, \quad h/H, \quad r = \rho'/\rho \quad (2.76)$$

We investigate the influence of the parameters by varying one parameter at a time. As before, the parameters in the base example are selected as $H = 1m$, $d = 0.2m$, $r = 0.926$, $T = 7s$, $\theta = 80^\circ$, $\nu = 3 \times 10^{-6}m^2/s$ with initial wave amplitudes of $a_0 = 0.01m$, $b_0 = 0.001m$.

As the directional angle, θ , is an independent parameter, mathematically there are an infinite number of interfacial wave pairs that can be in resonance with a given surface wave. Among these possible instabilities, the one which exhibits maximum growth rate is most likely to be observed. Therefore, the growth rate of the interfacial waves with variation of θ is evaluated by equation (2.71). Although the initial amplitudes of the waves affect their growth rate, the maximum amplitude gained by the interfacial waves is independent of their initial magnitudes (Tahvildari & Jamali, 2009). Figure 6 illustrates the variation of the initial growth rate, γ , against directional angle. As θ is reduced, the y component of the second interfacial wave (I_2) decreases while its x component becomes larger in magnitude in the opposite direction

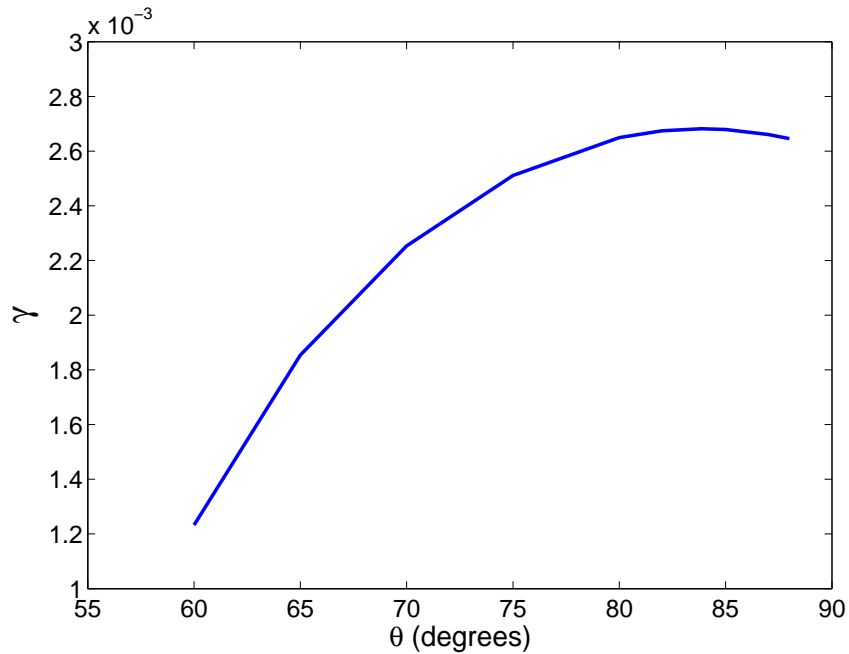


Fig. 6. Variations of initial growth rate of interfacial wave I against θ . $h = 0.8m$, $d = 0.2m$, $r = 0.926$, $T = 7s$, $a_0 = 0.01m$, $b_0 = 0.001m$

of the surface wave. When one of the interfacial waves and the surface wave are parallel and plane ($\theta = 0$) the second interfacial wave propagates in the same plane but in opposite direction. With the aforementioned specifications, the interfacial waves do not grow until $\theta \simeq 67^\circ$ and have maximum growth rate when the directions of interfacial wave pair are symmetric and form an angle of about 84° with respect to the surface wave. Figure (7) shows this configuration. S_1 denotes the surface wave and I_1 and I_2 represent the interfacial waves. In this condition (referred to as the symmetric case hereafter), the two interfacial wave amplitudes become identical in amplitude and phase.

Since the growth rate of the wave amplitudes is a function of wave forcing and the damping coefficient is independent of directional angle, the influence of directional angle can be observed in the inviscid analysis. As the symmetric pair is the most

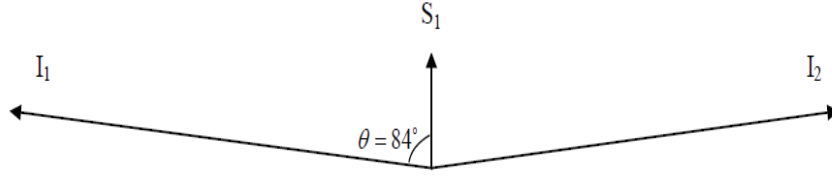


Fig. 7. Symmetric configuration of interfacial waves exhibits maximum growth rate; $\theta = 84^\circ$ when $h = 0.8m$, $d = 0.2m$, $r = 0.926$ and $T = 7s$, $a_0 = 0.01m$, $b_0 = 0.001m$

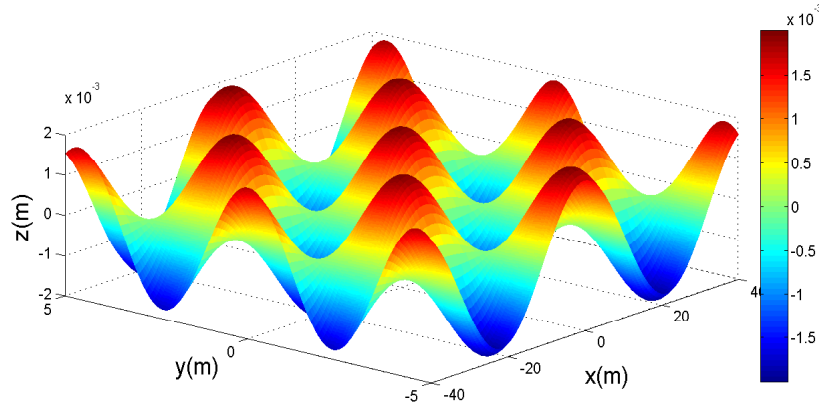


Fig. 8. Three-dimensional pattern of nearly-standing interfacial waves. $\theta = 84^\circ$, $h = 0.8m$, $d = 0.2m$, $r = 0.926$ and $T = 7s$, $a_0 = 0.01m$, $b_0 = 0.001m$

likely to occur, its conditions ($\omega_1 = \omega_2$ and $|\mathbf{k}_1| = |\mathbf{k}_2|$) will be used in the rest of the parametric studies ($b_1 = b_2 = b$). The three dimensional nearly-standing wave pattern at the interface is illustrated in Figure (8).

Temporal variation of the wave amplitudes with alteration of viscosity in the lower layer is illustrated in Figure 9. Based on the viscosity, the interfacial waves grow to reach a maximum amplitude and attenuate afterwards. Surface wave undergoes attenuation likewise. As expected, with increase in lower layer viscosity, the rates of attenuation of surface and interfacial waves increase. Figure 10 shows the variation of damping rate against lower layer viscosity. As mentioned by Macpherson (1980), the rate of attenuation of surface wave appears to be smaller than that of the interfacial

waves. It is noted that in the present approach, damping rate is independent of forcing and furthermore, all the parameters except θ influence the damping coefficient. In the present example, when viscosity increases to $1.3 \times 10^{-5} m^2/s$, interfacial waves exhibit no growth indicating that the forcing from the surface wave is inadequate to overcome viscous damping. To allow the generation of interfacial waves for a wide range of values of the other parameters, we hereafter assume that the lower layer has a viscosity of $3 \times 10^{-6} m^2/s$.

Figure 11 illustrates the evolution of interfacial waves and surface wave amplitudes for various values of surface wave frequency. It is interesting to note that although the initial growth rate is larger when $T = 45s$, the maximum amplitude of interfacial wave is larger at $T = 8s$. Therefore, the interfacial wave pair exhibiting maximum initial growth rate does not necessarily acquire maximum amplitude.

For various surface wave frequencies, the growth rate of the interfacial wave is illustrated in Figure 12. At $k_3H = 0.21206$ the growth rate is maximum. The damping rate of the surface and interfacial waves are shown in Figure 13. Dimensionless surface wave number, k_3H , is used as a measure of surface wave frequency (T_3). Surface wave attenuation rate appears to be smaller than the interfacial damping rate for all the frequencies and all waves undergo weaker damping as the surface wave (and consequently the interfacial waves) becomes deeper. It is also seen that with the increase in surface wave frequency, the attenuation and viscous growth rate (equations 2.74) of the interfacial wave decrease regardless of the wave length.

Stratification has significant effects on generation of interfacial waves. Figure 14 shows the variation of interacting interfacial and surface modes with variation of density ratio of $1.00 < 1/r \leq 1.20$. Variation of growth and attenuation rate of interfacial waves and the attenuation rate of surface wave with density ratio are illustrated in Figure 15. As shown, the variation of density ratio does not significantly affect

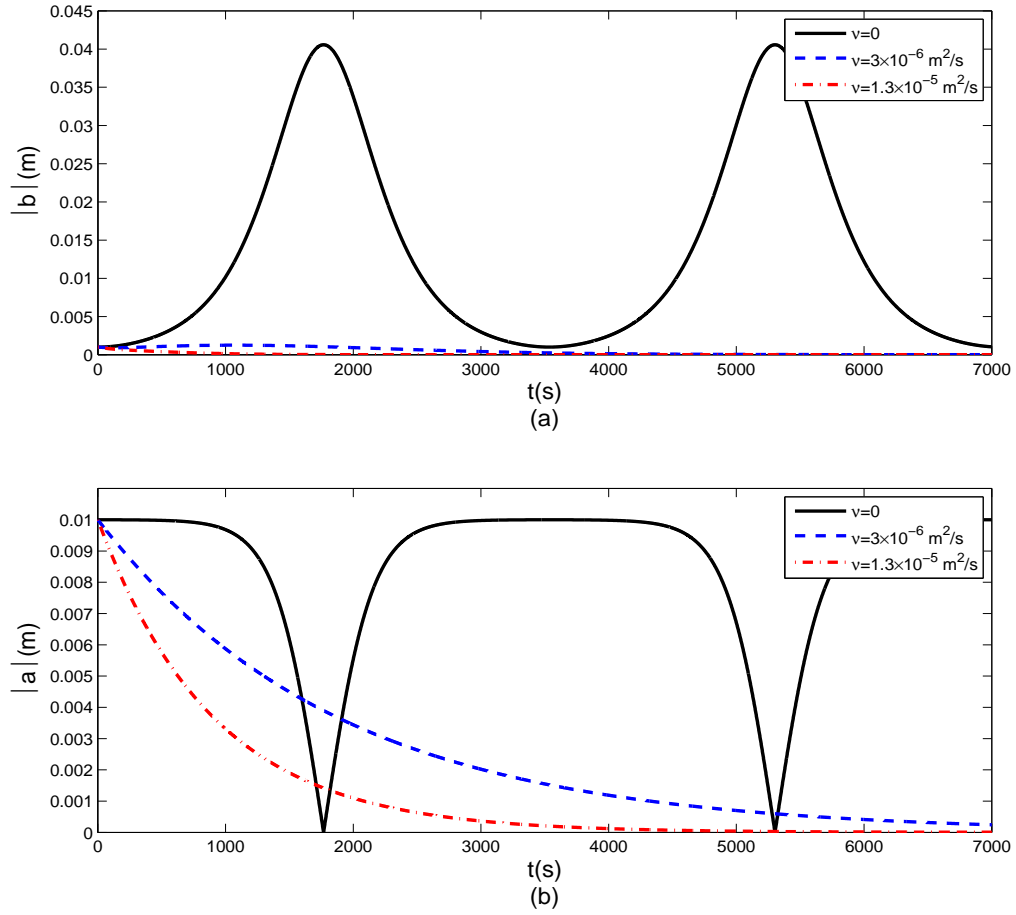


Fig. 9. Temporal variation of (a) interfacial wave amplitude, (b) surface wave amplitude for different values of lower layer viscosity ν . $h = 0.8m$, $d = 0.2m$, $r = 0.926$, $T = 7s$, $a_0 = 0.01m$, $b_0 = 0.001m$

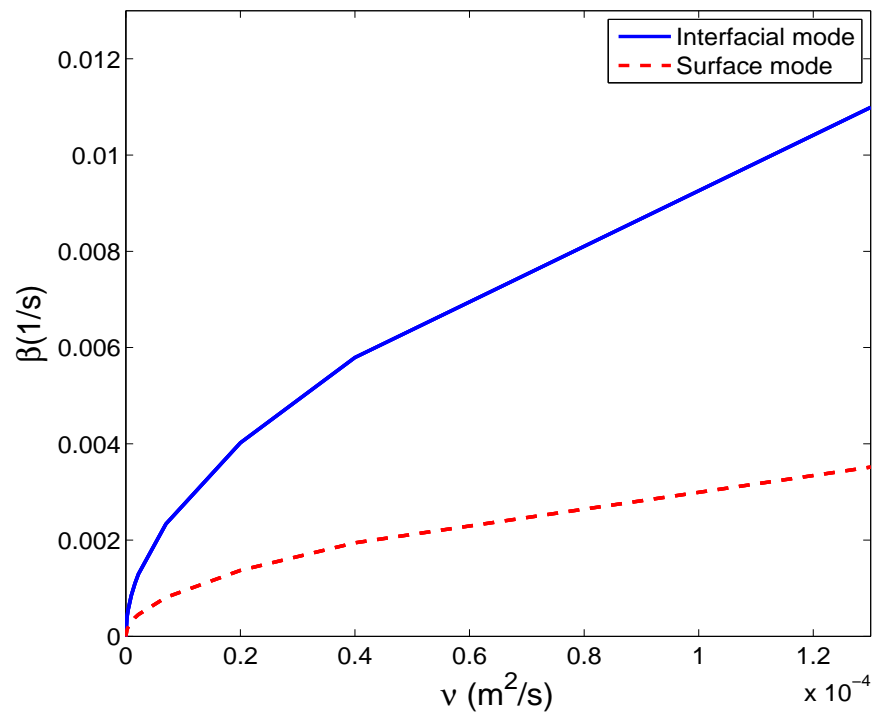


Fig. 10. Variation of temporal damping rate, β , against viscosity ν . $h = 0.8m$, $d = 0.2m$, $r = 0.926$, $T = 7s$, $a_0 = 0.01m$, $b_0 = 0.001m$

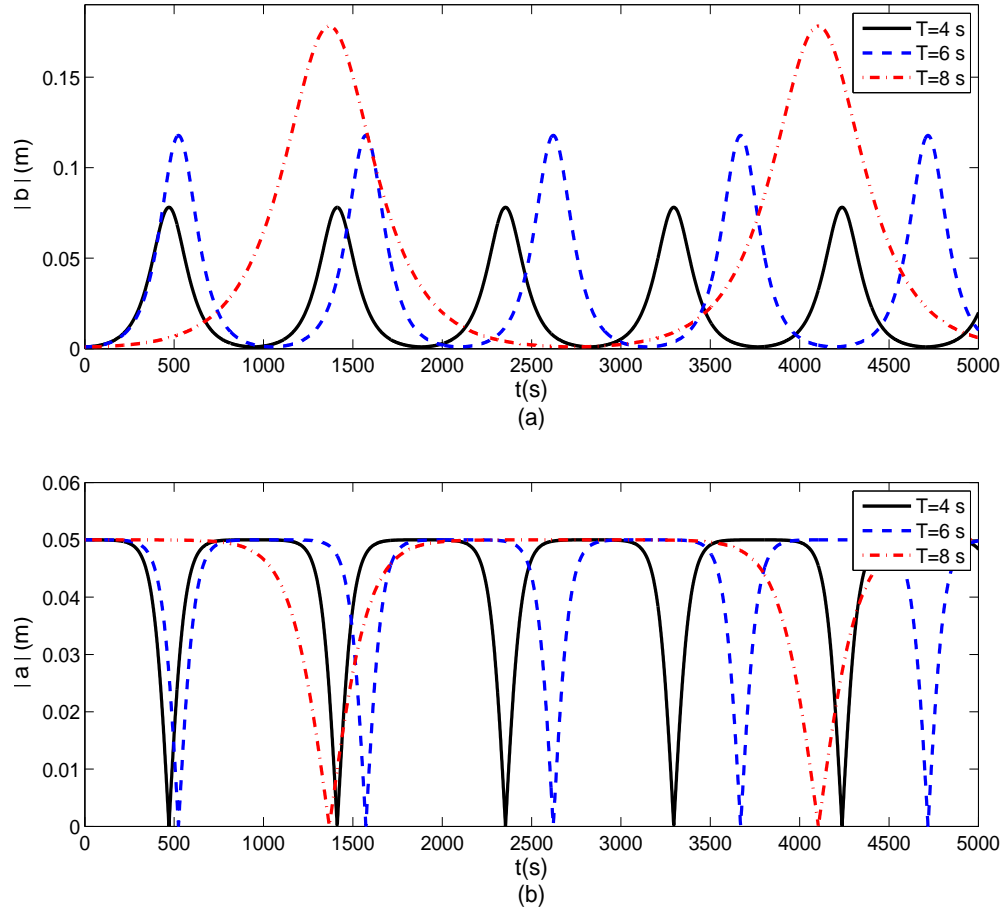


Fig. 11. Temporal variation of (a) interfacial wave amplitude, (b) surface wave amplitude for values of surface wave frequency T_3 . $h = 0.8m$, $d = 0.2m$, $r = 0.926$, $a_0 = 0.01m$, $b_0 = 0.001m$

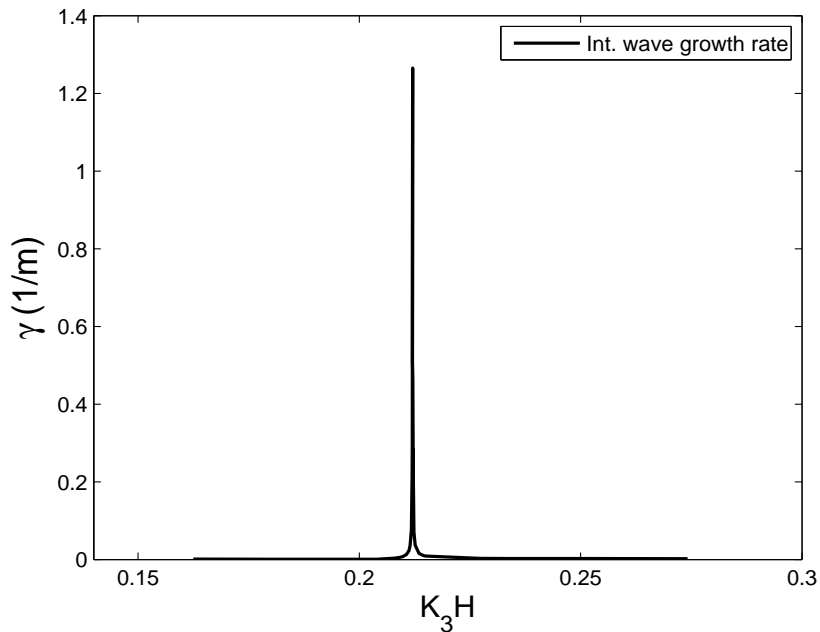


Fig. 12. Magnitudes of growth rate of interfacial mode against $k_3 H$. $h = 0.8m$, $d = 0.2m$, $r = 0.926$, $a_0 = 0.05m$.

the surface wave dissipation; surface wave damping rate slightly decreases in higher density gradients. As $1/r$ increases within the range of 1 to 1.05, the growth and dissipation rate of the interfacial wave increase dramatically. With further increase in the density gradient up to $1/r = 1.20$, the attenuation rate mildly increases approaching a constant. In this range, the damping and forcing effects balance and the growth rate approaches a constant as well.

Figure 16 shows the time variation of the surface and interfacial wave amplitude with alteration of the upper layer depth, h . As mentioned, the total depth, H , is kept constant. It is noted in this figure that the depth configuration which gives the largest maximum amplitude gives the smallest initial growth rate.

The interfacial wave growth rate exhibits an interesting behavior with variation of upper layer depth. As shown in Figure 17, the growth rate decreases as the upper

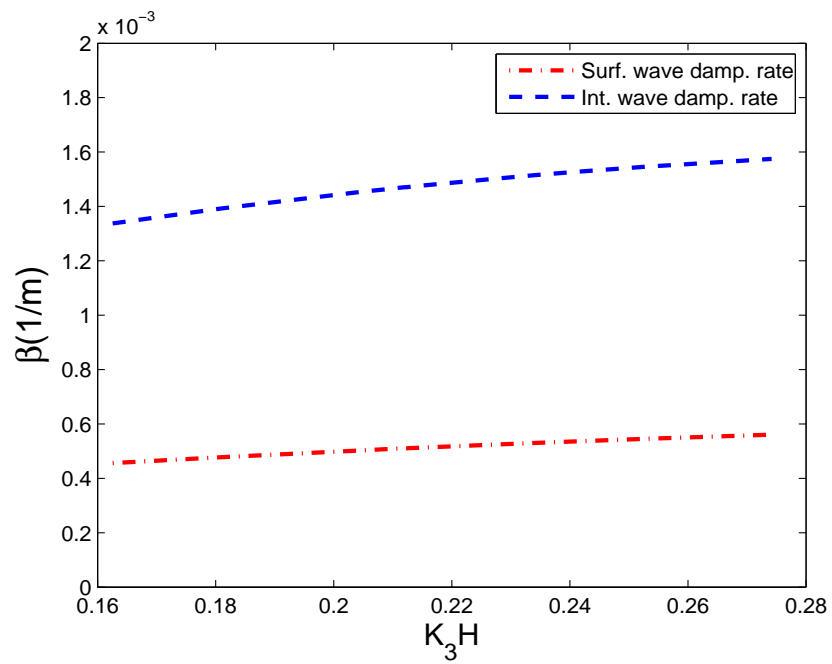


Fig. 13. Magnitudes of damping rate of surface and interfacial mode against k_3H .
 $h = 0.8m$, $d = 0.2m$, $r = 0.926$, $\nu = 3.00 \times 10^{-6}m^2/s$, $a_0 = 0.05m$,
 $b_0 = 0.001m$

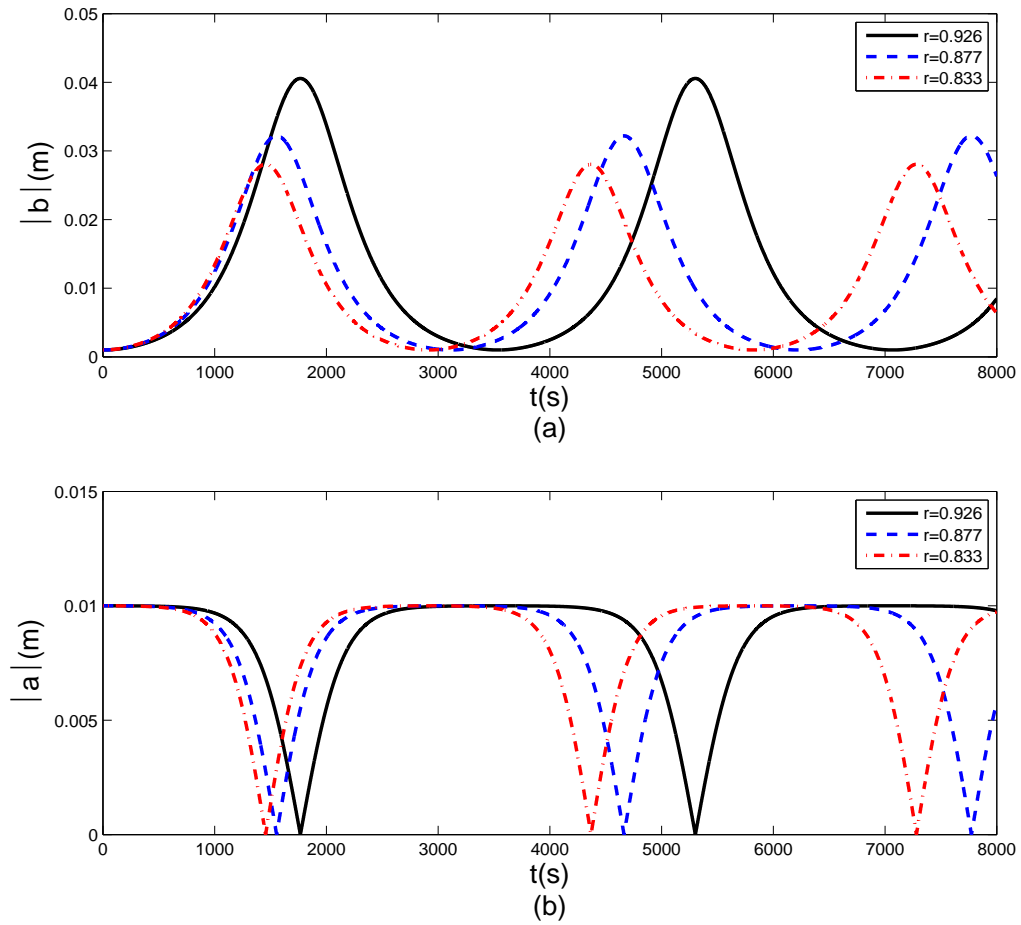


Fig. 14. Temporal variation of mode amplitudes for various values of $1/r$. $h = 0.8m$, $d = 0.2m, T = 7s, a_0 = 0.01m, b_0 = 0.001m$

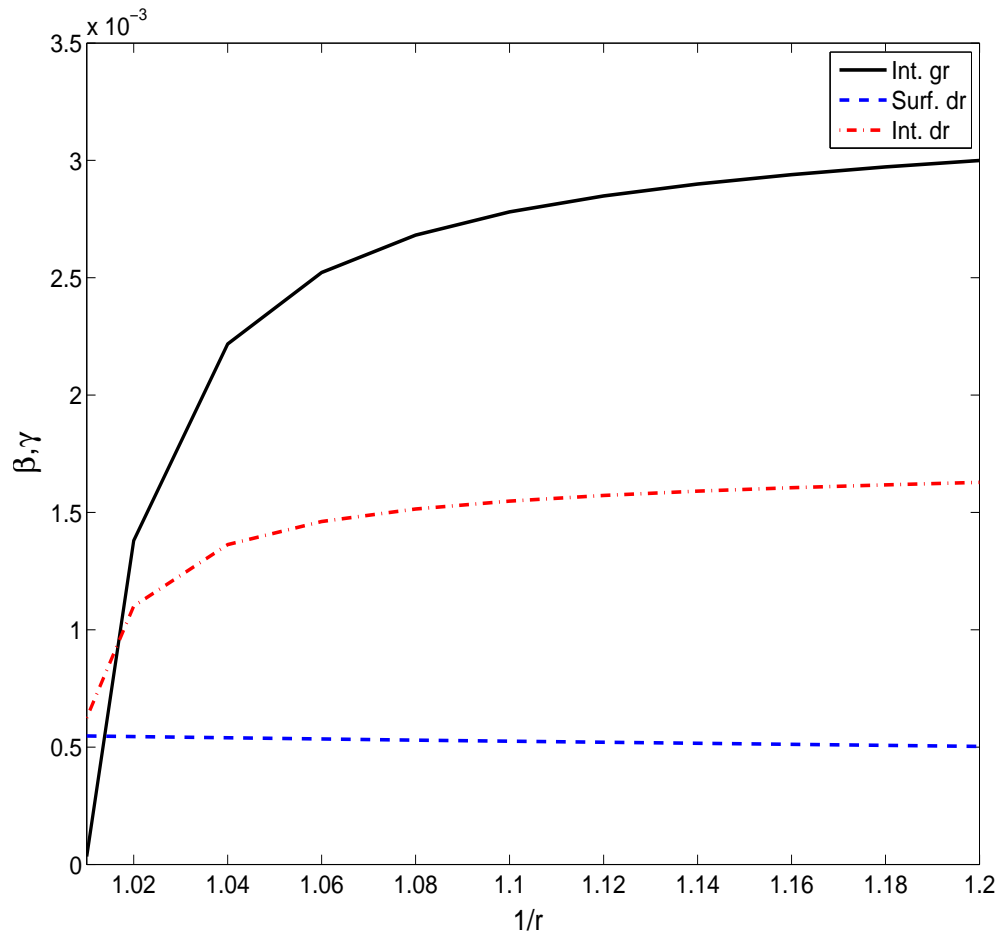


Fig. 15. Growth rate of interfacial mode and dissipation rate of surface and interfacial mode against variation of density ratio $1/r$. $h = 0.8m$, $d = 0.2m$, $T = 7s$, $\nu = 3.00 \times 10^{-6}m^2/s$, $a_0 = 0.01m$, $b_0 = 0.001m$.

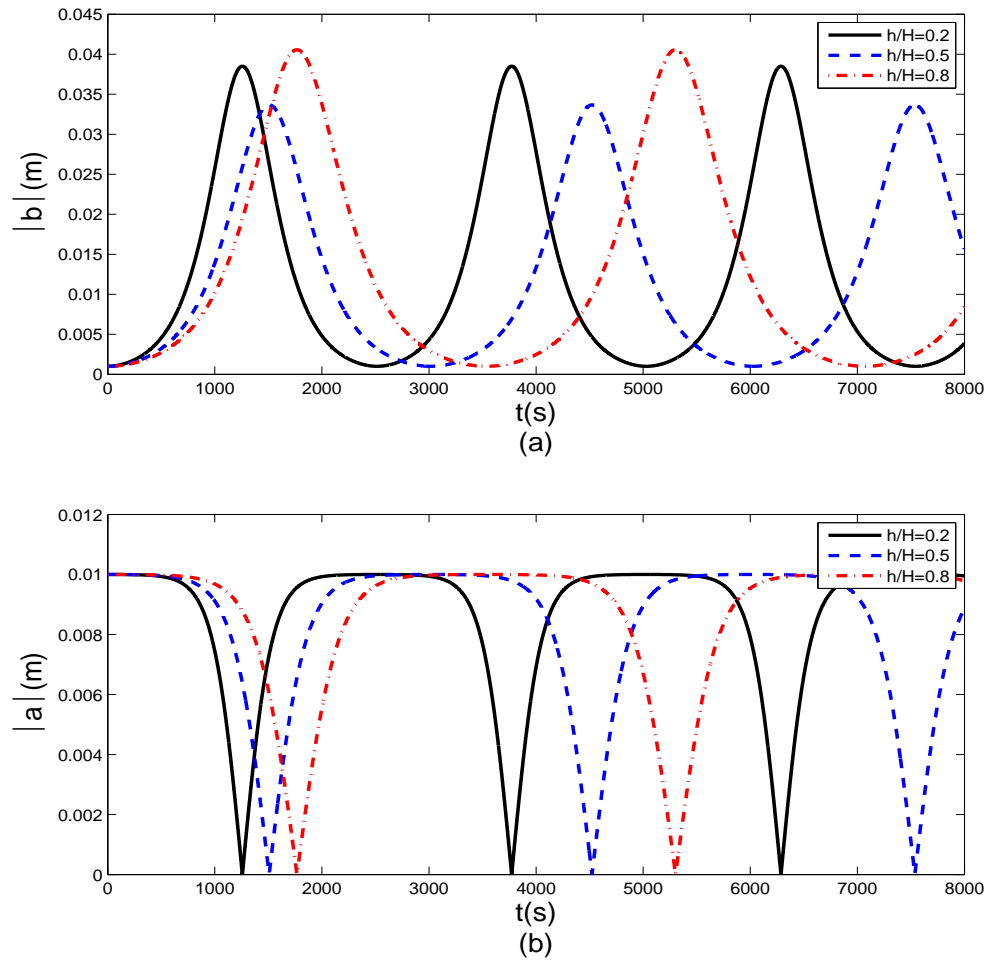


Fig. 16. Temporal variation of mode amplitudes for different upper layer depths h/H .
 $r = 0.926$, $T = 7s$, $a_0 = 0.01m$, $b_0 = 0.001m$

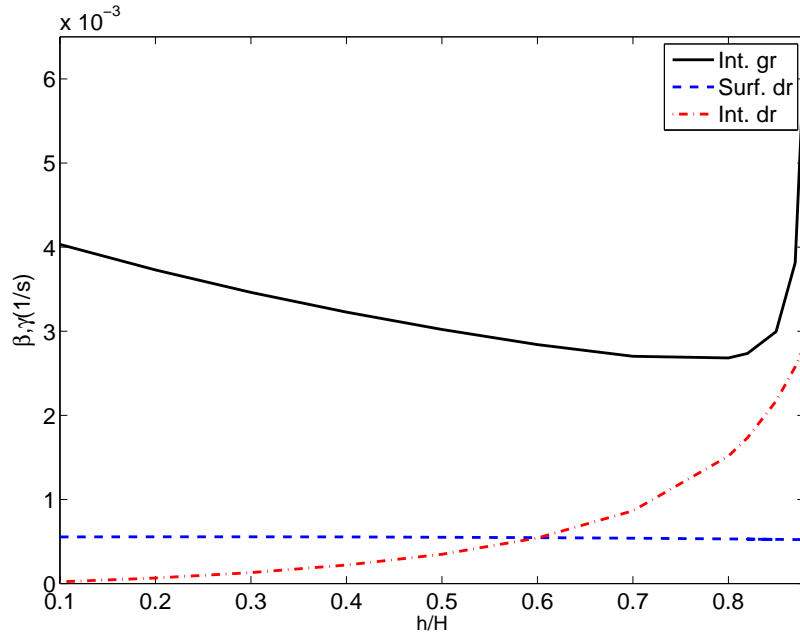


Fig. 17. Growth rate of interfacial mode (Int. gr) and dissipation rate of surface (Surf. dr) and interfacial modes (Int. dr) against variations of relative upper layer depth, h/H . $r = 0.926$, $T = 7s$, $\nu = 3.00 \times 10^{-6}m^2/s$, $a_0 = 0.01m$, $b_0 = 0.001m$.

layer thickens, until it reaches a relative depth of $h/H = 0.8$. As the upper layer gets deeper from this point, the growth rate increases significantly. Interfacial damping rate is an increasing function of h/H with increasing rate as the lower layer becomes thinner. This result is expected from the physics; as the lower layer becomes thinner, the interfacial waves become shallower and hence, a larger bottom boundary layer is generated. Therefore, the damping rate increases substantially. The dissipation rate of the surface wave is a very mildly decreasing function of upper layer thickness.

Surface wave height is the main source of energy in the interaction with interfacial waves. In addition, relative surface wave amplitude is a measure of nonlinearity in the equations and the small parameter in the perturbation expansion. Consequently, initial surface wave amplitude is an important parameter in the resonant interaction.

Figure 18 illustrates the typical time variation of the interfacial and surface wave amplitude for three values of initial surface wave amplitude. When the surface wave amplitude is increased, the growth rate of the interfacial wave amplitude increases. As shown, interfacial waves excited by larger surface waves have larger initial growth rates as well as larger maximum amplitudes. Equation (2.74) suggests that $|a_{03}|$ should have a minimum to make exponential growth possible,

$$|a_{03}|^2 \geq \frac{-\beta_1^2 - \alpha_1 \alpha_3 |b_{01}|^2}{\alpha_1 \bar{\alpha}_2} \quad (2.77)$$

Figure 19 shows that the growth rate of an interfacial wave is a linear function of initial surface wave amplitude. In the present approach, the damping coefficient is independent of surface wave amplitude, and furthermore, the present theory does not account for the dissipation due to breaking of the waves. Similar to Hill (2004) and based on experiments of Thorpe (1968), we assume that the threshold of interfacial wave breaking is reached when its steepness becomes larger than 0.3, i.e. $4 |b_{01}|_{max} < 0.3 / |k_1|$. In the present typical case, the breaking occurs when $a/H = 0.023$, and thus the growth rate of interfacial waves is calculated up to this limit.

1. Comparison with Jamali (1998)

As mentioned, Hill & Foda (1998) and Jamali (1998) carried out a second order analysis to study the resonant interactions between a surface and two interfacial waves in intermediate depth. Jamali (1998) provided a parametric study to investigate the influence of important parameters on the growth of interfacial waves. A comparison with his study shows qualitative agreement between the results of parametric study in the present analysis and Jamali (1998) for some parameters and difference for others. Jamali (1998) predicts smaller growth rates for larger density differences (their Figure 2.7). However, as illustrated in Figure 15, the interfacial wave growth rate is expected

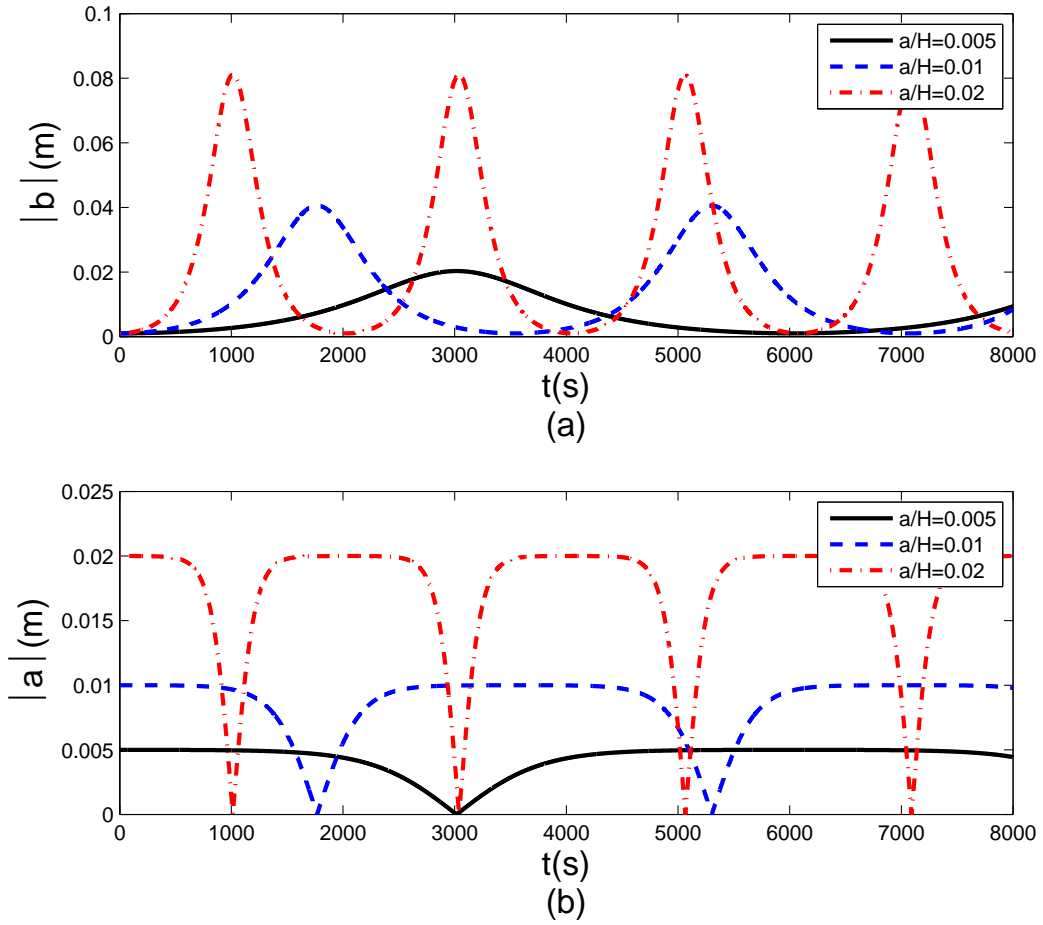


Fig. 18. Temporal variation of mode amplitudes for different initial values of surface wave amplitude a_{30} . $r = 0.926$, $T = 7s$, $h = 0.8m$, $d = 0.2m$, $b_0 = 0.001m$

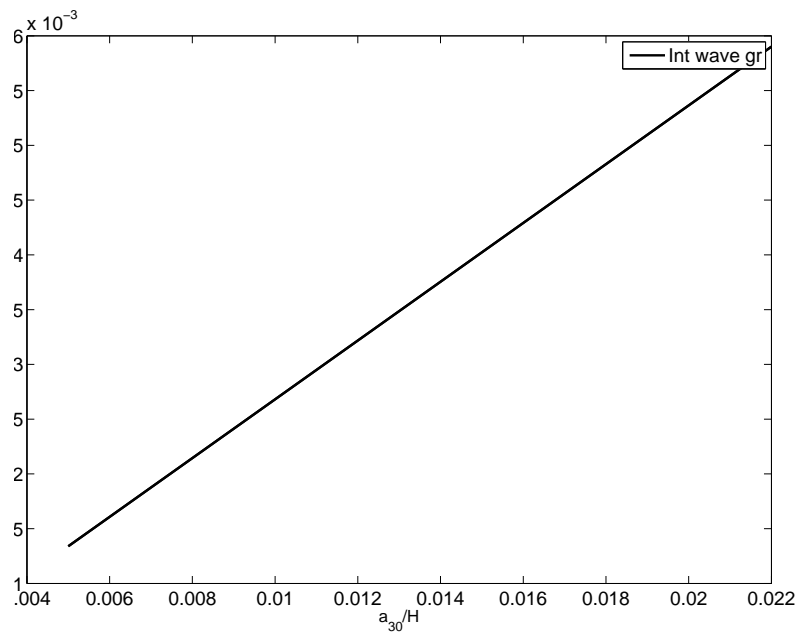


Fig. 19. Growth rate of interfacial mode against variations of surface wave initial amplitude a_{30} . $r = 0.926$, $T = 7s$, $h = 0.8m$, $d = 0.2m$, $\nu = 3.00 \times 10^{-6}m^2/s$, $b(0) = 0.001m$.

to increase in stronger stratifications in shallow water. In finite depth, Jamali (1998) predicts that the interfacial wave growth rate increases with the ratio of the lower layer to the total depth (their Figure 2.8). In the present study, the same result is obtained for depth ratios $h/H < 0.8$. For larger depth ratios the growth rate increases significantly (Figure 17). Similar to Jamali (1998), the damping ratio is an increasing function of viscosity and the interaction coefficients are independent of viscosity (10). The behavior of the growth of the interfacial waves with surface wave frequency is also similar in the present study and Jamali (1998) (their Figure 2.10); The growth increases with the frequency and reaches its maximum at a frequency in shallow water but decreases thereafter (Figure 13). The predicted direction of interfacial waves which exhibits the maximum growth rate is also similar in the two studies. Based on the comparison of the growth rates, both studies show interfacial waves are generated in an angle about 84° with respect to the surface wave direction.

F. Near-resonant interactions

In the Boussinesq formulation, the secondary harmonics can grow in amplitude and attain a magnitude comparable to the primary waves (Mei *et al.*, 2005). Three harmonics can be present at the surface and each can give rise to a pair of harmonics at the interface. In addition, near-resonant interactions are likely between the harmonics on either surface or interface.

In this section, to generalize the study of nonlinear interactions in shallow water, a triad of surface waves are considered on the surface. The choice of a triad is due to the fact that it forms the basic structure of quadratic nonlinear interactions in shallow water and allows for studying the interactions between components of a surface waves or interfacial wave train as well as coupling between the surface

and interface. Figure 20 shows the configuration of 9 interacting waves. This basic structure can be further generalized to wave spectra with numerous harmonics. In the next chapter, a formulation for spatial evolution of interacting time-harmonic waves will be presented. The kinematic conditions of exact resonance in the present case will be:

$$\omega_{s1} = \omega_{i11} + \omega_{i12} \quad (2.78)$$

$$\omega_{s2} = \omega_{i21} + \omega_{i22} \quad (2.79)$$

$$\omega_{s3} = \omega_{i31} + \omega_{i32} \quad (2.80)$$

$$\mathbf{k}_{s1} = \mathbf{k}_{i11} + \mathbf{k}_{i12} \quad (2.81)$$

$$\mathbf{k}_{s2} = \mathbf{k}_{i21} + \mathbf{k}_{i22} \quad (2.82)$$

$$\mathbf{k}_{s3} = \mathbf{k}_{i31} + \mathbf{k}_{i32} \quad (2.83)$$

in which, for instance, frequency ω_{i21} is the frequency of interfacial wave 1 in triad 2. It is assumed that the surface wave frequencies have the following relationship,

$$\omega_{s2} = 2\omega_{s1}, \quad \omega_{s3} = 3\omega_{s1} \quad (2.84)$$

and therefore, ω_{s1} can be considered the base frequency in this triad. In addition, the three surface waves will form a near-resonant triad which satisfies,

$$\omega_{s1} + \omega_{s2} = \omega_{s3} \quad (2.85)$$

$$\mathbf{k}_{s3} - \mathbf{k}_{s2} - \mathbf{k}_{s1} = \Delta\mathbf{k}_s \quad (2.86)$$

$$\mathbf{k}_{s2} - 2\mathbf{k}_{s1} = \delta\mathbf{k}_s \quad (2.87)$$

where $\delta\mathbf{k}_s$ and $\Delta\mathbf{k}_s$ are the mismatch from the exact resonance condition. It will be shown that δk is small relative to the wave numbers. As the interfacial waves, $(\omega_{i11}, \mathbf{k}_{i11})$ and $(\omega_{i12}, \mathbf{k}_{i12})$ are generated due to subharmonic resonant interactions,

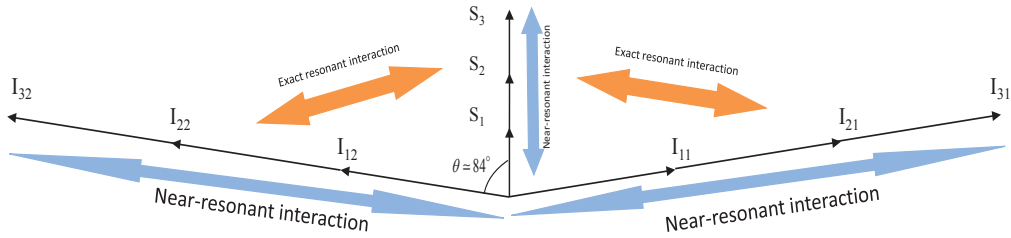


Fig. 20. Sketch of the configuration of the interactions between 3 surface waves and corresponding interfacial wave pairs. Surface (or interface) waves in the same direction exchange energy due to near-resonant condition. Surface and interfacial waves exchange energy due to exact resonance condition.

they have half the frequency of the surface wave, i.e. $\omega_{i11} = \omega_{i12} = \omega_{s1}/2$. Similarly, $\omega_{i21} = \omega_{i22} = \omega_{s2}/2$ and $\omega_{i31} = \omega_{i32} = \omega_{s3}/2$. Therefore, the following relationship is the near-resonant condition among interfacial waves in direction 1:

$$\omega_{i11} + \omega_{i21} = \omega_{i31} \quad (2.88)$$

$$\mathbf{k}_{i31} - \mathbf{k}_{i21} - \mathbf{k}_{i11} = \Delta \mathbf{k}_{i1} \quad (2.89)$$

$$\mathbf{k}_{i21} - 2\mathbf{k}_{i11} = \delta \mathbf{k}_{i1} \quad (2.90)$$

The same expression can be written for interfacial waves in direction 2. It is instructive to see the relative smallness of δk . The interfacial root of the dispersion relation can be written as follows (Pond & Pickard, 1983):

$$\omega_i^2 = \frac{\Delta \rho g k_i}{\rho \coth k_i h + \rho \coth k_i d} \quad (2.91)$$

By inserting $\omega_{2i} = 2\omega_i$ and $\mathbf{k}_{i2} = 2\mathbf{k}_{i1} + \delta \mathbf{k}$ in the above expression, we will obtain the following expression for the relative magnitude of mismatch between wavenumbers,

$$\frac{\delta k}{k_i} = \frac{\rho' d (k_i h)^2 + \rho h (k_i d)^2}{\rho' d + \rho h - \rho' d (k_i h)^2 - \rho h (k_i d)^2} = \mathcal{O}(\mu^2) \quad (2.92)$$

Therefore, the mismatch between the wave numbers is of order of frequency dispersion. A similar expression can found for Δk . The forcing function for the near-resonant terms has the same form as forcing functions in equations (2.57) and (2.58). However, since the phase mismatch should be considered, the components forcing each harmonic will be different. For instance, in the forcing term $(\mathbf{u}'_0 \cdot \nabla \mathbf{u}'_0)_t$, a term proportional to $\widehat{\mathbf{u}}'_{0s1} \widehat{\mathbf{u}}'_{0s2} a_2 \widehat{a}_1 e^{i(k_{s2}-k_{s1})x} e^{-i\omega_{s1}t}$ will be forcing surface wave 1. Similarly in the forcing term $(\mathbf{u}_0 \cdot \nabla \mathbf{u}_0)_t$, a term proportional to $\widehat{\mathbf{u}}_{0i1} \widehat{\mathbf{u}}_{0i2} b_2 \widehat{b}_1 e^{i(k_{i2}-k_{i1})x} e^{-i\omega_{i1}t}$ will be forcing interfacial wave 1. The variables are expanded to include all the interacting terms,

$$\eta(x, y, t) = \sum_{k=1}^3 a_{sk}(t) e^{i\Omega_{sk}} + \sum_{k=1}^3 b_{ik}(t) \widehat{\eta}_{ik} e^{i\Omega_{ik}} + \sum_{k=1}^3 b_{imk}(t) \widehat{\eta}_{imk} e^{i\Omega_{imk}} \quad (2.93)$$

$$\xi(x, y, t) = \sum_{k=1}^3 \frac{a_{sk}(t)}{\widehat{\eta}_{sk}} e^{i\Omega_{sk}} + \sum_{k=1}^3 b_{ik}(t) e^{i\Omega_{ik}} + \sum_{k=1}^3 b_{imk}(t) e^{i\Omega_{imk}} \quad (2.94)$$

$$\begin{aligned} \mathbf{u}'(x, y, t) = & \sum_{k=1}^3 \frac{a_{sk}(t)}{\widehat{\eta}_{sk}} \mathbf{k}_{sk} \widehat{u}'_{sk}(t) e^{i\Omega_{sk}} + \sum_{k=1}^3 b_{ik}(t) \mathbf{k}_{ik} \widehat{u}'_{ik} e^{i\Omega_{ik}} + \\ & \sum_{k=1}^3 b_{imk}(t) \mathbf{k}'_{imk} \widehat{u}'_{sk} e^{i\Omega_{imk}} \end{aligned} \quad (2.95)$$

$$\begin{aligned} \mathbf{u}(x, y, t) = & \sum_{k=1}^3 \frac{a_{sk}(t)}{\widehat{\eta}_{sk}} \mathbf{k}_{sk} \widehat{u}_{sk} e^{i\Omega_{sk}} + \sum_{k=1}^3 b_{ik}(t) \mathbf{k}_{ik} \widehat{u}_{ik} e^{i\Omega_{ik}} + \\ & \sum_{k=1}^3 b_{imk}(t) \mathbf{k}_{imk} \widehat{u}_{sk} e^{i\Omega_{imk}} \end{aligned} \quad (2.96)$$

where $\Omega = \mathbf{k} \cdot \mathbf{x} - \omega t$ is the phase function. The system of evolution equations which govern the energy transfer between the 9 waves are derived as follows,

$$\frac{da_1}{dt} = \alpha_{s1} a_2 \bar{a}_1 + \alpha_{s2} a_3 \bar{a}_2 + \alpha'_1 b_1 b_2 \quad (2.97)$$

$$\frac{db_1}{dt} = \alpha_{i1} b_3 \bar{b}_1 + \alpha_{i2} b_5 \bar{b}_3 + \alpha'_2 a_1 \bar{b}_2 \quad (2.98)$$

$$\frac{db_2}{dt} = \alpha_{i3} b_4 \bar{b}_2 + \alpha_{i4} b_6 \bar{b}_4 + \alpha'_3 a_1 \bar{b}_1 \quad (2.99)$$

$$\frac{da_2}{dt} = \alpha_{s3} a_1^2 + \alpha_{s4} a_3 \bar{a}_1 + \alpha'_4 b_3 b_4 \quad (2.100)$$

$$\frac{db_3}{dt} = \alpha_{i5}b_1^2 + \alpha_{i6}b_5\bar{b}_1 + \alpha'_5a_2\bar{b}_4 \quad (2.101)$$

$$\frac{db_4}{dt} = \alpha_{i7}b_2^2 + \alpha_{i8}b_6\bar{b}_2 + \alpha'_6a_2\bar{b}_3 \quad (2.102)$$

$$\frac{da_3}{dt} = \alpha_{s5}a_1a_2 + \alpha'_7b_5b_6 \quad (2.103)$$

$$\frac{db_5}{dt} = \alpha_{i9}b_1b_3 + \alpha'_8a_3\bar{b}_6 \quad (2.104)$$

$$\frac{db_6}{dt} = \alpha_{i10}b_2b_4 + \alpha'_9a_3\bar{b}_5 \quad (2.105)$$

It was shown in section (II-E) that the two subharmonic interfacial waves are identical. Therefore, above set of equations reduces to,

$$\frac{da_1}{dt} = \alpha_{s1}a_2\bar{a}_1 + \alpha_{s2}a_3\bar{a}_2 + \alpha'_1b_1^2 \quad (2.106)$$

$$\frac{db_1}{dt} = \alpha_{i1}b_3\bar{b}_1 + \alpha_{i2}b_5\bar{b}_3 + \alpha'_2a_1\bar{b}_1 \quad (2.107)$$

$$\frac{da_2}{dt} = \alpha_{s3}a_1^2 + \alpha_{s4}a_3\bar{a}_1 + \alpha'_4b_3^2 \quad (2.108)$$

$$\frac{db_3}{dt} = \alpha_{i5}b_1^2 + \alpha_{i6}b_5\bar{b}_1 + \alpha'_5a_2\bar{b}_3 \quad (2.109)$$

$$\frac{da_3}{dt} = \alpha_{s5}a_1a_2 + \alpha'_8b_3^2 \quad (2.110)$$

$$\frac{db_5}{dt} = \alpha_{i10}b_1b_3 + \alpha'_9a_3\bar{b}_5 \quad (2.111)$$

The above equations are solved numerically and the temporal evolution of waves are obtained for a typical example. The parameters in this typical example are $\omega_{s1} = 0.1rad/s, \omega_{s2} = 0.2rad/s, \omega_{s3} = 0.3rad/s, H = 1m, d = 0.2m, r = 0.91, \nu = 3 \times 10^{-6}m^2/s, a_1(0) = a_2(0) = a_3(0) = 0.05m$ and $b_1(0) = b_2(0) = b_3(0) = 0.001m$. As there are a large number of variables and equations in the system, there may be computational difficulties due to stiffness of the system. In such condition, the numerical scheme fails to converge to a solution. In the parameter ranges studied here, only one instance of stiffness was encountered in very long term and generally the stiffness was not an issue. Figure 21(a) shows the evolution of the 3 surface waves

in interaction with their corresponding interfacial wave pair. The interactions among surface waves or among interfacial waves is turned off here. Figure 21(b) shows the evolution of the interfacial waves in these triads. These two figures only include the exact resonance conditions (2.34), and look into three triads of surface-interfacial waves without any coupling between the triads.

In Figure 22(a), the evolution of the three surface waves, decoupled from their corresponding interfacial waves, and only in interaction with other surface waves is illustrated. As expected, the evolution of the surface wave triad in a two-layer fluid differs from its evolution in a single layer fluid (e. g. see Dingemans, 1993, Figure 7.23). Figure 22(b) shows the time variation of the triad of interfacial waves decoupled from surface waves.

Figures (23)-(28) show the evolution of surface and interfacial waves where all the possible interactions are active. It is evident that the addition of all the interactions results in a more complicated evolution. Figures (23)-(25) shows the evolution of surface waves and Figures (26)-(28) show the evolution of interfacial waves.

Although the evolution is far more complicated than the surface-interface exact resonant triad, it would be instructive to investigate the influence of the important physical parameters on the evolution of waves in the system. We investigate the influence of density ratio, $1/r$, upper layer relative depth, h/H , and highest surface wave frequency, ω_{s3} , on the evolution of waves. Frequencies, ω_{s1} , and ω_{s2} are proportional to ω_{s3} and thus, their variation will have the same result as the variation of ω_{s3} .

Figures (29) and (30) illustrates the time variation of surface and interfacial waves for three different density ratios respectively. Examination of the figures shows that surface wave 1 and 3 exhibits an initial oscillatory behavior as they loose energy from the beginning of the interaction. However, surface wave 2 experiences growth and its amplitude increases from the initial stages of interaction. The growth of surface wave

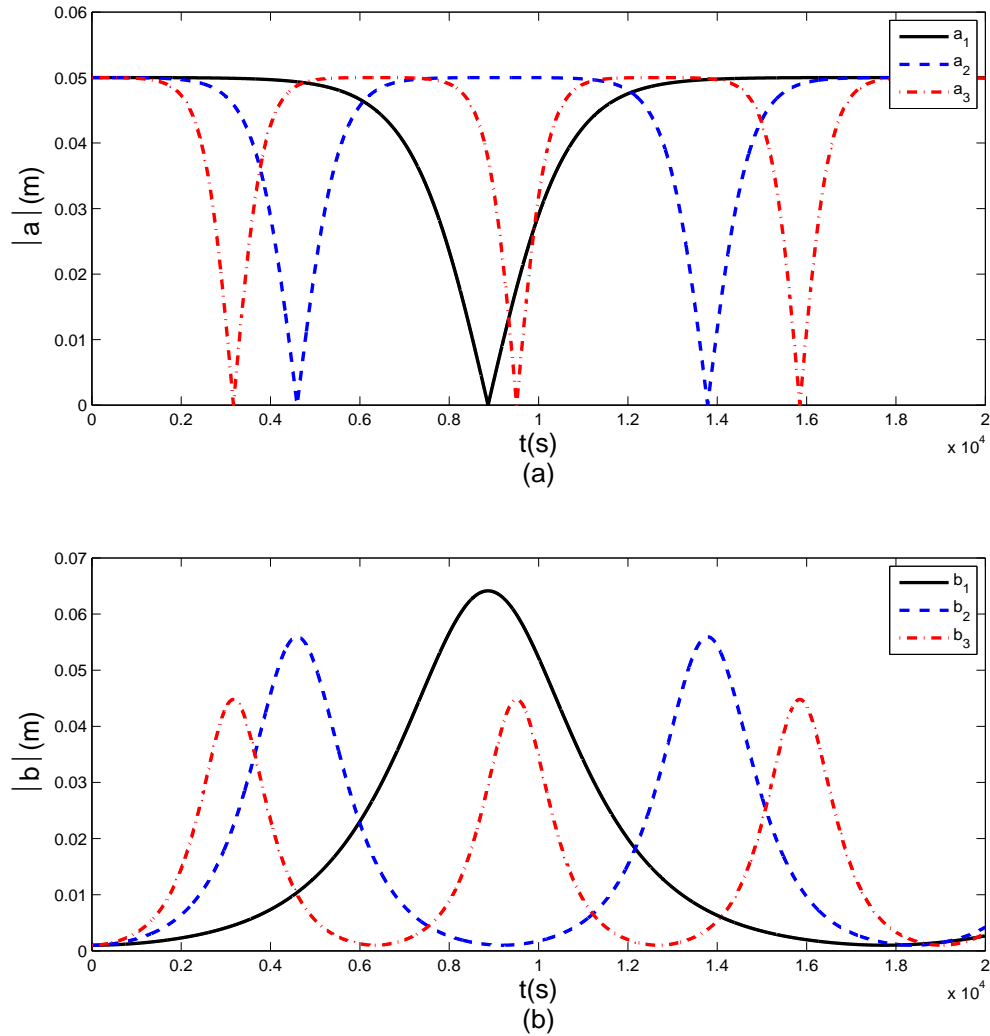


Fig. 21. Temporal evolution of (a) surface waves amplitudes in interaction with their subharmonic interfacial waves and (b) Subharmonic interfacial wave amplitudes in resonant triads with corresponding surface waves (the interaction is decoupled from other resonant triads), $H = 2.00\text{m}$, $d = 0.50\text{m}$, $\omega_3 = 0.3\text{rad/s}$, $r = 0.926$, $a_1(0) = a_2(0) = a_3(0) = 0.05\text{m}$ $b_1(0) = b_2(0) = b_3(0) = 0.001\text{m}$.

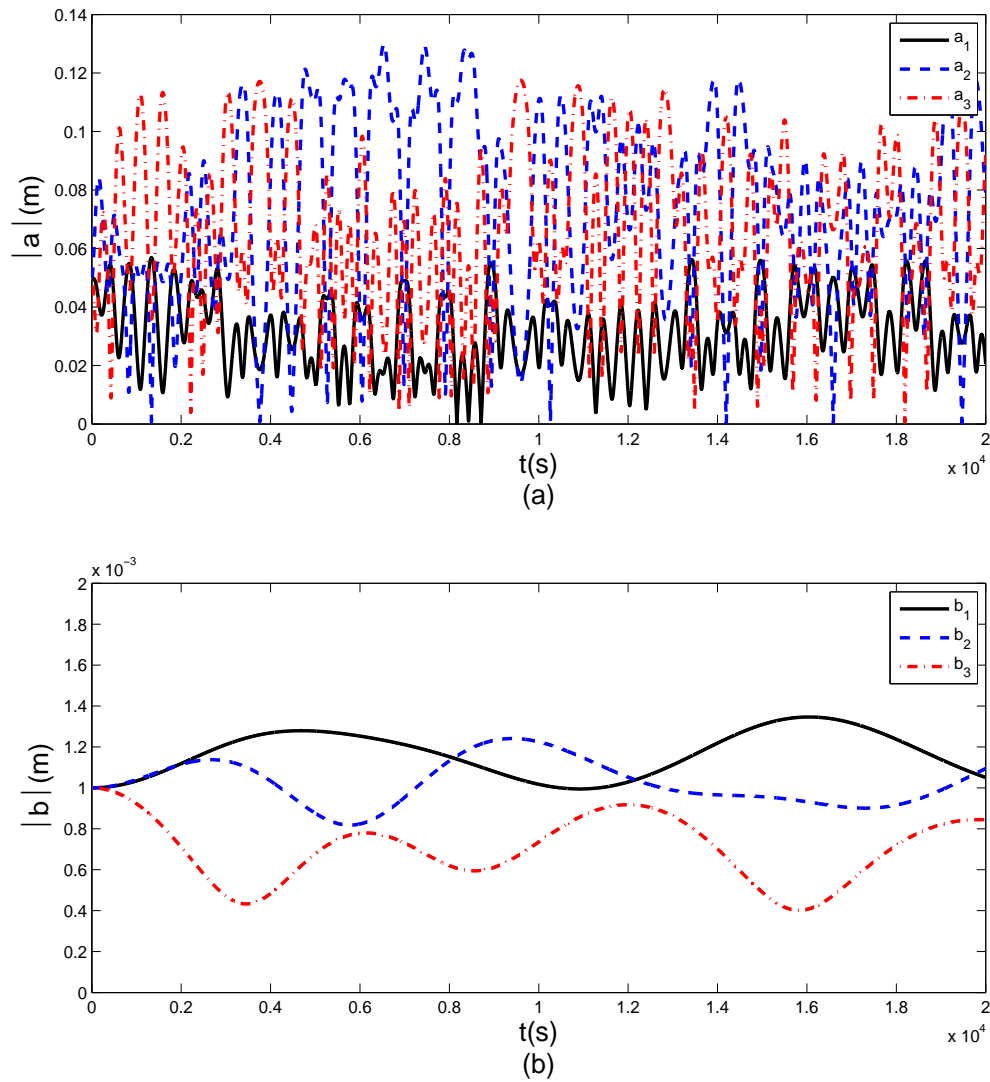


Fig. 22. Temporal evolution of (a) surface wave amplitudes in interaction triad with other surface waves (decoupled from interfacial waves) and (b) interfacial wave amplitudes in resonant triads with other interfacial waves (decoupled from surface waves) $H = 2.00m$, $d = 0.50m$, $\omega_3 = 0.3rad/s$, $r = 0.926$, $a_1(0) = a_2(0) = a_3(0) = 0.05m$.

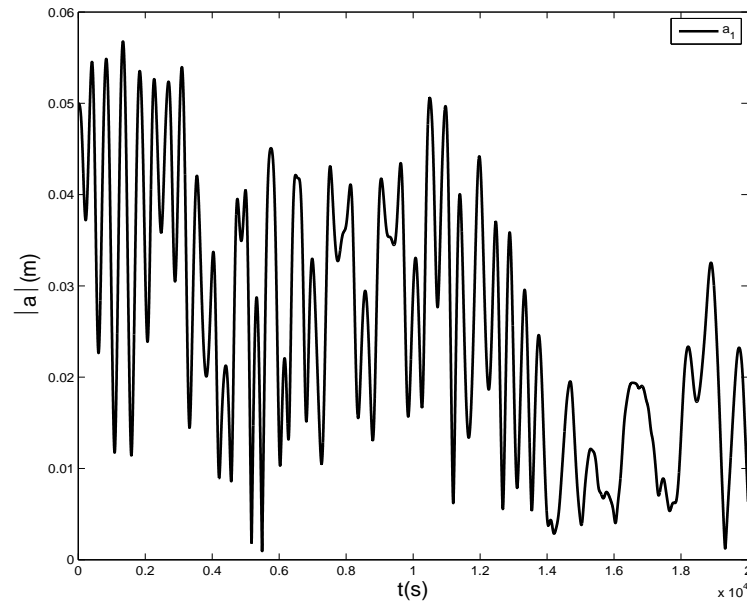


Fig. 23. Time variation of the amplitude of surface wave 1, $H = 2.00m$, $d = 0.50m$, $\omega_3 = 0.3rad/s$, $r = 0.926$, $a_1(0) = a_2(0) = a_3(0) = 0.05m$.

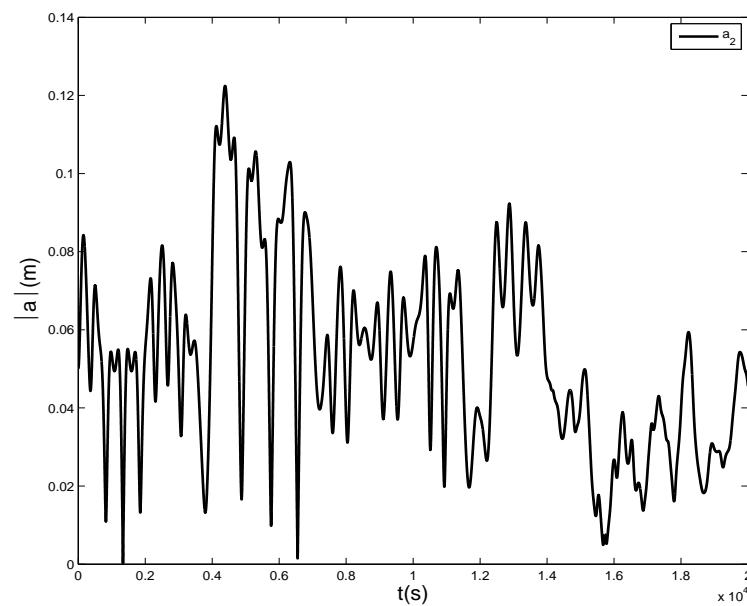


Fig. 24. Time variation of the amplitude of surface wave 2, $H = 2.00m$, $d = 0.50m$, $\omega_3 = 0.3rad/s$, $r = 0.926$, $a_1(0) = a_2(0) = a_3(0) = 0.05m$.

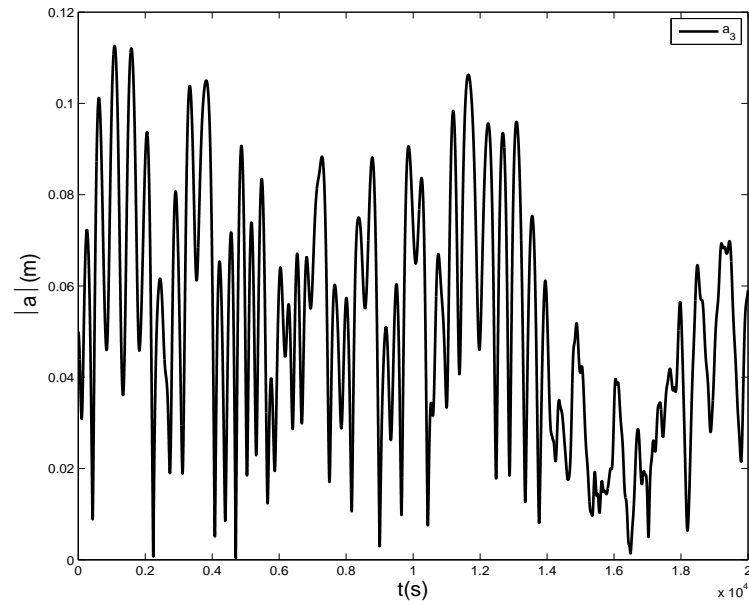


Fig. 25. Time variation of the amplitude of surface wave 3, $H = 2.00m$, $d = 0.50m$, $\omega_3 = 0.3rad/s$, $r = 0.926$, $a_1(0) = a_2(0) = a_3(0) = 0.05m$.

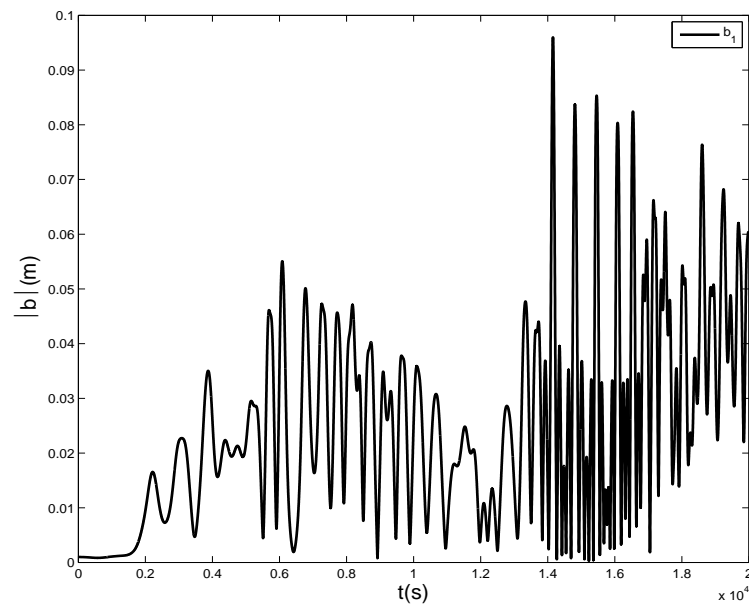


Fig. 26. Time variation of the amplitude of interfacial wave 1, $H = 2.00m$, $d = 0.50m$, $\omega_3 = 0.3rad/s$, $r = 0.926$, $a_1(0) = a_2(0) = a_3(0) = 0.05m$.

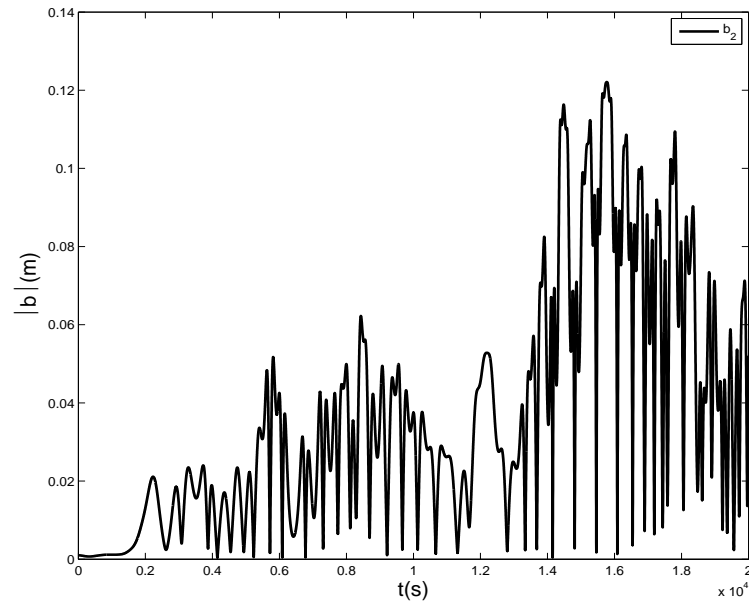


Fig. 27. Time variation of the amplitude of interfacial wave 2, $H = 2.00m$, $d = 0.50m$, $\omega_3 = 0.3rad/s$, $r = 0.926$, $a_1(0) = a_2(0) = a_3(0) = 0.05m$.

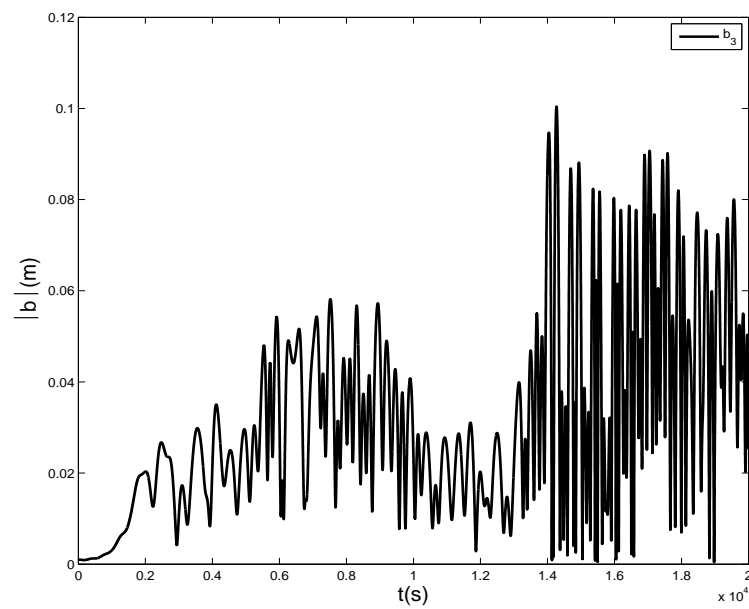


Fig. 28. Time variation of the amplitude of interfacial wave 3, $H = 2.00m$, $d = 0.50m$, $\omega_3 = 0.3rad/s$, $r = 0.926$, $a_1(0) = a_2(0) = a_3(0) = 0.05m$.

2 is intensified when the stratification becomes weaker. The three interfacial waves show initial growth. Unlike the 3 wave problem, in the 9 wave problem, the interfacial waves show stronger growth when the density ratio is closer to 1. In addition, it is observed that the surface wave amplitudes start oscillation with a slight phase-shift until about $t = 1700s$. After this time, a considerable change in the pattern and relative phase of the surface wave amplitudes occurs. This change is due to the entrance of the interfacial waves to the energy exchange. As seen in Figure (30), the interfacial waves do not exhibit significant growth until about $t = 1700s$. Therefore, the presence of subharmonic interfacial waves affects the evolution of interacting surface waves.

Figures (31) and (32) respectively illustrate the time variation of the surface and interfacial waves for three values of relative depth of the upper layer. Similar to density ratio, only surface wave 2 exhibits initial growth among surface waves. It is noteworthy that its growth rate is maximum when the interface is closer to the surface. Interfacial waves 1 and 2 show largest growth rates when the lower layer thickness is the least. This is generally in accordance with the three wave problem where interfacial wave growth decreases with h/H . In contrast, b_3 shows the maximum growth rate when $h/H = 0.7$.

Figures (33) and (34) show the time variation of harmonic amplitudes for various surface wave frequencies ω_{s3} . It is seen that for larger ω_{s3} , surface wave 3 exhibits growth. As before, surface wave 2 shows growth and its growth rate is highest for the largest ω_{s3} . By close examination of Figure (34), the interfacial waves show the largest growth rate with the lowest ω_{s3} but they gain the largest long term amplitude and variations with $\omega_{s3} = 0.3rad/s$.

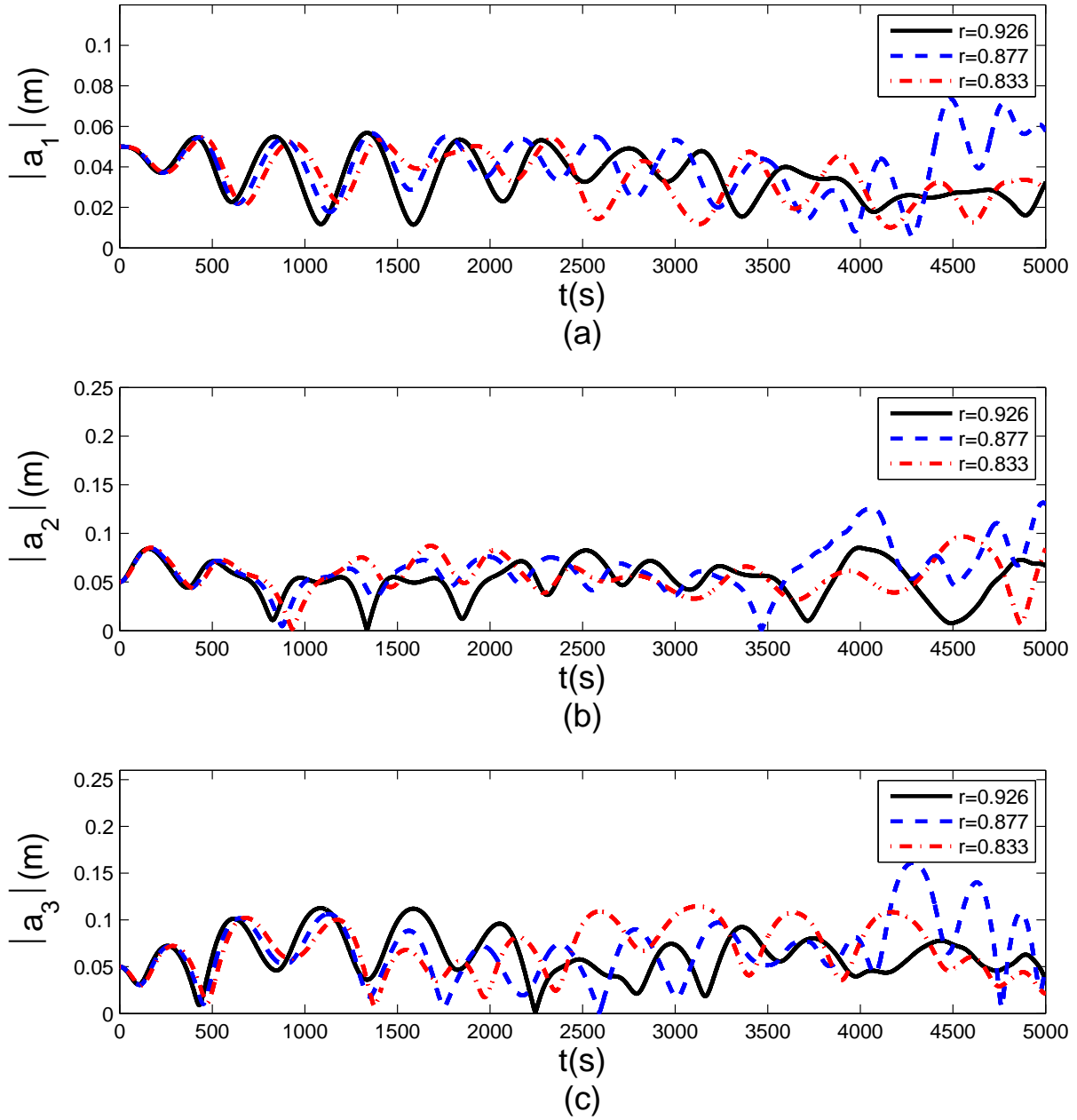


Fig. 29. Temporal evolution of surface waves for different density ratios, $H = 2m$, $d = 0.5m$, $\omega_3 = 0.3rad/s$, $a_1(0) = a_2(0) = a_3(0) = 0.05m$, $b_1(0) = b_2(0) = b_3(0) = 0.001m$.

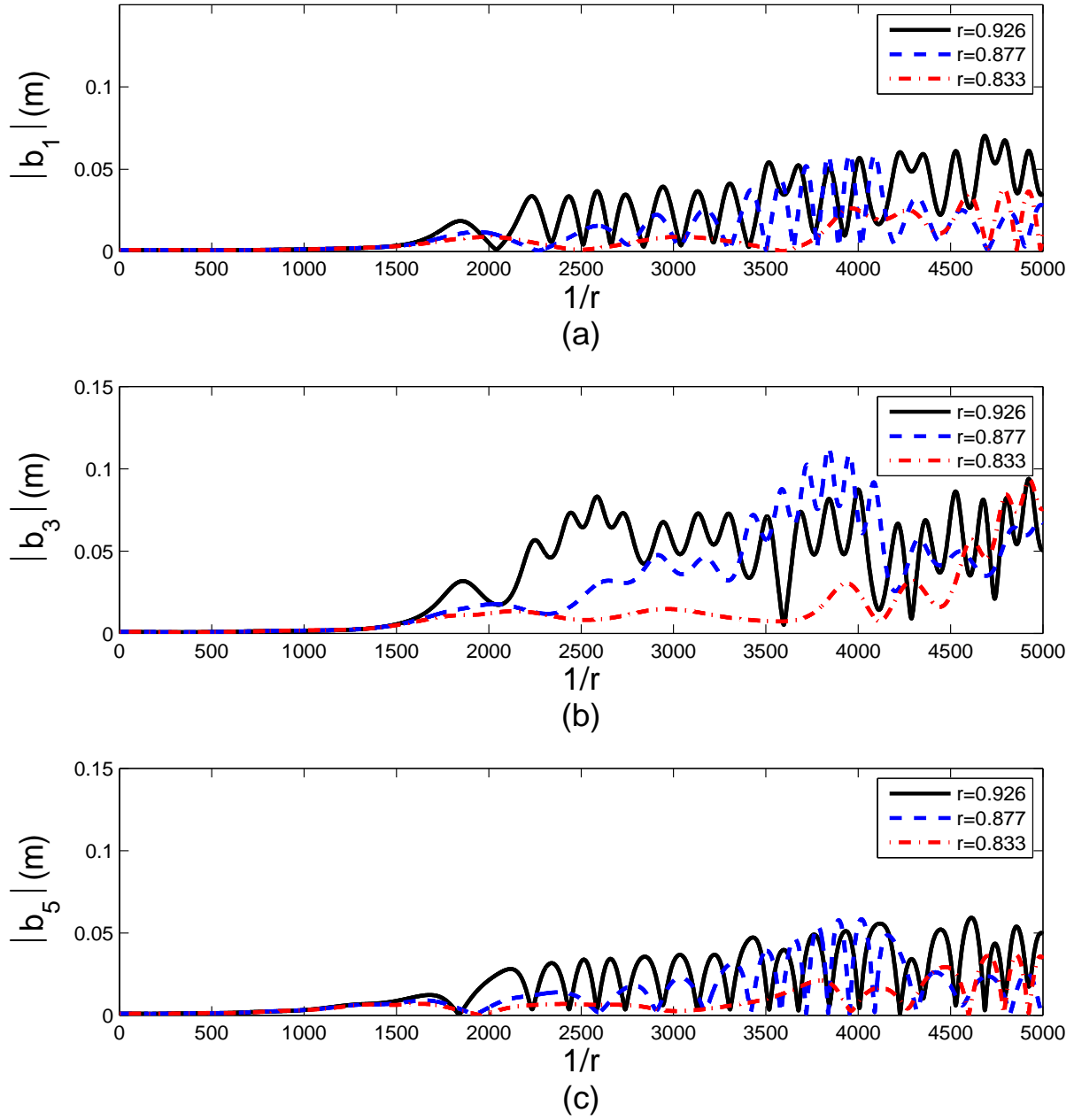


Fig. 30. Temporal evolution of interfacial waves for different density ratios, $H = 2m$, $d = 0.5m$, $\omega_3 = 0.3\text{rad/s}$, $a_1(0) = a_2(0) = a_3(0) = 0.05m$, $b_1(0) = b_2(0) = b_3(0) = 0.001m$.

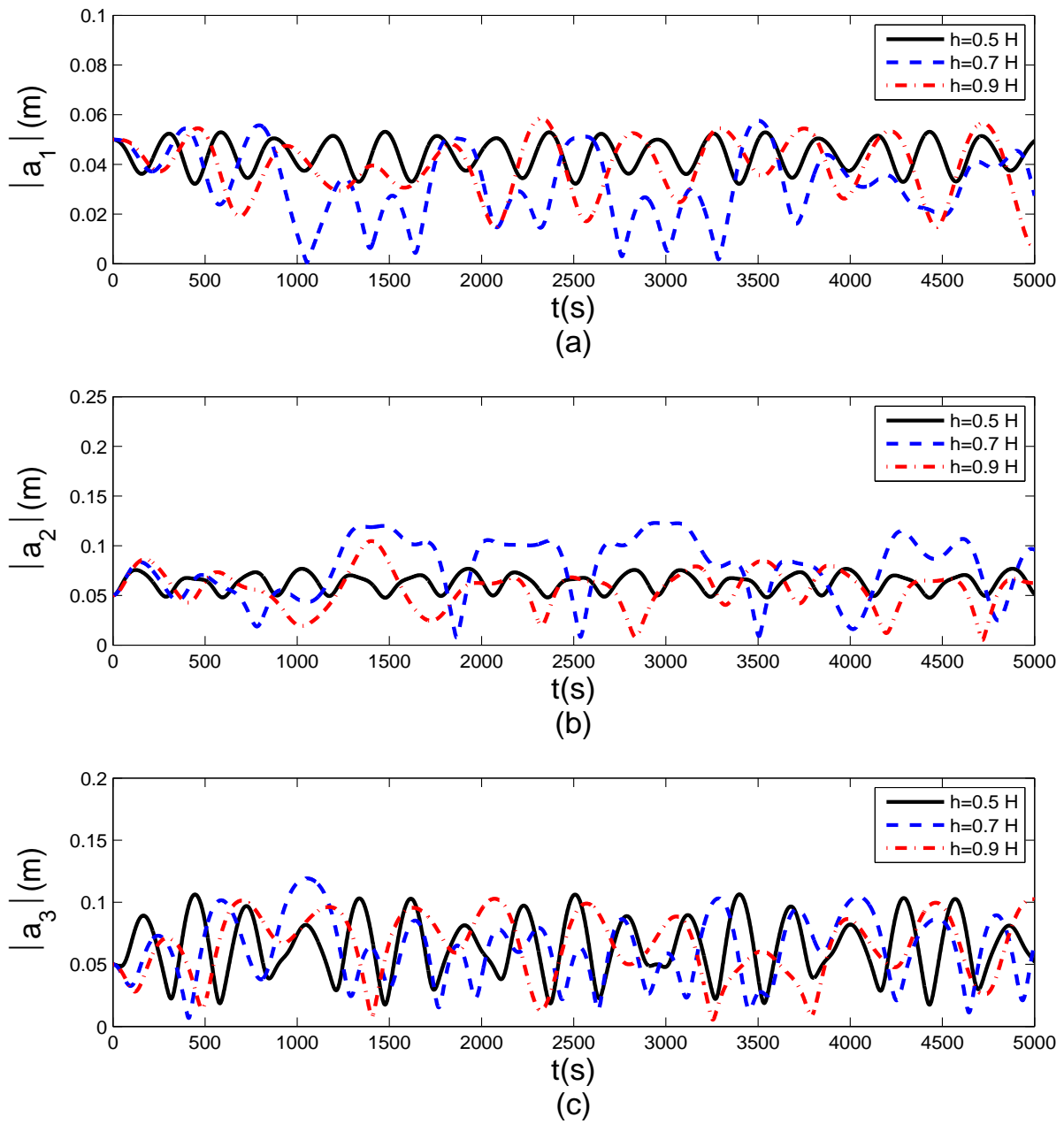


Fig. 31. Temporal evolution of surface waves for different depth ratios, $H = 2m$, $\omega_3 = 0.3rad/s$, $r = 0.926$, $a_1(0) = a_2(0) = a_3(0) = 0.05m$, $b_1(0) = b_2(0) = b_3(0) = 0.001m$.

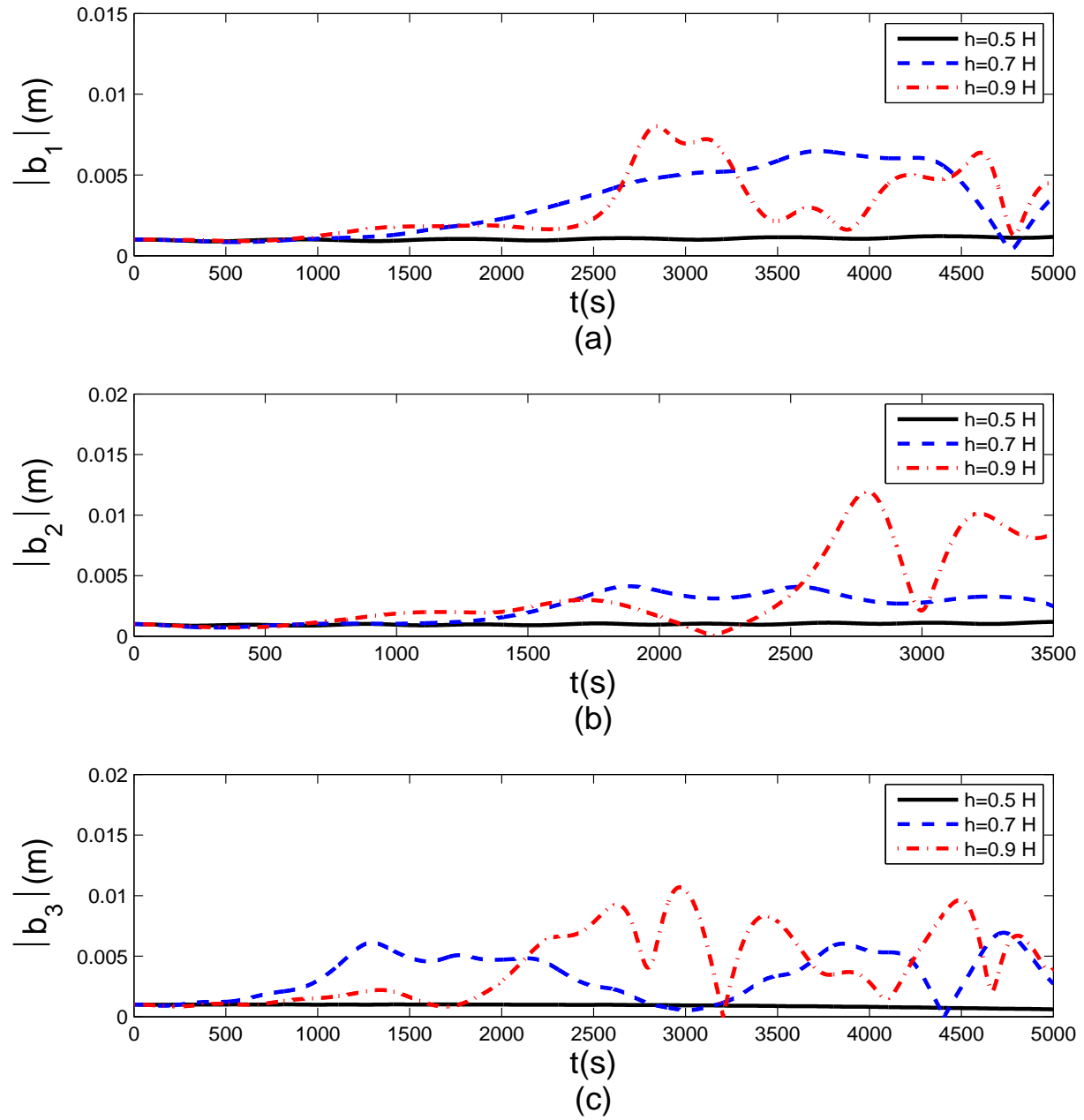


Fig. 32. Temporal evolution of interfacial waves for different depth ratios, $H = 2m, \omega_3 = 0.3 \text{ rad/s}, r = 0.926, a_1(0) = a_2(0) = a_3(0) = 0.05m, b_1(0) = b_2(0) = b_3(0) = 0.001m$.

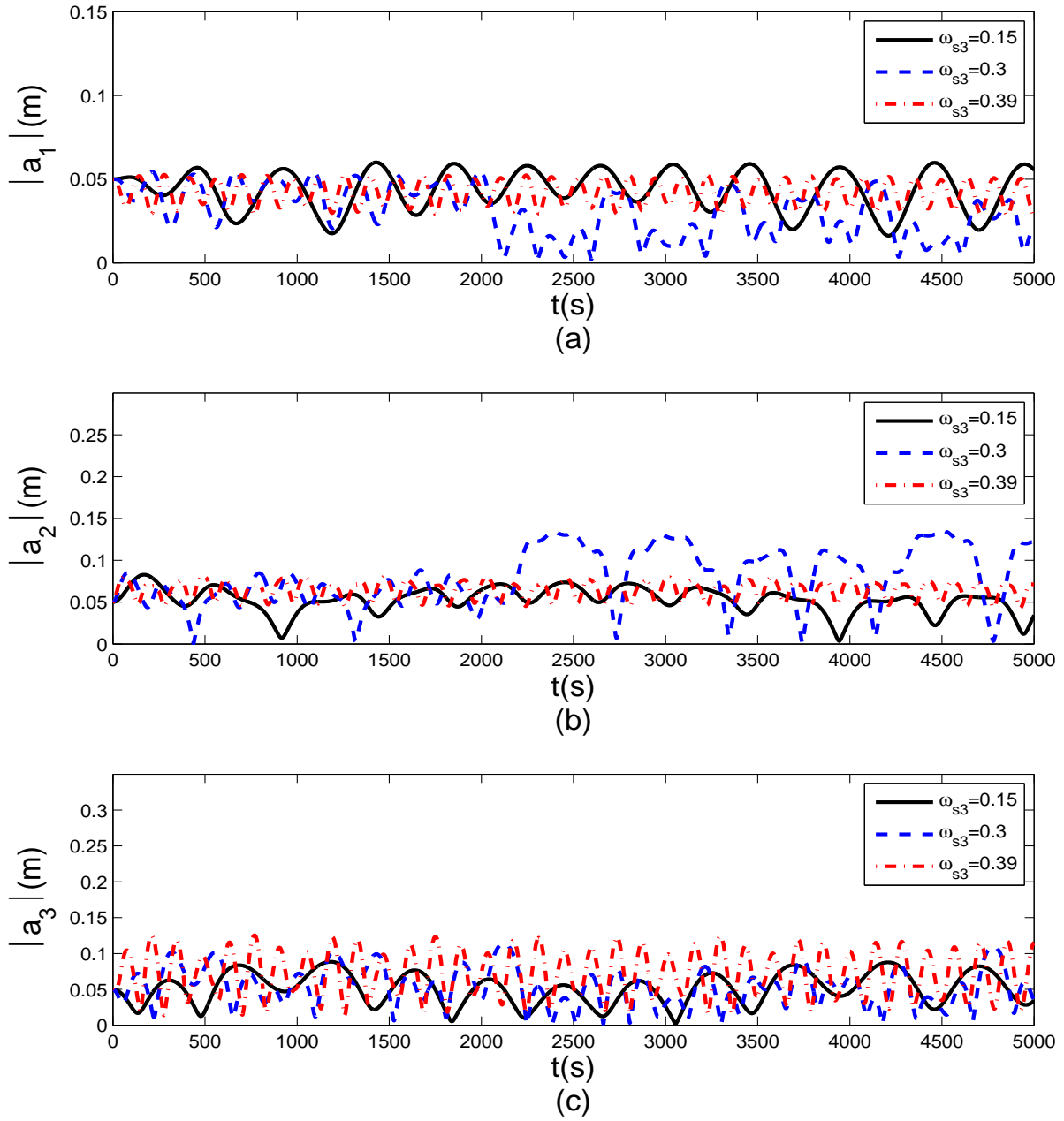


Fig. 33. Temporal evolution of surface waves for different frequencies ratios, $H = 2m$, $d = 0.5m$, $r = 0.926$, $a_1(0) = a_2(0) = a_3(0) = 0.05m$, $b_1(0) = b_2(0) = b_3(0) = 0.001m$.

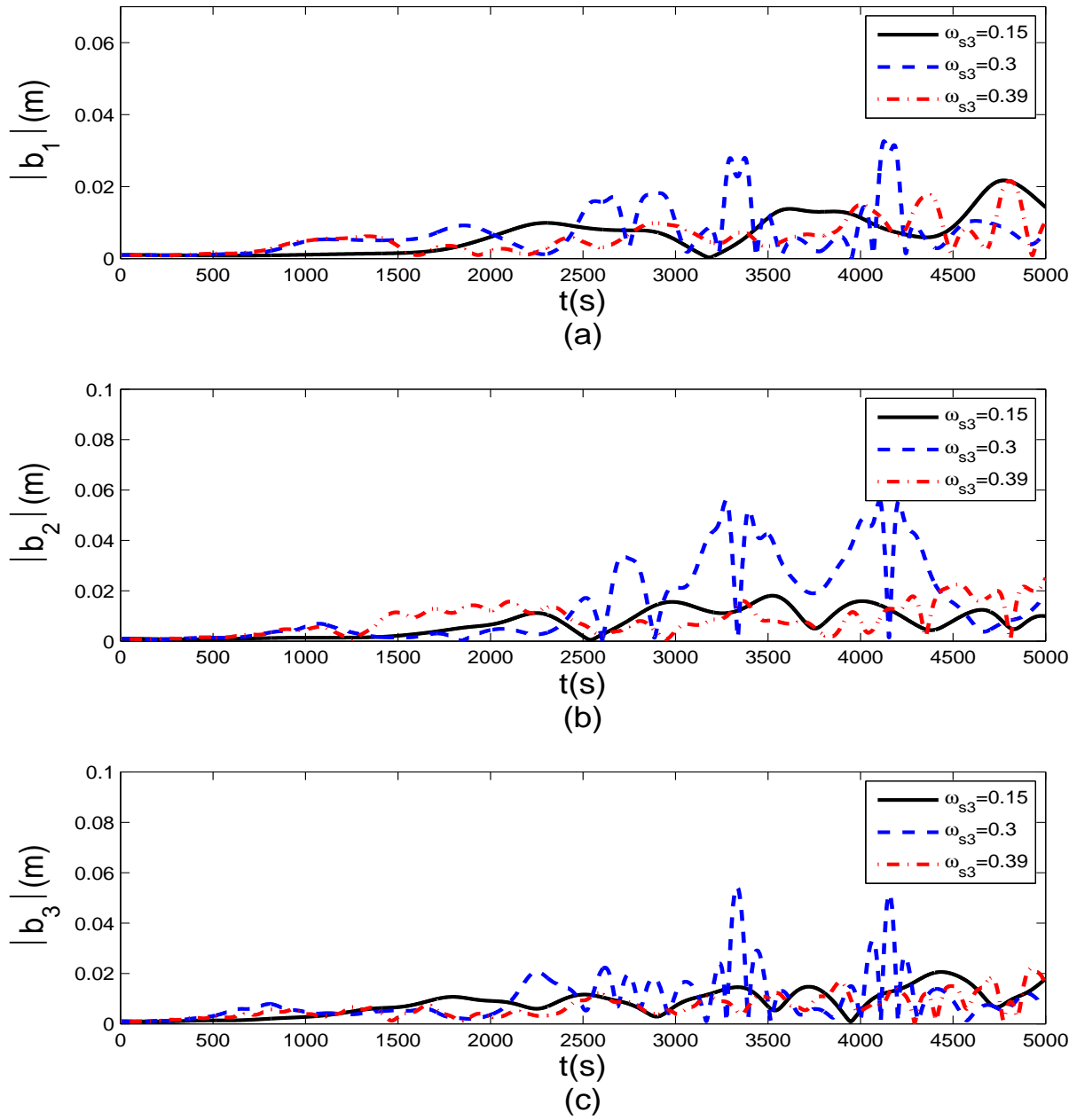


Fig. 34. Temporal evolution of surface waves for different frequency ratios, $H = 2m$, $d = 0.5m$, $r = 0.926$, $a_1(0) = a_2(0) = a_3(0) = 0.05m$, $b_1(0) = b_2(0) = b_3(0) = 0.001m$.

G. Concluding remarks

In this chapter, the nonlinear interactions between the long waves in a two-layer fluid are analyzed. A two-layer Boussinesq system of equations is derived to analyze the shallow water wave processes. The formulation is verified by favorable comparison with Choi & Camassa (1996). The equations are then analyzed for the interaction between one surface and two interfacial waves. A standard approach using a second order perturbation analysis is applied to obtain the evolution of the amplitudes of the interacting waves. Damping effect of weak viscosity is added to the evolution equations. A parametric study is also carried out to investigate the influence of each of the important physical parameter in the system. A typical case with, $H = 1m$, $d = 0.2m$, $r = 1/1.08$, $T = 7s$, $a(0) = 0.01m$, and $b(0) = 0.001m$ is used as the base of the numerical study. The evolution of waves are studied by changing one parameter at the time and keeping other parameters constant. The parametric study shows that interfacial waves exhibit maximum growth rate when they form a symmetric pair forming a 84° angle with respect to the surface wave direction (Figure 7) and thus, a surface wave can excite two oblique interfacial waves. The results indicate that the interfacial wave damping rate is larger than the surface wave damping rate (Figure 10). Weak viscosity effects suppress the generation of the interfacial waves (Figure 9). It is shown that the growth rate of interfacial waves increases with surface wave frequency up to a frequency of about $k_3H = 0.22$ and decreases thereafter (Figure 13). Stratification enhances the interfacial wave growth as well as its damping but slightly reduces surface wave damping rate (Figure 15). As upper layer thickness increases the growth rate of the interfacial waves decreases until about $h/H = 0.8$ and increases thereafter. Finally, it is shown that the interfacial wave growth rate is an increasing linear function of surface wave amplitude. The results of the parametric study are

in qualitative agreement with previous study of Jamali (1998) which was carried out for intermediate depth. However, the effect of stratification in the present study differs from Jamali (1998): While in intermediate depth the stratification weakens the interfacial waves growth, for the range of parameters in this study, stratification enhanced the wave growth.

Unlike intermediate depths, second order nonlinear interactions can occur among a triad of waves in shallow water. To generalize the problem, we expanded the surface wave to 3 surface harmonics to make the study of these interactions possible. The 3 long surface waves are in near-resonant conditions in which their frequency exactly and their wavenumbers approximately satisfy the kinematic conditions of resonance. On the other hand, based on the instability analysis, each of these surface waves can generate a pair of oblique interfacial waves. Therefore, a system of 9 interacting waves is formed. The system is solved numerically. The results of increasing the number of frequencies in the system considerably affect the evolution pattern of the waves. The smooth energy exchange in the 3 wave problem will vanish in the 9 wave system. In addition, the larger system of equation in which oscillators can vary in different time scales, make the system vulnerable to stiffness. In the parameter range of the present problem, this computational issue occurred only in one case in very long time.

CHAPTER III

FREQUENCY DOMAIN FORMULATION

A. Introduction

The theoretical study in Chapter (2) provides invaluable insight in the generation of interfacial waves and temporal evolution of surface waves at initial stages of the interaction. It is also desirable to look into the interaction problem when waves have passed this transient stage and the evolution occurs in space. The of evolution of waves can be described using two approaches: 1- Assuming spatial periodicity and use Fourier series with amplitudes varying with time (Bryant, 1973, e.g.), 2- Or assuming time periodicity and using Fourier series with spatially varying amplitudes (Liu *et al.*, 1985; Kaihatu & Kirby, 1995, e.g.). The spatial evolution of waves of time-harmonic waves has practical significance as most of the available data on waves are recorded as time series at fixed points.

In addition, it is invaluable to obtain a formulation to study the evolution of coupled spectra of surface and interfacial waves. The Boussinesq-type equations in a two layer system, (2.30)-(2.33), can serve as a base for setting up a formulation for spectral evolution. The waves are assumed to be time-periodic. The time-periodic or steady state behavior of the interfacial waves in long term has been verified by experiments (Jamali, 1998) and predicted in theory (Tahvildari & Jamali, 2009).

The instability analysis in Chapter (2) showed that for a range of parameters, a surface wave can generate two oblique interfacial waves. If the surface wave harmonic is generalized to a spectrum, the generated interfacial waves can potentially form a pair of interfacial wave spectra. In the parametric study in the previous chapter, the variation of growth of interfacial waves with directional angle was studied. Table (I)

$T(s)$	$\theta(degrees)$
4	84.33
6	83.94
8	83.82
10	83.76

Table I. Variation of θ (directional angle) with variation of T (surface wave period)

shows that the directional angles of the most energetic interfacial waves are nearly independent of the surface wave frequency. It is seen that in a typical problem with parameters $T = 4 - 10s$ (surface wave period), $H = 1m$, $d = 0.20m$, $r = 0.926$ and $\epsilon = 0.01$, the interfacial waves are generated in an angle of about 84° with respect to the surface wave direction. Therefore, it is confirmed that a spectrum of surface wave can potentially generate two spectrum of oblique interfacial waves and the interfacial wave harmonics in each spectrum form a nearly unidirectional wave train.

In this chapter, we derive a formulation for the spatial evolution of a coupled system formed of one surface wave spectrum and two oblique interfacial wave spectra. As the frequency domain framework allows for explicit treatment of nonlinear interaction terms, it is a suitable platform to study the nonlinear dynamics in the system (Kaihatu, 2003). In the first section, based on two-layer Boussinesq system derived in the previous chapter, we derive a time-harmonic formulation. The solutions are assumed to be periodic in time and represent the spatial evolution of the waves in steady-state condition of the system. The weak two-dimensionality of each of the wave trains suggests that we can apply the parabolic approximation for surface waves in x direction and for interfacial waves in $\pm y$ direction. Therefore, the parabolic equations for spatial evolution of propagating surface and interface waves spectra are

derived.

B. Boussinesq equations for a two-layer fluid

The problem configuration is the same as Figure 1 with the difference that the individual waves in previous chapter are now unidirectional wave spectra. The overbars of depth-averaged velocities are dropped hereafter. The two-layer system (2.30)-(2.33) will be used as the base of the frequency domain model. The long wave approximation allows for substituting the hyperbolic functions in the full dispersion relation with polynomials of dispersiveness (μ^2) orders, and thus, compared to the fully dispersive system, numerical modeling of the Boussinesq equations are significantly facilitated. It is more convenient to eliminate the spatial derivatives of the velocities in nonlinear terms using linear relationships between surface and interface displacements and velocities through continuity equations:

$$\nabla \cdot \mathbf{u}'_t = -\frac{1}{h}(\eta_{tt} - \xi_{tt}) \quad (3.1)$$

$$\nabla \cdot \mathbf{u}_t = -\frac{1}{d}\xi_{tt} \quad (3.2)$$

By these substitutions, equations (2.30)-(2.33) become,

$$(\eta - \xi)_t + h\nabla \cdot \mathbf{u}' + \mathbf{u}' \cdot \nabla(\eta - \xi) - \frac{1}{h}(\eta - \xi)(\eta - \xi)_t = O(\epsilon^2, \epsilon\mu^2) \quad (3.3)$$

$$\mathbf{u}'_t + \mathbf{u}' \cdot \nabla \mathbf{u}' + g\nabla\eta = \frac{-h}{3}\nabla\eta_{tt} - \frac{h}{6}\nabla\xi_{tt} + O(\epsilon^2, \epsilon\mu^2) \quad (3.4)$$

$$\xi_t + d\nabla \cdot \mathbf{u} + \mathbf{u} \cdot \nabla\xi - \frac{1}{d}\xi\xi_t = O(\epsilon^2, \epsilon\mu^2) \quad (3.5)$$

$$\mathbf{u}_t + \mathbf{u} \cdot \nabla \mathbf{u} + g(1-r)\nabla\xi + gr\nabla\eta = -r\frac{h}{2}\nabla\eta_{tt} - \left(\frac{d}{3} + r\frac{h}{2}\right)\nabla\xi_{tt} + O(\epsilon^2, \epsilon\mu^2) \quad (3.6)$$

In the frequency-domain approach, it is assumed that the nonlinear evolution of

wave spectrum is due to resonant triad interactions and non-resonant terms would be neglected. However, the time domain approach does not make any distinction between these interactions. Such differences can lead to discrepancies between the results of the two approaches (Kaihatu & Kirby, 1995). In the present problem, a surface wave train is propagating in x direction and two interfacial waves are propagating in opposite directions and primarily along $\pm y$ axis. The first step in the frequency domain formulation is to assume that variables are periodic in time. Therefore, the variables are expanded in the Fourier series with fundamental frequencies ω_s , denoting the base frequency in surface wave spectrum, and ω_{i1} and ω_{i2} denoting the base frequency of interfacial wave trains 1 and 2, respectively. From parametric study in the previous chapter, it is concluded that the two trains of interfacial waves are identical and thus $\omega_{i1} = \omega_{i2}$. This distinction is made only to clarify the possible triads of interaction. The equations are transformed by assuming the following forms for the variables,

$$\eta = \sum_{n'=1}^{N'} \frac{\hat{\eta}_{sn}(x,y)}{2} e^{in'\omega_s t} + \sum_{n_1=1}^{N_1} \frac{\hat{\eta}_{in1}(x,y)}{2} e^{in_1\omega_{i1}t} + \sum_{n_2=1}^{N_2} \frac{\hat{\eta}_{in2}(x,y)}{2} e^{in_2\omega_{i2}t} + c.c. \quad (3.7)$$

$$\xi = \sum_{n'=1}^{N'} \frac{\hat{\xi}_{sn}(x,y)}{2} e^{in'\omega_s t} + \sum_{n_1=1}^{N_1} \frac{\hat{\xi}_{in1}(x,y)}{2} e^{in_1\omega_{i1}t} + \sum_{n_2=1}^{N_2} \frac{\hat{\xi}_{in2}(x,y)}{2} e^{in_2\omega_{i2}t} + c.c. \quad (3.8)$$

$$\mathbf{u} = \sum_{n'=1}^{N'} \frac{\hat{\mathbf{u}}_{sn}(x,y)}{2} e^{in'\omega_s t} + \sum_{n_1=1}^{N_1} \frac{\hat{\mathbf{u}}_{in1}(x,y)}{2} e^{in_1\omega_{i1}t} + \sum_{n_2=1}^{N_2} \frac{\hat{\mathbf{u}}_{in2}(x,y)}{2} e^{in_2\omega_{i2}t} + c.c. \quad (3.9)$$

$$\mathbf{u}' = \sum_{n'=1}^{N'} \frac{\hat{\mathbf{u}}'_{sn}(x,y)}{2} e^{in'\omega_s t} + \sum_{n_1=1}^{N_1} \frac{\hat{\mathbf{u}}'_{in1}(x,y)}{2} e^{in_1\omega_{i1}t} + \sum_{n_2=1}^{N_2} \frac{\hat{\mathbf{u}}'_{in2}(x,y)}{2} e^{in_2\omega_{i2}t} + c.c. \quad (3.10)$$

where N' , N_1 and N_2 are the total number of harmonics in surface wave spectrum and interfacial wave spectra 1 and 2 respectively. The amplitudes, $\hat{\eta}$, $\hat{\xi}$, $\hat{\mathbf{u}}$ and $\hat{\mathbf{u}}'$ are complex magnitudes and *c.c.* denotes complex conjugates. The terms proportional to $e^{-in'\omega_s t}$ represent the contribution of n th harmonic of the surface wave spectrum on the velocity fields, the surface and interface displacements. Similarly, the terms

proportional to $e^{-in_1 w_{i1} t}$ and $e^{-in_2 w_{i2} t}$, respectively show the representation of interfacial waves 1 and 2 in the motion field. As mentioned, the interfacial waves are identical and thus, in the following calculations, n is used to represent both n_1 and n_2 . By substituting these expansions in the above system, the couplings between the harmonics due to nonlinear interactions are revealed.

C. Resonant triad interaction

Resonant interactions occur due to the nonlinear coupling in equations (2.30)-(2.33). The use of resonant triads will result in factoring out the time periodic terms and gives sets of equations for the Fourier coefficients in equations (3.7)-(3.10) which are essentially the evolution equations of the harmonics.

In the present chapter, the nonlinear interactions due to near-resonance condition between the triad of surface (or interface) harmonics, as discussed in Section (II-E), is generalized to several harmonics forming a spectrum. The quadratic nonlinearity couples the harmonics in the spectra in form of triads. For instance, a surface wave can be assumed to have the following form,

$$\eta_s = a(X)e^{i\psi_n} + a^*(X)e^{-i\psi_n} \quad (3.11)$$

where a is the complex amplitude and is a function of large spatial scale X , and $\psi = \mathbf{k} \cdot \mathbf{x} - \omega t$ is the phase function. Complex conjugate of the amplitude is denoted by a^* . With this definition, the quadratic terms in the equation (3.3) will give rise to the terms proportional to the following components,

$$a_l a_m e^{i(\psi_l + \psi_m)} \quad (3.12)$$

$$a_l a_m^* e^{i(\psi_l - \psi_m)} \quad (3.13)$$

$$a_l^* a_m e^{i(-\psi_l + \psi_m)} \quad (3.14)$$

$$a_l^* a_m^* e^{i(-\psi_l - \psi_m)} \quad (3.15)$$

And thus, a particular component in the free surface wave train oscillating with phase ψ_n , can be forced if two other arbitrary harmonics l , and m , satisfy any of the following conditions,

$$\psi_n = \psi_l + \psi_m \quad (3.16)$$

$$\psi_n = \psi_l - \psi_m \quad (3.17)$$

$$\psi_n = -\psi_l + \psi_m \quad (3.18)$$

$$\psi_n = -\psi_l - \psi_m \quad (3.19)$$

$$(3.20)$$

The above equations result in kinematic resonance condition between triads,

$$\omega_n = \omega_l + \omega_m \quad (3.21)$$

$$\omega_n = \omega_l - \omega_m \quad (3.22)$$

$$\omega_n = -\omega_l + \omega_m \quad (3.23)$$

$$\omega_n = -\omega_l - \omega_m \quad (3.24)$$

The same relationships hold between vector wave numbers but in near-resonant condition; as discussed in Section (II-E), there will be an incremental difference between the wave numbers, as an example:

$$k_n - k_l - k_m = \delta k \quad (3.25)$$

The same discussion applies for the nonlinear terms involving the velocities and interface displacements. The exact resonance between the frequencies allows for factoring out of the time dependence.

D. Time-harmonic equations

Equations (3.7)-(3.10) are inserted in the governing equations and the concept of resonant triads are used to obtain time-harmonic equations for spatial evolution of waves. It is more convenient to obtain the equations in terms of free surface and interface displacements. The velocities are related to derivatives of surface and interface displacements through first order momentum equations as,

$$\hat{\mathbf{u}}'_{sn} = \frac{-ig}{n'\omega_s} \nabla \hat{\eta}_{sn} + O(\epsilon, \mu^2) \quad (3.26)$$

$$\hat{\mathbf{u}}'_{inp} = \frac{-ig}{n_p\omega_{ip}} \nabla \hat{\eta}_{inp} + O(\epsilon, \mu^2) \quad (3.27)$$

$$\hat{\mathbf{u}}_{sn} = \frac{-ig}{n'\omega_s} \nabla [(1-r)\xi_{sn} + r\eta_{sn}] + O(\epsilon, \mu^2) \quad (3.28)$$

$$\hat{\mathbf{u}}_{inp} = \frac{-ig}{n'\omega_{ip}} \nabla [(1-r)\xi_{inp} + r\eta_{inp}] + O(\epsilon, \mu^2) \quad (3.29)$$

where $p = 1, 2$ denotes the two distinct interfacial wave trains. These relationships are used to substitute surface and interface displacements for velocities in the nonlinear terms. The nonlinear terms, forcing the n' th harmonic in surface wave train or the n th harmonic in interfacial wave train can be written as follows,

$$[\eta_s(\eta_s)_t]_{n'} = \frac{-i\omega_s n'}{8} \left[\sum_{l'=1}^{n'-1} \eta_{s,l'} \eta_{s,n'-l'} + 2\eta_{s,l'}^* \eta_{s,n'+l'} \right] \quad (3.30)$$

$$\begin{aligned} (\mathbf{u}_s \cdot \nabla \mathbf{u}_s)_{n'} &= \frac{-g^2}{8\omega_s^2} \left[\sum_{l'=1}^{n'-1} \frac{1}{l'(n'-l')} (\nabla \eta_{s,l'} \cdot \nabla \nabla \eta_{s,n'-l'} + \nabla \eta_{s,n'-l'} \cdot \nabla \nabla \eta_{s,l'}) \right] + \\ &\frac{g^2}{4\omega_s^2} \left[\sum_{l'=1}^{N'-n'} \frac{1}{l'(n'+l')} \nabla \eta_{s,l'}^* \cdot \nabla \nabla \eta_{s,n'+l'} + \nabla \eta_{s,n'+l'} \cdot \nabla \nabla \eta_{s,l'}^* \right] \end{aligned} \quad (3.31)$$

$$\begin{aligned} (\mathbf{u}'_s \cdot \nabla \eta_s)_{n'} &= \frac{-ign'}{8\omega_s} \left[\sum_{l'=1}^{n'-1} \frac{1}{l'(l'-n')} \nabla \eta_{s,l'} \cdot \nabla \eta_{s,n'-l'} \right] + \\ &\frac{ign'}{4\omega_s} \left[\sum_{l'=1}^{N'-n'} \frac{1}{l'(l'+n')} \nabla \eta_{s,l'}^* \cdot \nabla \eta_{s,n'+l'} \right] \end{aligned} \quad (3.32)$$

The nonlinear terms involving interfacial wave amplitude and /or lower layer velocity are derived similarly. These terms become important in near-resonant interactions. However, it is recalled that there is coupling due to exact resonance between each surface wave harmonic and two interfacial harmonics through equation (2.34). For interface wave 2, these coupling are written as follows,

$$[\eta_s(\xi_{i1})_t]_{n_2} = \frac{in_2\omega_{i2}}{4}\eta_{s,l'}\xi_{i1,l'-n_2} \quad (3.33)$$

$$[\xi_{i1}(\eta_s)_t]_{n_2} = \frac{-in_2\omega_{i2}}{2}\eta_{s,l'}\xi_{i1,l'-n_2} \quad (3.34)$$

$$(\mathbf{u}'_s \cdot \nabla \xi_{i1})_{n_2} = \frac{-ig}{4l'\omega_s}\nabla\eta_{s,l'} \cdot \nabla \xi_{i1,l'-n_2} \quad (3.35)$$

$$(\mathbf{u}_s \cdot \nabla \xi_{i1})_{n_2} = \frac{-igr}{4l'\omega_s}\nabla\eta_{s,l'} \cdot \nabla \xi_{i1,l'-n_2} \quad (3.36)$$

Nonlinear terms for interface wave 1 are obtained similarly. Substituting the expansions (3.7)-(3.10) in (3.3)-(3.6) and using above equations for nonlinear terms, the transformed continuity and momentum equations are obtained. By cross differentiation of the continuity and momentum equations in each layer, the velocities are eliminated and the time periodic equations for $\eta_{s,n'}$, $\eta_{i,n}$, $\xi_{s,n'}$, $\xi_{i,n}$ are obtained. Combining upper layer continuity and momentum equations gives,

$$\begin{aligned} & n'^2\omega_s^2(\eta_{s,n'} - \xi_{s,n'}) - G'_n \nabla^2 \eta_{s,n'} + \frac{h^2}{6}n'^2\omega_s^2 \nabla^2 \xi_{s,n'} = \\ & \frac{-gn'^2}{4} \left[\sum_{l'=1}^{n'-1} \frac{\nabla\eta_{s,l'} \cdot \nabla\eta_{s,n'-l'}}{l'(n'-l')} - 2 \sum_{l'=1}^{N'-n'} \frac{\nabla\eta_{s,l'}^* \cdot \nabla\eta_{s,n'+l'}}{l'(n'+l')} \right] + \\ & \frac{n'^2\omega_s^2}{4h} \left[\sum_{l'=1}^{n'-1} \eta_{s,l'}\eta_{s,n'-l'} + 2 \sum_{l'=1}^{N'-n'} \eta_{s,l'}^*\eta_{s,n'+l'} - h\xi_{i,l1}\xi_{i,n'-l1} \right] - \\ & \frac{g^2h}{4\omega_s^2} \left[\sum_{l'=1}^{n'-1} \frac{1}{l'(n'-l')} \nabla \cdot (\nabla\eta_{s,l'} \cdot \nabla(\nabla\eta_{s,n'-l'}) + \nabla\eta_{s,n'-l'} \cdot \nabla(\nabla\eta_{s,l'})) \right] - \\ & \frac{g^2h}{2\omega_s^2} \left[\sum_{l'=1}^{N'-n'} \frac{1}{l'(n'+l')} \nabla \cdot (\nabla\eta_{s,l'}^* \cdot \nabla(\nabla\eta_{s,n'+l'}) + \nabla\eta_{s,n'+l'} \cdot \nabla(\nabla\eta_{s,l'}^*)) \right] \quad (3.37) \\ & n^2\omega_i^2(\eta_{i,n} - \xi_{i,n}) - G_n \nabla^2 \eta_{i,n} + \frac{h^2}{6}n^2\omega_i^2 \nabla^2 \xi_{i,n} = \end{aligned}$$

$$\begin{aligned} & \frac{-n^2\omega_i^2}{h} \left[\frac{1}{2}\eta_{s,l'}\xi_{i,l'-n'} - \frac{1}{4} \left(\sum_{l=1}^{n-1} \xi_{i,l}\xi_{i,n-l} + 2 \sum_{l=1}^{N-n} \xi_{i,l}^*\xi_{i,n+l} \right) \right] + \\ & \frac{g}{4}\nabla\eta_{s,n} \cdot \nabla\xi_{i,n}^* \end{aligned} \quad (3.38)$$

where $G'_n = gh - \frac{n'^2\omega_s^2h^2}{3}$, and similarly $G_n = gh - \frac{n^2\omega_s^2h^2}{3}$. Combination of lower layer momentum and continuity equations results in,

$$\begin{aligned} & n'^2\omega_s^2\xi_{s,n'} - rd \left(g - \frac{h}{2}n'^2\omega_s^2 \right) \nabla^2\eta_{s,n'} - d \left[g(1-r) - \left(\frac{d}{3} + \frac{rh}{2}n'^2\omega_s^2 \right) \right] \nabla^2\xi_{s,n'} = \\ & \frac{g^2r^2d}{4\omega_s^2} \left[\sum_{l'=1}^{n'-1} \frac{1}{l'(n'-l')} \nabla \cdot (\nabla\eta_{s,l'} \cdot \nabla\nabla\eta_{s,n'-l'} + \nabla\eta_{s,n'-l'} \cdot \nabla\nabla\eta_{s,l'}) \right] - \\ & \frac{g^2r^2d}{2\omega_s^2} \left[\sum_{l'=1}^{N'-n'} \frac{1}{l'(n'+l')} \nabla \cdot (\nabla\eta_{s,l'}^* \cdot \nabla\nabla\eta_{s,n'+l'} + \nabla\eta_{s,n'+l'} \cdot \nabla\nabla\eta_{s,l'}^*) \right] - \\ & \frac{2g^2(1-r)^2d}{n'^2\omega_s^2} \nabla \cdot (\nabla\xi_{i,l1} \cdot \nabla\nabla\xi_{i,m2}) - g(1-r)(\nabla\xi_{i,l1} \cdot \nabla\xi_{i,m2}) + \\ & \frac{n'^2\omega_s^2}{4d} (\xi_{i,l1}\xi_{i,m2}) \end{aligned} \quad (3.39)$$

$$\begin{aligned} & n^2\omega_i^2\xi_{i,n} - rd \left(g - \frac{h}{2}n^2\omega_i^2 \right) \nabla^2\eta_{i,n} - d \left[g(1-r) - \left(\frac{d}{3} + \frac{rh}{2}n^2\omega_i^2 \right) \right] \nabla^2\xi_{i,n} = \\ & -\frac{g(1-r)^2d}{4n^2\omega_i^2} \left[\sum_{l=1}^{n-1} \frac{1}{l(n-l)} \nabla \cdot (\nabla\xi_{i,l} \cdot \nabla\nabla\xi_{i,n-l} + \nabla\xi_{i,n-l} \cdot \nabla\nabla\xi_{i,l}) \right] + \\ & \frac{g(1-r)^2d}{2\omega_i^2} \left[\sum_{l=1}^{N-n} \frac{1}{l(n+l)} \nabla \cdot (\nabla\xi_{i,l}^* \cdot \nabla\nabla\xi_{i,n+l} + \nabla\xi_{i,n+l} \cdot \nabla\nabla\xi_{i,l}^*) \right] - \\ & \frac{gn^2(1-r)}{4} \left[\sum_{l=1}^{n-1} \frac{1}{l(n-l)} \nabla\xi_{i,l} \cdot \nabla\xi_{i,n-l} - 2 \sum_{l=1}^{N-n} \frac{1}{l(n+l)} \nabla\xi_{i,l}^* \cdot \nabla\xi_{i,n+l} \right] + \\ & \frac{g^2r(1-r)d}{4n^2\omega^2} \nabla \cdot [\nabla\xi_{i2}^* \cdot \nabla\nabla\eta_{s,l'} \cdot \nabla\nabla\xi_{i2}^*] + \frac{n^2\omega^2}{4d} \left[\sum_{l=1}^{n-1} \xi_{i,l}\xi_{i,n-l} + 2 \sum_{l=1}^{N-n} \xi_{i,l}^*\xi_{i,n+l} \right] \end{aligned} \quad (3.40)$$

The above set of equations give the transformed surface and interface displacements. The order of truncation of above equations is the same as the governing equations and equal to $O(\epsilon^2, \epsilon\mu^2)$. The equations are elliptic. Therefore, boundary conditions in the entire domain should be known to solve them which is generally not possible

in open ocean. Furthermore, the discretization of the domain needs to be sufficiently fine which results in high computational demands. The parabolic approximation, discussed in the next section, can ease these modeling issues.

E. Parabolic approximation

The parabolic approximation transforms the elliptic boundary value problem to a parabolic initial value problem (Radder, 1979; Lozano & Liu, 1980). The parabolic system requires only the information on lateral boundaries and the initial value and thus, is suitable for studying the propagation of waves in an open coast. The method has the limitation of small angle of approach and thus is most useful in weakly-two dimensional problems. However, this limitation does not violate the conditions of our study. The results from the instability analysis in previous chapter indicates that the direction of generated interfacial waves is almost normal to the direction of the surface wave and furthermore, as mentioned earlier in the chapter, is almost independent of the surface wave frequency. Therefore, a surface wave train can generate two nearly unidirectional oblique interfacial wave trains. The interfacial wave trains will propagate in a symmetric direction with respect to the surface wave. Consequently, if the surface wave spectrum is primarily propagating in $+x$ direction, the interfacial waves will primarily propagate in $\pm y$ direction. Based on weakly two-dimensional nature of each wave train, parabolic approximation can be used for the surface spectrum in x and for interface wave spectrum in y ,

$$\eta_{sn} = A_{sn}(x)e^{in'k_sx} \quad (3.41)$$

$$\xi_{inp} = B_{inp}(x, y)e^{in_pk_ipy} \quad (3.42)$$

where $A_{sn}(x)$ and $B_{in}(x, y)$ are complex amplitudes and slowly varying function of space. The direction of propagation of surface wave is set as x axis and for simplifying the problem, we assume the water depth is constant. With this assumption, the interfacial waves propagate with a small angle relative to y axis. To account for this weak two dimensional behavior, the fast varying term (oscillation) of the interfacial waves is assumed to be a function of y and the slow varying component of the wave (B_{in}) is assumed to be a function of both x and y . Therefore, the interfacial waves are primarily propagating along y axis but can have evolution along x axis. The parabolic approximation is applied on the derivatives and the terms are ordered in advance using (similar to Liu *et al.*, 1985):

$$\frac{\partial^s A_{sn}}{\partial x^s} \approx \frac{\partial^s B_{inp}}{\partial y^s} \approx O(\epsilon^s) \quad (3.43)$$

$$\frac{\partial^s B_{inp}}{\partial x^s} \approx O(\epsilon^{s/2}) \quad (3.44)$$

where $s = 1, 2$. One consequence of having the phase as a function of only one direction is that the fast varying part of the solution is only retained in the phase accumulation in that direction (y for the interfacial wave, and x for surface wave). Orderings (3.43) and (3.44) allow for retention of higher order derivatives of interfacial wave amplitudes in x direction to mimic their wave-like variation along this axis. In addition, this ordering results in elimination of derivatives in the nonlinear terms. Substituting (3.41) and (3.42) in equations (3.38)-(3.40) and applying above approximations gives the parabolic models. The upper layer continuity equation gives,

$$p_1 A_{sn} + p_2 B_{sn} + p_3 (A_{sn})_x + p_4 (B_{sn})_x = Q_1 \left[\sum_{l'=1}^{n'-1} A_{s,l'} A_{s,n'-l'} + 2 \sum_{l'=1}^{N'-n'} A_{s,l'}^* A_{s,n'+l'} \right] + Q_2 B_{il}^2 \quad (3.45)$$

where

$$p_1 = n'^2 \omega_s^2 + G'_n k_{sn}^2 \quad (3.46)$$

$$p_2 = -n'^2 \omega_s^2 \left(1 + \frac{k_{sn}^2 h^2}{6}\right) \quad (3.47)$$

$$p_3 = -2i G'_n k_{sn} \quad (3.48)$$

$$p_4 = i \frac{h^2}{3} n'^2 \omega_s^2 k_{sn}^2 \quad (3.49)$$

$$Q_1 = \frac{k_s^2}{4} \left(g n'^2 + \frac{\alpha_s^2 n'^2}{h} - \frac{g^2 h}{\alpha_s^2} \right) \quad (3.50)$$

$$Q_2 = \frac{n'^2 \alpha_s^2 k_s^2}{4} \quad (3.51)$$

The transformed momentum equation in the upper layer is,

$$p_5 A_{in} + p_6 B_{in} + p_7 (A_{in})_y + p_8 (B_{in})_y + p_9 (A_{in})_{xx} + p_{10} (B_{in})_{xx} = Q_3 \left[\sum_{l=1}^{n-1} B_{i,l} B_{i,n-l} + 2 \sum_{l=1}^{N-n} B_{i,l}^* B_{i,n+l} \right] + Q_4 A_{sl} B_{im}^* \quad (3.52)$$

where

$$p_5 = (n^2 \omega_i^2 + G_n k_{in}^2) \quad (3.53)$$

$$p_6 = -n^2 \omega_i^2 \left(1 + \frac{k_{in}^2 h^2}{6}\right) \quad (3.54)$$

$$p_7 = -2i G_n k_{in} \quad (3.55)$$

$$p_8 = i \frac{h^2}{3} n^2 \omega_i^2 k_{in}^2 \quad (3.56)$$

$$p_9 = -G_n \quad (3.57)$$

$$p_{10} = \frac{h^2}{6} n^2 \omega_i^2 \quad (3.58)$$

$$Q_3 = -\frac{n^2 \alpha_i^2 k_i^2}{4h} \quad (3.59)$$

$$Q_4 = \frac{n^2 \alpha_i^2 k_i^2}{2h} - \frac{g}{8} n^2 k_{s,l}^2 \quad (3.60)$$

Similarly, parabolic version of lower layer continuity equation will be,

$$p_{11}A_{sn} + p_{12}B_{sn} + p_{13}(A_{sn})_x + p_{14}(B_{sn})_x = Q_5 \left[\sum_{l'=1}^{n'-1} A_{s,l'} A_{s,n'-l'} + 2 \sum_{l'=1}^{N'-n'} A_{s,l'}^* A_{s,n'+l'} \right] + Q_6 B_{il}^2 \quad (3.61)$$

where

$$p_{11} = rdk_{sn}^2 \left(g - \frac{h}{2} n'^2 \omega_s^2 \right) \quad (3.62)$$

$$p_{12} = n'^2 \omega_s^2 \left(1 - k_{sn}^2 d \left[\frac{d}{3} + \frac{rh}{2} \right] \right) + k_{sn}^2 g d (1 - r) \quad (3.63)$$

$$p_{13} = -2irdk_{sn} \left(g - \frac{h}{2} n'^2 \omega_s^2 \right) \quad (3.64)$$

$$p_{14} = -2idk_{sn} \left(g[1 - r] - \left[\frac{d}{3} + \frac{rh}{2} \right] n'^2 \omega_s^2 \right) \quad (3.65)$$

$$Q_5 = \frac{g^2 r^2 d n'^2 k_s^2}{4\alpha_s^2} \quad (3.66)$$

$$Q_6 = n'^2 \frac{k_s^2}{2} \left(1 - \frac{k_i^2}{2k_{ix}^2} \right) \left[\frac{-gd(1-r)^2}{\alpha_s^2} \left(1 - \frac{k_i^2}{2k_{ix}^2} \right) + g(1-r) \right] + \frac{n'^2 \alpha_s^2 k_s^2}{4d} \quad (3.67)$$

And finally, equation (3.40) gives,

$$p_{15}A_{in} + p_{16}B_{in} + p_{17}(A_{in})_y + p_{18}(B_{in})_y + p_{19}(A_{in})_{xx} + p_{20}(B_{in})_{xx} = Q_7 \left[\sum_{l=1}^{n-1} B_{i,l} B_{i,n-l} + 2 \sum_{l=1}^{N-n} B_{i,l}^* B_{i,n+l} \right] + Q_8 A_{sl} B_{im}^* \quad (3.68)$$

where

$$p_{15} = rdk_{in}^2 \left(g - \frac{h}{2} n^2 \omega_i^2 \right) \quad (3.69)$$

$$p_{16} = n^2 \omega_i^2 \left(1 - k_{in}^2 d \left[\frac{d}{3} + \frac{rh}{2} \right] \right) + k_{in}^2 g d (1 - r) \quad (3.70)$$

$$p_{17} = 2irdk_{in} \left(g - \frac{h}{2} n^2 \omega_i^2 \right) \quad (3.71)$$

$$p_{18} = -2idk_{in} \left(g[1 - r] - \left[\frac{d}{3} + \frac{rh}{2} \right] n^2 \omega_i^2 \right) \quad (3.72)$$

$$p_{19} = -rd \left(g - \frac{h}{2} n^2 \omega_i^2 \right) \quad (3.73)$$

$$p_{20} = -d \left(g[1-r] - \left[\frac{d}{3} + \frac{rh}{2} \right] n^2 \omega_i^2 \right) \quad (3.74)$$

$$Q_7 = \frac{k_i^2}{4} \left[\frac{-gd(1-r)^2}{\alpha_i^2} - g(1-r)^2 n^2 + \frac{n^2 \alpha_i^2}{d} \right] \quad (3.75)$$

$$Q_8 = \frac{g^2 r d (1-r) n^2}{2\alpha_i^2} k_{il,x}^2 \quad (3.76)$$

Equations (3.45) and (3.61) can be further combined to obtain a single parabolic equation for evolution of surface wave amplitude (A_{sn}). Similarly, combining equations (3.52) and (3.68) gives the evolution equation of interfacial wave amplitude (B_{in}),

$$\lambda_1 A_{sn} + \lambda_2 (A_{sn})_x = R_1 \left[\sum_{l'=1}^{n'-1} A_{s,l'} A_{s,n'-l'} + 2 \sum_{l'=1}^{N'-n'} A_{s,l'}^* A_{s,n'+l'} \right] + R_2 B_{il}^2 \quad (3.77)$$

$$\lambda_3 B_{in} + \lambda_4 (B_{in})_y + \lambda_5 (B_{in})_{xx} = R_3 \left[\sum_{l=1}^{n-1} B_{i,l} B_{i,n-l} + 2 \sum_{l=1}^{N-n} B_{i,l}^* B_{i,n+l} \right] + R_4 A_{sl} B_{i,l'-n}^* \quad (3.78)$$

where

$$\lambda_1 = p_1 - \frac{p_2}{p_{12}} p_{11} \quad (3.79)$$

$$\lambda_2 = p_3 - \frac{p_2}{p_{12}} p_{13} - \left(p_4 - \frac{p_2}{p_{12}} \right) \frac{p_{11}}{p_{12}} p_{14} \quad (3.80)$$

$$\lambda_3 = p_6 - \frac{p_5}{p_{15}} p_{16} \quad (3.81)$$

$$\lambda_4 = p_8 - \frac{p_5}{p_{15}} p_{18} - \left(p_7 - \frac{p_5}{p_{15}} p_{17} \right) \frac{p_{16}}{p_{15}} \quad (3.82)$$

$$\lambda_5 = p_{10} - \frac{p_5}{p_{15}} p_{20} - \left(p_9 - \frac{p_5}{p_{15}} p_{19} \right) \frac{p_{16}}{p_{15}} \quad (3.83)$$

$$R_1 = Q_1 - \frac{p_2}{p_{12}} Q_5 \quad (3.84)$$

$$R_2 = Q_2 - \frac{p_2}{p_{12}} Q_6 \quad (3.85)$$

$$R_3 = Q_3 - \frac{p_5}{p_{15}} Q_7 \quad (3.86)$$

$$R_4 = Q_4 - \frac{p_5}{p_{15}} Q_8 \quad (3.87)$$

$$(3.88)$$

Based on approaches in previous investigation to model the two-dimensional parabolic equations, it is suggested to model the present parabolic equations using Crank-Nicholson scheme. The scheme has second order accuracy in x and y and is unconditionally stable. The finite difference model obtained will be similar to the KP model in Liu *et al.* (1985) where the numerical scheme is given in detail (albeit for a single layer).

A two-layer dispersion relation is provided by Pond & Pickard (1983) for $\Delta\rho \ll 1$:

$$\left[\omega^2 - gk \tanh(kh + kd) \right] \left[\omega^2 - \frac{\Delta\rho gk}{\rho' \coth kh + \rho \coth kd} \right] = 0 \quad (3.89)$$

By comparing the roots from this equation with the quartic two-layer dispersion relation (Lamb, 1932), it is found that the above relationship provides very good estimates of surface and interfacial roots in the range of parameters studied here. Using this equation in the non-dispersive limit, $kh \approx kd \ll \mathcal{O}(1)$, the surface and interfacial wave numbers and frequencies can be written in terms of the base frequencies at surface and interface respectively,

$$k_{sn} = n' k_s, \quad k_{in} = n k_i \quad (3.90)$$

Base wave number and frequencies are the lowest mode in the spectra, and using the above expressions, the wave numbers for the harmonics are written in terms of the base wave number. Furthermore, base wavenumbers, k_s and k_i , can be obtained as

functions of the base wave frequencies as:

$$k_s = \frac{\omega_s}{\sqrt{g(h+d)}}, \quad k_i = \omega_i \sqrt{\frac{\rho'd + \rho h}{\Delta \rho g h d}} \quad (3.91)$$

The above expressions can be used to exchange wave numbers and frequencies.

It is instructive to look into the relationship between primary surface wave, A_s , and its signature on the interface, B_s , and also the relationship between primary interfacial wave, B_i , and its surface signature, A_i . From the linear theory, the relationship between the primary waves and their signatures are readily obtained in long wave limit:

$$\frac{b}{a} = 1 + \frac{k^2 h^2}{2} - \frac{g k^2 h}{\omega^2} \left(1 + \frac{k^2 h^2}{6} \right) \quad (3.92)$$

Using the dispersion relation (3.89), the expression for the surface and interfacial wave signatures is obtained as follows,

$$\frac{b_s}{a_s} \approx \mathcal{O}\left(\frac{d}{H}\right) + \mathcal{O}(\mu^2), \quad \frac{b_i}{a_i} \approx \mathcal{O}\left(\frac{\rho' + \rho \frac{h}{d}}{\Delta \rho}\right) + \mathcal{O}(\mu^2) \quad (3.93)$$

From above equations, it is evident that the amplitude of the signature wave depends on the magnitude of the primary wave and physical parameters. The amplitude of the interface signature of the surface wave depends primarily on the depth ratio and the magnitude of the surface signature of the interfacial wave mainly is a function of stratification. In ocean environment the stratification is weak and thus, the surface signature of the interfacial wave will be significantly smaller than the primary interfacial wave. In addition, if the lower layer is significantly thinner than the total fluid depth (e.g. a thin layer of fluidized mud), the interface signature of the surface wave will be considerably smaller than the primary surface wave. From (3.93), and by obtaining the evolution of primary surface and interfacial waves. The evolution of their signature can be obtained at the first order.

F. Summary

Based on the two-layer Boussinesq equation derived in Chapter (2), a frequency domain model is derived for spatial evolution of long surface and interfacial waves. In this approach, the variables are assumed to be periodic in time and the concept of resonant triads is used. As a result, a time-harmonic elliptic model for the spatial evolution of the waves in a two-layer system is derived. Based on the weak two-dimensionality of surface and interfacial wave trains, parabolic approximation was used to alleviate the computational demands and restrictions of the boundary condition requirements in the original elliptic model.

CHAPTER IV

CONCLUSIONS

A. Summary

In this dissertation, nonlinear interactions between long gravity waves in a two-layer fluid are studied. The previous studies on surface-interface wave interactions either used deep water (Stokes) scaling and thus were limited to intermediate-deep waters, or investigated the problem in very shallow waters (non-dispersive limit). We extend the study to shallow-intermediate depth where waves are in weakly dispersive domain, derive and verify a formulation to study the waves, and analyze the system for dynamics of subharmonic generation of a pair of oblique interfacial waves due to resonant interaction with a monochromatic surface wave in shallow water. In addition, we expand the problem to include a triad of surface wave which exchange energy due to near-resonance condition and also are in coupling with their corresponding interfacial wave pairs. The near-resonant interactions between unidirectional interfacial wave harmonics are also accounted for. Therefore, unlike previous studies that isolated a triad of waves (one surface and two interface), we expand the 3 wave problem to 9 waves to include near-resonant interactions. Finally, a formulation for spatial evolution of a surface wave spectrum in interaction with two oblique interfacial wave spectra is derived in frequency domain.

In Chapter (2), a two-dimensional Boussinesq-type model for propagation of weakly-dispersive waves in a two fluid system is derived. The fluid layers are assumed to be inviscid and incompressible with potential flow. The model is verified as the assumptions of slow varying bottom and shallow lower layer are applied to the model by Choi & Camassa (1996), their equations reduce to the model presented in

this study. Then the resonant interaction between surface and interfacial waves, as a generation mechanism for long interfacial waves, is studied. A second order perturbation approach is applied and temporal evolution equations of the interacting waves amplitudes are derived. In the intermediate-deep water, the instability coefficients are extremely lengthy and complicated, whereas by using depth-averaged velocities in Boussinesq equations, the interaction coefficient has been greatly simplified. In addition, the damping effect of the viscosity, due to presence of a weakly viscous lower layer, is added to the evolution equations. By considering the nonlinear energy transfer from the surface mode to interfacial modes and adding the viscous decay in the evolution of the interfacial waves, we have considered an additional indirect mechanism of surface wave attenuation which was usually neglected in previous studies. Furthermore, a numerical parametric study is carried out to study the influence of important parameters namely directional angle, viscosity of the lower layer, surface wave amplitude and frequency, thickness of the top layer and density difference on the growth rate of the interfacial waves (2.72). In the typical for the parametric study we use $H = 1m$, $d = 0.2m$, $r = 1/1.08$, $T = 7s$, $a(0) = 0.01m$, and $b(0) = 0.001m$.

The maximum growth rate of interfacial waves occurs when $\theta = 84^\circ$ (Figure 6). In the absence of strong interfacial shear in weakly viscous layers, viscosity only suppresses the generation of interfacial waves. Damping rate is an increasing function of viscosity (figure 10). Interfacial growth rate increases with surface wave frequency until it reaches a maximum in shallow water range and decreases thereafter. Similar behavior is predicted for interfacial damping rate. Furthermore, it appears that the damping rate of surface is not significantly sensitive to the surface wave frequency (Figure 13). Stratification increases both the growth and damping rate of the interfacial waves. However, the sensitivity of the growth and damping rate to density difference decreases in large density differences. In contrast to this result, in inter-

mediate depth, the theory predicts that the growth rate is a decreasing function of density ratio ($1/r$) (Jamali, 1998, e.g.). As the thickness of the top layer increases to comprise higher ratio of the total water depth, the growth rate of the interfacial waves decreases until $h/H \simeq 0.80$. Surface wave attenuation rate is a mild decreasing function of top layer thickness. Except for the density ratio, as mentioned above, the results of the analysis are in qualitative agreement of the previous work of Hill & Foda (1998) and Jamali (1998) which studied the waves in intermediate depth.

As mentioned, harmonics of surface (or interfacial) waves can form triads of nonlinear interaction if they satisfy kinematic conditions of near-resonance. Therefore, to generalize the study of nonlinear interactions in shallow water, we consider an interacting triad of waves on surface. According to the results in section (II-B), each surface wave generates two oblique subharmonic interfacial waves and thus, a system of 9 waves forms. The interfacial harmonics are also in shallow water range and are thereby in near-resonance condition. A system of 9 evolution equations is derived and the evolution of the waves under variation of different parameters is studied. It is concluded that as the number of waves in the system increases, the behavior of interacting waves changes significantly. In almost all the cases, surface waves 1 and 3 show initial oscillatory behavior while surface wave 2 exhibits initial growth. The growth of surface wave 2 is increased when the density difference is reduced (Figure 29). The three interfacial waves show growth after about $t = 1700s$. The introduction of the interfacial waves in the interaction results in the significant change in the pattern and phase of the surface waves. In contrast to the 3 wave problem, in the 9 wave system, the interfacial waves growth is a decreasing function of density ratio (Figure 30). Variation of waves with depth ratio is also examined. The growth rate of surface wave 2 is maximum when the interface is closer to the interface (Figure 31). In agreement with the 3 wave problem, interfacial waves 1 and 2 exhibit the largest

growth rate when the interface is closest to the surface (Figure 32). In contrast, b_3 has the maximum growth rate at $h/H = 0.7$. Unlike previous cases, if ω_{s3} is increased, surface wave 3 shows initial growth. Surface wave 2 has the largest growth rate at the largest ω_{s3} (Figure 33). All the interfacial waves show the largest growth rate with the lowest frequency, $\omega_{s3} = 0.15$, but they gain largest long term amplitude and variations with $\omega_{s3} = 0.3$ (Figure 34).

In Chapter (3), based on the derived two-layer Boussinesq equation, a frequency domain model is formulated for spatial evolution of time-harmonic interacting surface and interfacial wave trains. Frequency domain formulation facilitates the investigation of evolution of waves due to nonlinear interactions. The derived time-harmonic model is elliptic and thus, its modeling requires fine grid resolution and also has to have defined boundary conditions a priori. Based on the weak two-dimensional nature of surface and interfacial wave trains, the parabolic approximation is used. This approximation alleviates the computational demands as well as restrictions of the boundary condition in the original elliptic model. The derived model can be used to model the propagation of the interacting surface and interfacial wave trains.

B. Recommendations

In the interaction analysis, we do not account for complications in the field type conditions. An example is the sea bed modulation in large time and space scales which can result in shoaling and breaking of both surface and interfacial waves.

The study of long-term behavior of waves requires inclusion of higher order non-linearity in the system. In addition, highly nonlinear waves are common in coastal areas and thus, a higher order nonlinear model can capture wave with larger amplitudes.

In the analysis, the effect of viscosity is limited to damping and is reflected in the evolution equations of waves. such treatment of viscous effects is justifiable when the the system is weakly viscous. However, in highly viscous media, the destabilizing effect of viscosity as a result of shear stress at the interface should also be considered.

Although in the two-layer Boussinesq equations we considered mildly varying bathymetry, in modeling the equations in frequency domain we assumed constant depth. The study can be generalized to include evolution of waves due to varying bathymetry.

REFERENCES

- AGNON, Y., SHEREMET, A., GONSALVES, J. & STIASSNIE, M. 1993 Nonlinear evolution of a unidirectional shoaling wave field. *Coast. Engng.* **20**, 29–58.
- BALL, F. K. 1964 Energy transfer between external and internal gravity waves. *J. Fluid Mech.* **19**, 465–478.
- BENJAMIN, T. B. 1966 Internal waves of finite amplitude and permanent form. *J. Fluid Mech.* **25**, 241–270.
- BRYANT, P. J. 1973 Periodic waves in shallow water. *J. Fluid Mech.* **59**, 625–644.
- BRYANT, P. J. 1974 Stability of periodic waves in shallow water. *J. Fluid Mech.* **66**, 81–96.
- CACCHOINE, D. A., DRAKE, D. E., KAYEN, R. W., STERNBERG, R. W., KINEKE, G. C. & TATE, G. B. 1995 Measurements in the bottom boundary layer on the amazon subaqueous delta. *Mar. Geol.* **125**, 235–258.
- CHEN, Q., KIRBY, J. T., DALRYMPLE, R. A., SHI, F. Y. & THORNTON, E. B. 2003 Boussinesq modeling of longshore currents. *J. Geophys. Res.* **108**, 3362.
- CHOI, W. & CAMASSA, R. 1996 Weakly nonlinear internal waves in a two-fluid system. *J. Fluid Mech.* **313**, 83–103.
- CHOI, W. & CAMASSA, R. 1999 Fully nonlinear internal waves in a two-fluid system. *J. Fluid Mech.* **396**, 1–36.
- DALRYMPLE, R. A. & LIU, P. L. F. 1978 Waves over soft muds: a two-layer fluid model. *J. Phys. Oceanogr.* **8**, 1121–1131.

- DAVIS, R. E. & ACRIVOS, A. 1967 The stability of oscillatory internal waves. *J. Fluid Mech.* **30**, 723–736.
- DEBSARMA, S., DAS, K. P. & KIRBY, J. T. 2010 Fully nonlinear higher-order model equations for long internal waves in a two-fluid system. *J. Fluid Mech.* **654**, 281–303.
- DINGEMANS, M. W. 1993 *Water Wave Propagation over Uneven Bottoms*. World Scientific.
- ELGAR, S. & GUZA, R. T. 1985 Observations of bispectra of shoaling surface gravity waves. *J. Fluid Mech.* **161**, 425–448.
- FODA, M. A. & HILL, D. F. 1998 Nonlinear energy transfer from semidiurnal barotropic motion to near-inertial baroclinic motion. *J. Phys. Oceanogr.* **28**, 1865–1872.
- FREILICH, M. H. & GUZA, R. T. 1984 Nonlinear effects on shoaling surface gravity waves. *Proc. R. Soc. Lond. A* **311**, 1–41.
- HELLAND-HANSEN, B. & NANSEN, F. 1909 The Norwegian sea. *Rep. Norweg. fish and Mar. Invest.* **2**, N.1 and 2.
- HILL, D. F. 2002 The faraday resonance of interfacial waves in weakly viscous fluids. *Phys. Fluids* **14**, 158–169.
- HILL, D. F. 2004 Weakly nonlinear cubic interactions between surface waves and interfacial waves :an analytic solution. *Phys. Fluids* **16**, 839–842.
- HILL, D. F. & FODA, M. A. 1996 Subharmonic resonance of short internal standing waves by progressive surface waves. *J. Fluid Mech.* **321**, 217–233.

- HILL, D. F. & FODA, M. A. 1998 Subharmonic resonance of oblique interfacial waves by a progressive surface wave. *Proc. R. Soc. Lond. A* **454**, 1129–1144.
- HSIAO, S. V. & SHEMDIN, O. H. 1980 Interaction of ocean waves with a soft bottom. *J. Phys. Oceanogr.* **10**, 605–610.
- JAMALI, M. 1998 Surface wave interaction with oblique internal waves. PhD thesis, The University of British Columbia.
- JARAMILLO, S. A., SHEREMET, A., ALLISON, M. A., REED, A. H. & HOLLAND, K. T. 2009 Wave-mud interactions over the muddy atchafalaya subaqueous clinof orm, louisiana, united states: wave-supported sediment transport. *J. Geophys. Res.* **114**, C04002.
- KAIHATU, J. M. 2003 Frequency domain wave models in the nearshore and surf zones. In *Advances in Coastal Modeling* (ed. V. C. Lakhan), pp. 43–72. Elsevier Science B. V.
- KAIHATU, J. M. & KIRBY, J. T. 1995 Nonlinear transformation of waves in finite water depth. *Phys. Fluids* **7**, 1903–1914.
- KAIHATU, J. M. & KIRBY, J. T. 1998 Two-dimensional parabolic modeling of extended boussinesq equations. *J. Waterw. Port C-ASCE* **124**, 57–67.
- KAIHATU, J. M., SHEREMET, A. & HOLLAND, K. T. 2007 A model for propagation of nonlinear surface waves over viscous muds. *Coast. Engng.* **10**, 752–764.
- KOOP, C. G. & BUTLER, G. 1981 An investigation of internal solitary waves in a two-fluid system. *J. Fluid Mech.* **112**, 225–251.
- LAMB, H. 1932 *Hydrodynamics*. Cambridge University Press.

- LEWIS, J., BRUCE, M. L. & DENNY, R. S. K. 1974 On the interaction of internal waves and surface gravity waves. *J. Fluid Mech.* **63**, 773–800.
- LIU, A. K. 1988 Analysis of nonlinear internal waves in the new york bight. *J. Geophys. Res.* **93**, 122–317.
- LIU, C. M. 2006 Second-order random internal and surface waves in a two-fluid system. *Geophys. Res. Lett.* **33**, L06610.
- LIU, P. L. F., YOON, S. B. & KIRBY, J. T. 1985 Nonlinear refraction/diffraction of waves in shallow water. *J. Fluid Mech.* **153**, 184–201.
- LOZANO, C. J. & LIU, P. L. F. 1980 Refraction/diffraction models for linear surface water waves. *J. Fluid Mech.* **101**, 708–720.
- LYNETT, P. J. & LIU, P. L. F. 2002 A two-dimensional depth-integrated model for internal wave propagation over variable bathymetry. *Wave Motion* **36**, 221–240.
- MACPHERSON, H. 1980 The attenuation of water waves over a non-rigid bed. *J. Fluid Mech.* **97**, 721–742.
- MADSEN, P. A., MURRAY, R. & SORENSEN, O. R. 1991 A new form of the boussinesq equations with improved linear dispersion characteristics. *Coast. Engng.* **15**, 371–388.
- MAXWORTHY, T. 1979 A note on the internal solitary waves produced by tidal flow over a three-dimensional ridge. *J. Geophys. Res.* **84**, 338–346.
- MEI, C. C., STIASSNIE, M. & YUE, D. K. P. 2005 *Theory and Applications of Ocean Surface Waves*. World Scientific.

- MEI, C. C. & UNLUATA, U. 1972 Harmonic generation in shallow water waves. In *Waves on Beaches and Resulting Sediment Transport* (ed. R. E. Meyer), pp. 181–202. Academic Press.
- NWOGU, O. 1993 Alternative form of boussinesq equations for nearshore wave propagation. *J. Waterw. Port C-ASCE* **119**, 618–638.
- OLBERS, M. J. & HERTERICH, K. 1979 The spectral energy transfer from surface to internal waves. *J. Fluid Mech.* **92**, 349–379.
- PARAU, E. & DIAS, F. 2001 Interfacial periodic waves of permanent form with free-surface boundary conditions. *J. Fluid Mech.* **137**, 325–336.
- PEREGRINE, D. H. 1967 Long waves on a beach. *J. Fluid Mech.* **27**, 815–827.
- PHILIPS, O. M. 1960 On the dynamics of unsteady gravity waves of finite amplitude. part i. *J. Fluid Mech.* **9**, 193–217.
- PHILIPS, O. M. 1981 Wave interactions- the evolution of an idea. *J. Fluid Mech.* **106**, 215–227.
- POND, S. & PICKARD, G. L. 1983 *Introductory Dynamical Oceanography*. Butterworth-Heinemann.
- RADDER, A. C. 1979 On the parabolic equation method for water-wave propagation. *J. Fluid Mech.* **95**, 159–176.
- RYGG, O. B. 1988 Nonlinear refraction-diffraction of surface waves in intermediate and shallow water. *Coast. Engng.* **12**, 191–211.
- SEGUR, H. 1980 Resonant interactions of surface and internal gravity waves. *Phys. Fluids* **23**, 2556–2557.

- SHEREMET, A. & STONE, G. W. 2003 Observations of nearshore wave dissipation over muddy seabeds. *J. Geophys. Res.* **108**, 3357–3368.
- SOLTANPOUR, M., SAMSAMI, F. & SOROURIAN, S. 2010 Wave-flume experiments of dissipating waves on soft mud. In *Proceedings of the International Conference on Coastal Engineering (ICCE)*, pp. 181–202. ASCE.
- STAQUET, C. & SOMMERIA, J. 2002 Internal gravity waves: from instabilities to turbulence. *Ann. Rev. Fluid Mech.* **34**, 559–593.
- STOKES, C. G. 1847 On the theory of oscillatory waves. *Trans. Cambridge Philos. Soc.* **8**, 441–455.
- TAHVILDARI, N. & JAMALI, M. 2009 Analytical cubic solution to weakly nonlinear interactions between surface and interfacial waves. In *Proc. 28th International Conference on Ocean, Offshore and Arctic Engineering (OMAE2009)*, pp. 625–530. ASME.
- THORPE, S. A. 1966 On wave interactions in a stratified fluid. *J. Fluid Mech.* **24**, 737–751.
- THORPE, S. A. 1968 On standing internal internal gravity waves of finite amplitude. *J. Fluid Mech.* **32**, 489–528.
- THORPE, S. A. 1975 The excitation, dissipation, and interaction of internal waves in deep ocean. *J. Geophys. Res.* **80**, 328–338.
- TROY, C. D. & KOSEFF, J. R. 2006 The viscous decay of progressive interfacial waves. *Phys. Fluids* **18**, 1–14.
- TURNER, J. S. 1973 *Bouyancy Effects in Fluids*. Cambridge University Press.

- WATSON, K. M., WEST, B. J. & COHEN, B. I. 1976 Coupling of surface and internal gravity waves: a mode coupling model. *J. Fluid Mech.* **77**, 185–208.
- WEI, G. & KIRBY, J. T. 1995 Time-dependent numerical code for extended boussinesq equations. *J. Waterway Port Coastal Ocean Engng* **121**, 251–261.
- WEI, G., KIRBY, J. T., GRILLI, S. T. & SUBRAMANYA, R. 1995 A fully nonlinear Boussinesq model for surface waves. Part 1. Highly nonlinear unsteady waves. *J. Fluid Mech.* **294**, 71–92.
- WELLS, J. T. & COLEMAN, J. M. 1981 Physical processes and fine-grained sediment dynamics, coast of surinam, south america. *J. Sediment. Petrol.* **51**, 1053–1068.
- WEN, F. 1995 Resonant generation of internal waves on the soft sea bed by a surface water wave. *Phys. Fluids* **7**, 1915–1922.

VITA

Navid Tahvildari was born in Iran. He received his Bachelor of Science degree in civil engineering in 2005 from Amirkabir University of Technology (Tehran Polytechnic). Immediately after graduation, he pursued his studies in Master of Science in civil engineering and received his degree from Sharif University of Technology in 2007. In Fall 2007, he began his doctoral studies in Ocean Engineering Program in Civil Engineering Department at Texas A&M University, graduating in December 2011. His research interests are theoretical and numerical studies in wave mechanics, environmental fluid mechanics, and wave-structure interactions.

Dr. Tahvildari may be reached by email at: navid.tahvildari@gmail.com or can be contacted at: Coastal & Ocean Engineering Division, Civil Engineering Department, Texas A&M University, 3136 TAMU, College station, TX 77843-3136, USA.